Chapter 4

Circulation of the Mediterranean Sea and its Variability

Katrin Schroeder[a], Jesus Garcìa-Lafuente[b], Simon A. Josey[c], Vincenzo Artale[d], Bruno Buongiorno Nardelli[e], Adriana Carrillo[d], Miroslav Gačić[f], Gian Pietro Gasparini[a], Marine Herrmann[g], Piero Lionello[h], Wolfgang Ludwig[i], Claude Millot[j], Emin Özsoy[k], Giovanna Pisacane[d], Jose C. Sánchez-Garrido[b], Gianmaria Sannino[d], Rosalia Santoleri[e], Samuel Somot[g], Mariavittoria Struglia[d], Emil Stanev[l], Isabelle Taupier-Letage[j], Michael N. Tsimplis[c], Manuel Vargas-Yáñez[m], Vassilis Zervakis[n], George Zodiatis

a. CNR-ISMAR, Forte Santa Teresa, 19036 Pozzuolo di Lerici (La Spezia), Italy
b. Departamento de Física Aplicada II, University of Málaga, Málaga, Spain
c. National Oceanography Centre, Southampton, United Kingdom
d. ENEA –Casaccia, via Anguillarese 301, 00123 Roma, Italy
e. CNR-ISAC, Via del fosso del Cavaliere 100, 00133 Roma, Italy
f. OGS, Borgo Grotta Gigante 42/c, I□34010 Trieste, Italy
g. CNRM-GAME, Météo-France / CNRS, Toulouse, France
h. University Lecce, Dept Mat Sci, via per Arnesano, km1.2,73100 Lecce, Italy
i. Cefrem, University Perpignan, 52, Avenue P. Alduy, 66860 Perpignan, France
j. LOPB-COM-CNRS, BP 330, 83150 La Seyne/mer, France
k. Institute of Marine Sciences, Middle East Technical University, Erdemli, Turkey
l. University Oldenburg, ICBM, Postfach 2503, D-26111 Oldenburg, Germany
m. IEO, Centro Oceanográfico de Málaga. 29640 Fuengirola, Málaga, Spain
n. University of the Aegean, Department of Marine Sciences, Mytilini, Greece
o. University of Cyprus, Oceanography Centre, P.O. 20537, 1678 Nicosia, Cyprus

1. Introduction

The Mediterranean Sea occupies an elongated area of about 2.5 million km^2 between Europe and Africa, and has only a restricted communication with the world ocean, through the narrow and shallow Strait of Gibraltar. It is further subdivided into two main basins, the Eastern Mediterranean (EMED) and the Western Mediterranean (WMED), communicating through the Sicily Channel. Due to its relatively small size, its geographical location, and its semi-land locked nature, the Mediterranean Sea is very sensitive and responds quickly to atmospheric forcings and/or anthropogenic influences. Demographic growth, climate change and overexploitation are exerting exceptional pressure on the Mediterranean environment, its ecosystems, services and resources. Further it is a region where major oceanic processes occur, though on smaller scales than those occurring in the world ocean, such as deep water formation (DWF) that contributes to sustain a basin-wide thermohaline circulation cell, a reduced version of the large-scale oceanic conveyor belt.

In addition to the obvious length-scale, the Mediterranean thermohaline circulation (MTHC) also differs from that of the world ocean in that it is an open cell: the MTHC starts in the Strait of Gibraltar with an inflow of Atlantic Water (AW) composed by Atlantic Surface Water (ASW) and North Atlantic Central Water (NACW), ends at the same site with an undercurrent of intermediate and deep Mediterranean Waters (MWs) and is driven by the net buoyancy flux toward the atmosphere that takes place on average in the Mediterranean Sea. The flux is mainly due to the freshwater deficit of the sea and transforms continuously the raw material of AW into the final product of MWs, which are 0.2% denser due basically to an increase of salinity. The volume of inflowing AW exceeds the one of outflowing MWs (both in the order of 0.8 Sv, Baschek et al., 2001 and Sánchez-Román et al., 2009; although historical references range from 0.6 to 1.8 Sv, see Bryden et al., 1994) by the needed amount to balance the freshwater deficit.

The upper branch of the MTHC that carries the relatively fresh AW towards the interior of the sea extends over the WMED and EMED and displays a rather complex surface circulation that could be considered as a superposition of interacting large-scale and mesoscale patterns, each of them showing their own variability (circulation schemes are given in Fig. 4.1). A debate on the surface circulation in the EMED is still open (as described more in detail in Sections 2.1. and 2.2). Thus for the AW path, the two schemes are shown in Fig. 4.1a and 4.1b. The lower branch of the MTHC is affected by the sea topography differently. While Levantine Intermediate Water (LIW), the most important intermediate water, resides in the EMED at depths from which it can flow without major topographic constrictions through the Sicily Channel into the WMED, depicting a rather continuous return flow, the deep MWs circulation cells are separated by the topography of the channel and driven by specific DWF processes in the Adriatic/Aegean (for EMED) and the Provençal (for WMED) subbasins. Even if intermediate and deep circulation forming the lower branch of the MTHC are partially coupled to each other, they also have their own scales of variability that do not coincide necessarily. Sections 2.1 and 2.2 deal with the temporal variability of large-scale and mesoscale circulation, respectively, issues that are obviously interconnected since the differentiation between large-scale and mesoscale is somewhat artificial. On the other hand, the expected quick response of a water body of reduced dimensions as the Mediterranean Sea to the forcing variability through its surface has propitiated a considerable amount of literature about changes in MWs properties inside the sea and in the rates of DWF (Béthoux et al., 2002; Rixen et al., 2005, López-Jurado et al., 2005; Schroeder et al., 2006, 2008b; Smith et al., 2008) that are revised and discussed. Recently a new possibility that changes in MWs properties are originated by changes in the properties of the inflowing AW (Millot, 2007) has opened new perspectives to the analysis of the observed variability of MWs. All these issues are addressed in Sections 2.3 and 2.4.

The Mediterranean Sea is of major interest for air-sea interaction research because it provides the opportunity to study heat budget closure (e.g. Bunker et al., 1982), the impacts of large-scale modes of atmospheric variability and the influence of extreme heat loss on DWF (Josey, 2003). The availability of estimates of the heat transport at the Strait of Gibraltar, and the semi-enclosed nature of the basin, place constraints on the Mediterranean Sea heat and freshwater budgets and allow it to be used as a test bed for evaluation of the accuracy of air-sea flux datasets for this region. These budgets are analyzed in detail in Section 3.1, which is completed with a comprehensive description of continental freshwater inputs (river runoff) in Section 3.2, both within Section 3 that deals with the forcing of the Mediterranean Sea. The straits play a fundamental role in this forcing, particularly the Gibraltar Strait whose topography is a key point in the functioning of the Mediterranean, since it limits the exchanged flows by establishing hydraulic controls that contribute to determine the final properties of the MWs. Another archetypical example of hydraulically controlled exchange is provided by the long and shallow system of Turkish straits whose influence in the nearby Aegean subbasin is obvious as the inflow of Black Sea Water (BSW) entering the Mediterranean through the Dardanelles Strait forms a thin layer of relatively fresh and buoyant water that hinders DWF processes. The DWF in the North Aegean would require the erosion of this layer, a fact that led Zervakis et al. (2000) to propose a mechanism connecting the rate of the Dardanelles outflow to the formation of North Aegean Deep Water (NAeDW) and, hence, to the triggering of the Eastern Mediterranean Transient (EMT, i.e. a shift of the formation site of deep waters, from the Adriatic to the Aegean, an event that has been extensively described in the first Medclivar book, Lionello et al., 2006; see also Sections 2.1, 2.3, 2.4, 3.5). The Sicily Channel differs from the former ones in the sense that internal hydraulics is not important; its importance stems from its connecting the WMED and the EMED, which makes it a very suitable place to monitor signals of the MTHC return flow from the latter to the former. Recent findings about the exchange through all these straits are presented in Sections 3.3, 3.4 and 3.5, respectively. Finally, a discussion about variability in the heat and freshwater characteristics at interannual to multi-decadal times cale is provided in Section 4, while some outlooks and future research priorities are proposed in the concluding Section 5.

Geographical names	
EMED/WMED	Eastern/Western Mediterranean Sea
Water masses	
AdDW	Adriatic Deep Water
AeDW	Aegean Deep Water
ASW	Atlantic Surface Water
AW	Atlantic Water
BSW	Black Sea Water
CDW	Cretan Deep Water
CIW	Cretan Intermediate Water
EMDW	Eastern Mediterranean Deep Water
LDW	Levantine Deep Water
LIW	Levantine Intermediate Water
MW	Mediterranean Water
NACW	North Atlantic Central Water
NAeDW	North Aegean Deep Water
NadDW	Northern Adriatic Dense Water
TDW	Tyrrhenian Dense Water
WIW	Winter Intermediate Water
WMDW	Western Mediterranean Deep Water
Processes	
DSWC	Dense Shelf Water Cascading
DWF	Dense/Deep Water Formation
EMT	Eastern Mediterranean Transient
MTHC	Mediterranean ThermoHaline Circulation
WMT	Western Mediterranean Transition
Currents and Gyres	
CD	Cretan Dipole
CYE	Cyprus Eddy
EAG	Eastern Alboran Gyre
IPG	Ierapetra Gyre
MMG	Mersa-Matruh Gyre
MMJ	Mid Mediterranean Jet
NC	Northern Current
NIG	North Ionian Gyre
PG	Pellops Gyre
RG	Rhodes Gyre
SAG	South Adriatic Gyre
SHG	Shikmona Gyre
WAG	Western Alboran Gyre

Table 4.1: List of the main acronyms used in this chapter

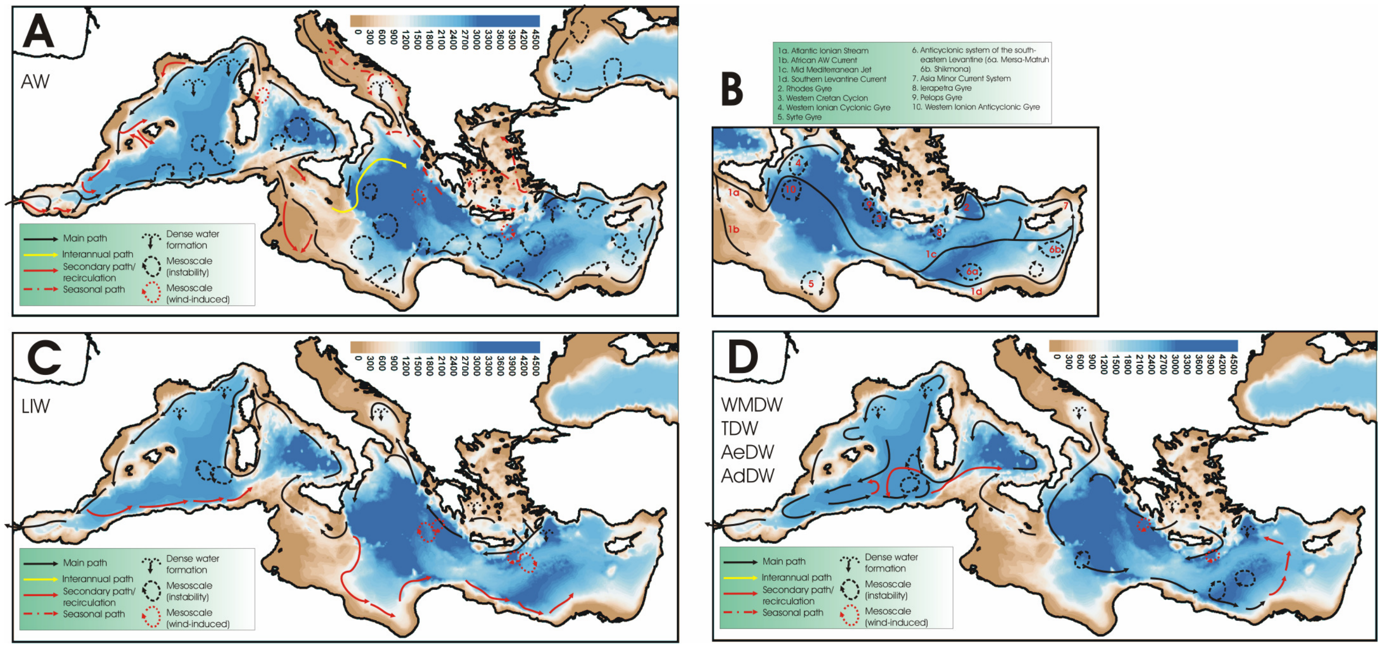

Figure 4.1: Circulation schemes: (a) and (b) surface layer (AW) according to Millot and Taupier-Letage, 2005a (redrawn) and Pinardi et al., 2004 (redrawn, only EMED), respectively; (c) intermediate layer (LIW) and (d) deep layer (WMDW, TDW, AeDW and AdDW) (redrawn from Millot and Taupier-Letage, 2005a).

2. Changes in the Thermohaline Circulation of the Mediterranean Sea

The thermohaline circulation of the Mediterranean Sea exhibits strong seasonal and interannual variability, and is extremely complex, consisting of numerous eddies and current meanders. It is occupied at different levels by a number of water masses, either formed inside the sea or imported from the Atlantic Ocean. The temporal variability of the large-scale and mesoscale circulation, as well as of the characteristics of the water masses is discussed firstly, and then the observed changes in water mass formation in the EMED and in the WMED are described.

2.1. Large-scale circulation variability

Bathymetric differences may have an important impact on the circulation patterns and are responsible for some documented differences in the circulation structure of the two Mediterranean basins. The EMED is characterized by a number of bottom features that can trap subbasin or mesoscale circulation features, while the WMED is characterized by an absence of well defined bottom features. Further, in the EMED deep water is formed in semi-enclosed areas, and spills over a sill into the main basin, while in the WMED the DWF site is located within the basin itself, not being separated by a sill. In spite of those differences, a number of circulation features are common for both basins, such as an eastward flow path, fed by AW, the general counterclockwise flow pattern as well as the presence of mesoscale eddies and meanders. Millot and Taupier-Letage (2005a) assert that the two basins display marked similarities. According to those authors, the AW flow behaves essentially in the same way, being prominently unstable in the south and relatively stable as a return flow to the north. For the following descriptions, we invite the reader to refer to the schematics of the large-scale circulation shown in Fig. 4.1.

In the WMED the alongslope current extending along the North African slope is commonly named the Algerian Current (Millot, 1985). It flows eastward, is characterized by a transport of about 2 Sv and divides into two branches, one weaker entering the Tyrrhenian (~0.7 Sv), and the other continuing through the Sicily Channel (~1.5 Sv) into the EMED (e.g. Schroeder et al., 2008a). The Algerian Current is unstable, leading to the generation of meanders and subsequently to a series of “coastal eddies” of 50-100 km in diameter (see Section 2.2 for further details), that propagate eastward along the slope at speeds of about 3-5 km day^{-1}. The coastal eddies interact and can be disturbed by “open-sea eddies” that are present in the centre of the WMED (Millot, 1999). Due to absence of strong bottom features, coastal eddies are not trapped but move mainly downstream and can be of both signs, even if anticyclones may become very prominent and last for months (Millot, 1999). They occasionally become open-sea eddies of ~200 km in diameter and may have lifetimes of up to ~3 years extending down to the bottom (~ 3000 m; Puillat et al., 2002; Millot and Taupier-Letage, 2005b). The only quasi stationary closed structures are the Western Alboran Gyre (WAG) and the Eastern Alboran Gyre (EAG), two anticyclonic vortices/meanders separated by the Alboran ridge (Viudez et al., 1996a, b).

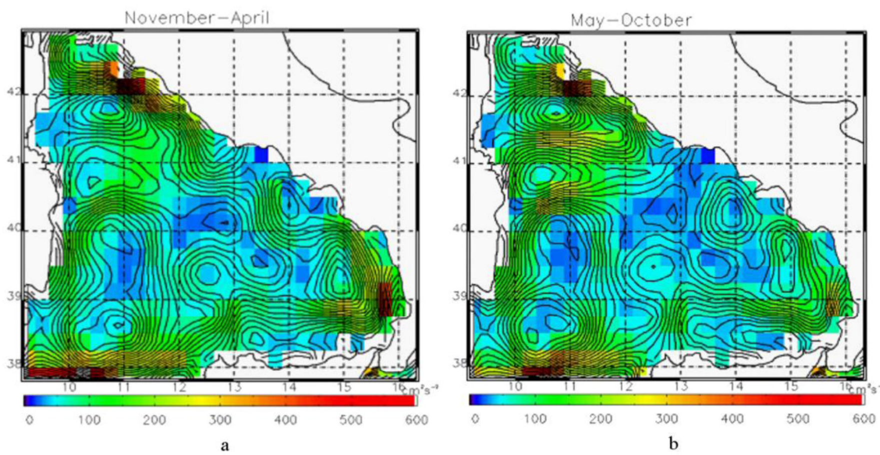

Figure 4.2: Seasonal variability of the Tyrrhenian circulation from altimeter data. Mean kinetic energy with superimposed the mean flow in (a) winter and (b) summer (from Rinaldi et al., 2010).

The flow that makes part of the return branch in the WMED is fed in the surface layer by the AW, in the intermediate layer by the LIW, in the deep layers by the WMDW. It extends along the northern coast of Sicily, then along the western Italian coastline and along the Ligurian and Provençal coasts. Subsequently the flow extends along the Catalan coast through the Ibiza Channel. Millot (1999) named this entire current system the Northern Current. The AW partly originates from the Algerian Current entrained by Algerian eddies and partly directly from the Algerian Current that, before entering the Sicily Channel, splits into two branches and propagates across the Tyrrhenian and along the western Corsican coast. The Tyrrhenian subbasin is characterized by a number of anticyclonic mesoscale eddies, as well as by the semi-permanent cyclonic/anticyclonic wind-induced dipole (North Tyrrhenian Cyclone and North Tyrrhenian Anticyclone) located in front of the Bonifacio Passage (Rinaldi et al., 2010). This complex pattern varies on a seasonal scale and makes it difficult to identify a consistent mean flow (see Fig. 4.2).

In the EMED both the eastward and the return (northern) flows are quite clearly evident. In addition, the EMED is characterized by the presence of a number of topography- or bottom-trapped, often wind-induced, gyres that are permanent, recurrent or semi-permanent such as Rhodes Gyre (RG), Ierapetra (IPG), Cretan Dipole (CD), Mersa-Matruh (MMG), Pellops (PG), South Adriatic Gyre (SAG), North Ionian Gyre (NIG), Shikmona Gyre (SHG) and Cyprus eddy (CYE). For several aspects of the EMED circulation there is a wide agreement, such as the AW crossing the Sicilian Channel, flowing eastward, becoming denser via evaporation exceeding precipitation, to sink in specific northern zones to create deep and intermediate water masses (Ovchinnikov, 1966; Hecht et al., 1988; Theocharis et al., 1993). Other aspects of the EMED circulation are still under debate (Amitai et al., 2010). One of the major controversial issues is the main pathway of the AW and the governing basin scale surface current (see Fig. 4.1a and 4.1b): is it basin centered, or does it flow along seashore slopes (Amitai et al., 2010)? On the basis of in-situ data, the POEM Group (1992) and Manca et al. (2002) showed the meandering flow spreading AW clockwise in the northern part of the Ionian and then crossing the southern Cretan Sea in the form of an offshore cross-basin jet (the Mid Mediterranean Jet – MMJ, see Fig. 4.1b). Rio et al. (2007) found from the Mean Dynamic Topography for the period 1993-1999 that the flow in the Ionian divides into two branches that cross the Ionian toward the Levantine subbasin. An overall clockwise circulation seems to dominate the southern Ionian and according to the same authors this is the main route of the AW. The second branch continues directly eastward, where it flows mainly along the Libyan and Egyptian slopes, and joins the other branch before entering Cretan Passage. New in-situ data (Zodiatis et al., 2010a) confirm the previous analyses carried out during the 80s (Özsoy et. al., 1991; POEM Group, 1992), i.e. that the MMJ enters the area from the southwest, meandering between Cyprus and the northern periphery of the Cyprus warm core eddy (Zodiatis et. al. 2005b). The MMJ is documented to transfer the AW eastward within the Levantine subbasin, particularly along the periphery of the Cyprus warm core eddy. AW has also been observed close to the Egyptian coast, as a result of a westward re-circulation, either of the MMJ or of a current flowing eastward close to the Egyptian coast (Zodiatis et. al., 2007).

On the other hand, Hamad et al. (2005) analysing satellite IR data suggested that the eastward flow in the EMED is alongslope, as in the WMED, continuing along the African coast. They also showed that this circulation is unstable generating mesoscale anticyclonic eddies that propagate offshore. Moreover, in a recent paper Millot and Gerin (2010) assert that the MMJ is an artefact, due to the limitations of the in-situ sampling, making in fact part of instabilities of the

AW flow (see Fig. 4.1a). The return flow extends along the Asia Minor coast (Asia Minor Current – AMC) and then presumably bifurcates to the north and to the south of Crete, perturbed by semi-permanent gyres. On its way westward from its formation site, the LIW follows more or less the same pathways and it is entrained within the IPG and PG (Millot and Taupier-Letage, 2005a).

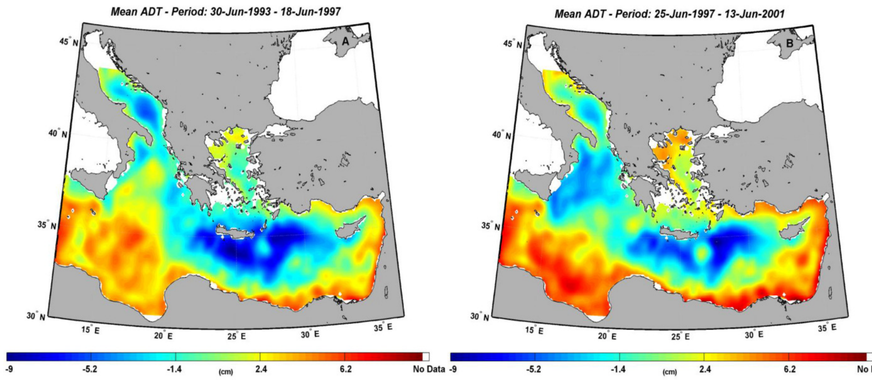

Figure 4.3 Mean distribution of absolute sea-level height in the EMED for two 4-years periods. The surface circulation inversion is evident in the NW- Ionian, passing from anticyclonic in the first period (left panel, before 1997) to cyclonic in the second period (right panel, after 1997). A number of mesoscale features are clearly evident in both periods (redrawn from Borzelli et al., 2009)

Most of the EMED gyres have well defined and unchanged rotation sign but vary in intensity on seasonal or more prominently on decadal time-scales. Conversely, the NIG is different from the others, since it changes on a decadal scale not only in intensity but also in sign of rotation (Borzelli et al., 2009; Gačić et al., 2010). The reversal of the NIG determines the direction of the spreading of the AW (see Fig. 4.3): it flows eastward when the NIG is cyclonic close to the African coast, while it propagates northward into the Ionian interior with an anticyclonic NIG (Manca et al., 2002; Malanotte-Rizzoli et al., 1997), eventually entering the Adriatic (Gačić et al., 2010). Also the flow of the LIW is determined by the sign of rotation of NIG: when NIG is cyclonic the LIW outflow through the Cretan Passage is intensified while during the NIG anticyclonic phase both flows (AW and LIW) through the Cretan Passage are weakened. In fact the NIG anticyclonic mode causes LIW to recirculate within the Levantine subbasin and the AW to fill the Ionian interior. Therefore, differences in the schematization of the Ionian and EMED circulation between e.g. Hamad et al. (2004) and Rio et al. (2007) may be explained in terms of the decadal variations of the NIG circulation. Evidently the water flow through the Cretan Passage and the thermohaline properties in the Adriatic, Ionian and Levantine are conditioned by the NIG and presumably vary on a decadal scale, as NIG rotation sign changes

(Gačić et al., 2010; Theocharis et al., 2002), changing the salt content in the three subbasins of the EMED. Thus the NIG circulation could be considered responsible for determining the intensity of the DWF processes in the Aegean and Adriatic that were out-of-phase, i.e. while the Aegean was producing the dense water the Adriatic was not and, vice versa, the Adriatic resumed the production of dense water when the Aegean stopped.

The Adriatic shows the occurrence of several high-salinity events (Vilibic and Orlic, 2001, and references therein) and this may confirm that the NIG inversions have taken place on a decadal scale. The NIG inversions have often been associated with changes in the wind stress curl (Pinardi et al., 1997; Korres et al., 2000; Molcard et al., 2002) that were documented from wind data time series (Lascaratos et al., 2002). On the other hand, Gačić et al. (2010) explained the NIG decadal variability in terms of a feedback mechanism between the Adriatic and the Ionian, the Adriatic being an important time-dependent potential vorticity source due to the outflow of dense water of varying thermohaline properties and density. The feedback mechanism has been named Adriatic-Ionian Bimodal Oscillating System (BiOS). In the early 70s a high-salinity event similar to the EMT was documented in the Levantine, but it was not followed by a temperature decrease in the Aegean and thus no Aegean Deep Water (AeDW) formed as during the EMT (Theocharis et al., 2002). High-salinity events represent a preconditioning for the Aegean DWF, but probably winter air-sea fluxes in the early 70s were not strong enough to trigger the Aegean DWF. The switch from the Adriatic to the Aegean, as the source for EMDW, and the consequent bottom water circulation changes, has been possible because the two DWF sites are separated from the rest of the basin by bathymetric features.

Also the WMED shows prominent circulation variability with a large contribution of mesoscale and seasonal variations in the southern and northern part, respectively, as documented by Millot (1999). The seasonal variability of the Northern Current (NC) between the Balearic Islands and the coastline (Ibiza Channel) is strongly pronounced with a maximum in winter and a minimum in summer (Pinot et al., 2002). On the other hand, anticyclonic eddies formed along the Algerian Current altered or even masked the seasonal signal driving the waters from the south, mainly the fresh AW through the Mallorca Channel or more to the east along the western coast of Sardinia and Corsica, that then feed the NC. Anticyclonic eddies are formed also to the north of the Balearic Islands and they alter the southward flow. Interannual variability is due to the varying dense water (WMDW) production, which in turn depends both on lateral advection and winter climatic conditions (Schroeder et al., 2010). Recently, a major production of salty deep water has been evidenced. The authors showed that the lateral advection played a major role in setting the change of the deep water properties in recent years (after 2005). More specifically, some authors suggest occasional inversions of the southward current, taking place at the Catalan shelf, that block the AW penetration with the NC leading to an increased salt content due to the massive presence of LIW (Salat et al., 2009).

Millot (1999) suggested that in the Gulf of Lions either WMDW or intermediate water (Winter Intermediate Water, WIW) is formed, as a function of the intensity of air-sea heat fluxes. According to the same author the outflow from the Sicily Channel or the thermohaline properties of the EMED waters and thus the DWF processes in the EMED play an essential role in mixing between the LIW/WIW and the WMDW. These waters cascade from 300 m depth at great depths (~2000 m) and if the amount of this water is large, the mixing between WMDW and cascading water is intense. The amount of the unmixed upwelled WMDW, that then mixes with the upper layer waters in the Tyrrhenian, is controlled by the density of the EMED water. This mechanism can thus explain how WMDW that lies at depths of about 2000 m, is lifted to 300 m at the Gibraltar Strait and makes part of the mixture of the exiting MWs. The important aspect of this mechanism is that the signal associated with the EMED waters determines the upwelling of the WMDW, its mixing with intermediate waters and thermohaline properties of the MWs, that presumably change in function of the EMED water characteristics (Millot, 1999). The water exiting the Strait of Gibraltar reflects changes of the mixing between four different types of the MWs (WMDW, TDW, WIW and LIW). It was shown that since mid 90s there have been continuous variations of the densest outflowing MWs. These variations are one order of magnitude larger than decadal trends in the thermohaline properties of the WMDW (Millot et al., 2006). In the early 2000s the contribution of the EMED waters to the outflowing MWs is especially prominent and it was hypothesized that this was linked to the EMT. Indeed, Millot et al. (2006) called the sudden increase in the contribution of the EMED waters to the outflowing MWs the Mediterranean Sea Transient.

Analysis of the sea surface height anomalies (SSHA) of the entire Mediterranean i.e. the surface geostrophic flow, confirms important differences between the two basins' low-frequency and mesoscale circulation variability (Cipollini et al., 2008). The altimetric data as shown by Wunsch (1997) reflect primarily the motion of the main thermocline, thus the SSHA variability presented here really reflects motions related to a first baroclinic mode. At longer time-scales (> 1y), variability is prominent mainly in the EMED and associated with the NIG, PG, IPG and MMG. Some low-frequency variations can also be seen along the Algerian Current. Generally, the RMS amplitude of the low-frequency signal is more prominent in the EMED than in the WMED. The annual signal shows isolated peaks associated with the IPG, due to the annual variations of the Etesian winds. At the shorter time scales, on the order of one month, SSHA show important mesoscale activity in the interior or the EMED (see detailed description in Section 2.2; see also Rio et al., 2007). Numerical simulations corroborated the fact that the EMED is characterized by a stronger interannual variability which can be explained in terms of the wind stress and heat fluxes (Pinardi et al., 1997).

2.2. Mesoscale Circulation Variability

The Mediterranean Sea is a region where mesoscale processes play a key role in determining the characteristics of the large-scale circulation, the distribution and mixing of water masses, with important consequences on the whole ecosystem functioning (e.g. Millot et al., 1990; Robinson et al., 2001; Salas et al., 2002; CIESM, 2005; and references therein). Mesoscale features (meanders, eddies, filaments) mainly originate as instabilities of larger-scale currents and density fronts and the scale of these spatial and temporal disturbances is set primarily by the internal properties of the ocean (i.e. scaled by the internal Rossby radius of deformation and rotation time).

In the Mediterranean, the internal Rossby radius does not exceed a few tens of km, about four times smaller than the typical values found in the world oceans. However, some features characterized by longer space and time scales (e.g. some eddies and gyres) are generally described as "mesoscale", even though the assumption of quasi-geostrophy is not necessarily valid for all of them, and other mechanisms may start to play an important role on their evolution (e.g β-effect, friction, topographical effects). It must be noted that also the definition of "eddy" and "gyre" is not unique, the two words being often used interchangeably to define a closed circulation path, or the "eddy" being associated with non-permanent features and the "gyre" being defined as a quasi-permanent eddy, or the "gyre" being associated only with the basin-wide along-slope circulation. The Mediterranean mesoscale features described hereafter thus encompass a wide range of different phenomena/features, with horizontal scales ranging from a few km to a few tens/hundreds of km, with vertical scales ranging from tens to thousands m (sometimes reaching the seafloor) and temporal scales from few days to several weeks/months. As an example, Puillat et al. (2002) and Taupier-Letage (2008), reported that Algerian eddies can last for up to 3 years, and Libyo-Egyptian eddies for 2 years, while at least one eddy in the Levantine was documented to be active for more than a decade (Zodiatis et al., 2005b).

The assessment of the energy associated with mesoscale at Mediterranean scale has significantly improved with the advent of satellite altimetry. In fact, through altimeter data, it was possible for the first time to estimate the surface geostrophic currents and the associated eddy kinetic energy at weekly (or longer) time scales in the whole sea. Altimeter data identified the AW flow as the main source of eddy variability (see as an example Fig. 4.4), both in the western and the eastern basins (Larnicol et al., 1995; Iudicone et al., 1998; Ayoub et al., 1998; 2002; Pujol and Larnicol, 2005; Pascual et al., 2007; Cipollini et al., 2008; Jordi and Wang, 2009). However, altimeter data have been shown to significantly underestimate the variability of mesoscale structures <100 km, not sufficiently resolved even with the best available combination of satellites (Pascual et al., 2007; Ferrari and Wunsch, 2010; Rinaldi et al., 2010). Actually, mesoscale features are observed all over the basin even at smaller scales (few tens of km) in thermal and colour imagery (see Fig. 4.5). In practice, the simple circulation schemes generally proposed for the Mediterranean surface layers, firstly proposed by Nielsen (1912) and later by Ovchinninkov et al. (1976), are complicated by the fact that the surface flow is markedly unstable (e.g. Millot and Taupier-Letage, 2005a; Zodiatis et al., 2005a, b; see also Fig. 4.1).

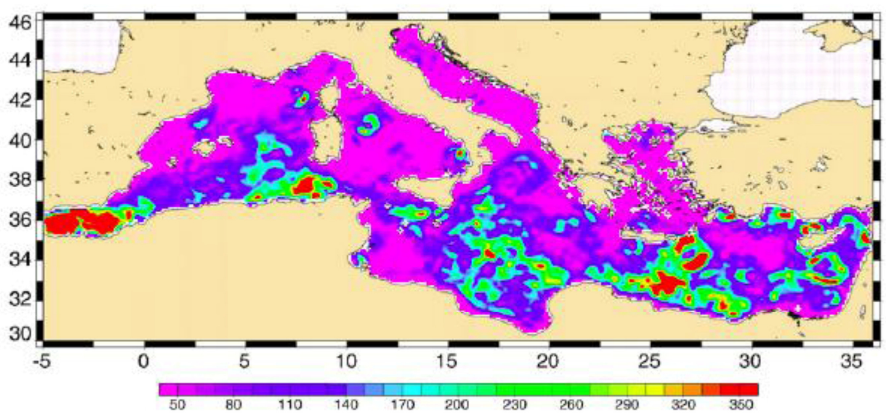

Figure 4.4: Mean EKE averaged over the period October 2002–June 2003, as estimated from Jason-1, ERS-2 and T/P altimeters. Units are $cm^2 s^{-2}$ (from Pascual et al., 2007).

Wind-driven coastal upwelling fronts, filaments and flow instabilities have also been recorded several times in many different places around the basin. In particular, several regional studies have been made (e.g. Millot, 1979; Johns et al., 1992; Buongiorno Nardelli et al., 1999; Borzelli et al., 1999; Lermusieaux and Robinson, 2001; Ribotti et al., 2004; Bignami et al., 2007) and some basin-wide analyses have also been performed on coastal upwelling and related mesoscale (and sub-mesoscale) features (e.g. Bignami et al., 2008).

Starting from the western basin, the surface circulation, dominated by the AW inflow (see Section 2.1), can be subdivided in "regional currents" (the Algerian Current, Northern Current, etc.) each having specific characteristics that lead to specific instability features. Along the Algerian slope, the AW flow (100–200 m deep) meanders and generates both cyclonic and anticyclonic eddies (e.g. Millot, 1985; Millot et al., 1997; Iudicone et al., 1998). Large anticyclones develop a few times per year, and can reach diameters over 100 km, often extending down to the bottom (2000–3000 m). These structures propagate eastward when they are embedded in their parent currents, so that their propagation speed matches that of a baroclinic instability in an unstable along-slope current. Since these eddies have a vertical extent much deeper than their parent currents, they follow deeper isobaths and can thus separate from them when the deeper isobaths diverge from the shallower ones. When separated from their parent currents, however, the β-effect (rotational and bathymetric) and the non-linearity of the system become essential and these features generally tend to drift southwestward at speeds up to a few km/day (Puillat et al., 2002; Testor et al., 2005a). Taupier-Letage et al. (2003) and Millot and Taupier-Letage (2005b) also showed that these eddies entrain significant amounts of AW and MWs from the periphery: lenses of slightly modified AW and LIW can be found in the central part of the subbasin. In the same way the vertical extent of Algerian eddies down to the bottommay modify locally and temporarily the deeper circulation (Millot and Taupier-Letage, 2005b). Eddies formed of LIW have also been observed at intermediate depths in the eastern part of the Algerian subbasin (Testor and Gascard, 2003; Testor et al., 2005b).

In the northern part of the western basin, the NC mainly develops meanders O(70km) (e.g. Albérola and Millot, 2003; Stemmann et al., 2008) and mesoscale activity shows a strong seasonal signal, with intensification during winter (e.g. Sammari et al., 1995). In fact, while the higher stability of the NC is clearly reflected in the eddy kinetic energy estimates from satellite altimetry, intense mesoscale processes are observed in the central part of the Provençal subbasin, off the Gulf of Lions, where open ocean DWF processes are regularly observed. In this area, intense air-sea interactions lead first to the progressive growth of a cyclonic circulation, and finally drive deep (and intermediate) winter convection events and subsequent isopycnal outcropping. Intense mesoscale instabilities originate at the density front between the well mixed dense waters and the lighter surrounding waters, acting to re-stratify the water column after convection. Small eddies formed mainly of WIW have also been observed north of the North

Balearic Front (frontal eddies, Fuda et al., 2000), as far as the Alboran (Allen et al., 2008).

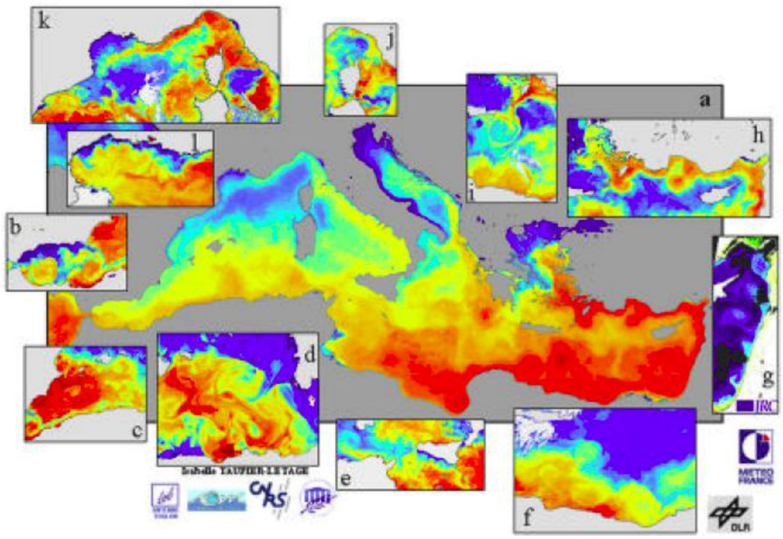

Figure 4.5: Mediterranean mesoscale features as seen in thermal images. Temperature increases from blue to red. Image credits:(a-h) monthly sea surface temperature composite for January 1998 (DLR imagery); (b-f and i-l) single AVHRR images (SATMOS imagery); (g) ocean colour from SeaWiFS (JRC imagery). (from Taupier-Letage, 2008).

Besides the debate already highlighted above, another strong debate still exists in the scientific community about the dynamics and role of mesoscale variability in modulating the mean surface circulation in the eastern Levantine and on the presence and origin of the Mid Mediterranean Jet (MMJ, see also Section 2.1, as well as Fig. 4.1a and 4.1b, Amitai et al., 2010 for details). We recall that on one hand, the first description of the Levantine mesoscale circulation, proposed during the late 80s, evidenced the presence of several alternating cyclonic and anticyclonic gyres and eddies (Robinson et al., 1987; Özsoy et. al., 1991; POEM Group, 1992), whose variability is the main cause of the signal found in the altimeter eddy kinetic energy maps. As a result of the interaction between these cyclonic (Rhodes) and anticyclonic (Ierapetra, Mersa Matruth and Shikmona) gyres, the mean kinetic energy presents an offshore maxima, generally related to the MMJ (e.g. Marullo et al., 2003, and references therein, see Fig. 4.1b). In the southeastern Levantine, the POEM Group (1992) defined the Shikmona gyre as a non-permanent multi-pole gyre, consisting of three eddies, of which the Cyprus one is the most pronounced (Brenner, 1989; 1993). The analysis of in-situ data collected in the southeastern Levantine (starting in the mid 90s, and lasting for a period of 15 years, as well as moored time series, mainly within the frame of the CYBO, CYCOFOS and CYCLOPS projects, see Zodiatis et al., 2005a, b), as well as the extended use of satellite remote sensing data (Groom et. al., 2005), made it possible to describe not only the daily and seasonal, but also the interannual variability of the mesoscale features and water masses displacements in the region. These long-term in-situ data sets (collected seasonally) revealed that the dominant and quasi-permanent Cyprus warm core eddy undergoes significant seasonal and interannual fluctuations in terms of shape, size, intensity and location (Zodiatis et al., 2005a). Moreover, the establishment of a secondary warm eddy in the southeastern part of the area was recorded. This secondary eddy appeared during periods when the Cyprus eddy became weaker. Recently, an analysis of drifters trajectories showed that the instability of the strong northward current along the Israel-Lebanese coast (see Fig. 4.5g) leads to the generation of a new anticyclonic eddy. This later detaches from the northward current towards the area of the secondary eddy, as observed during the CYBO cruises. During CYBO long-term observing campaigns, the re-establishment of the non permanent Shikmona gyre has been observed, with the co-existence of 2-3 warms eddies (Zodiatis et al., 2010b). The periodic re-appearance of these features was confirmed by satellite altimetry, as well by the operational forecasts of MOON-CYCOFOS. In this view, the AW is thus transported eastward by the MMJ along the periphery of the Cyprus warm core eddy. This eastward flow is also confirmed by several drifters trajectories deployed in the SE Levantine (Gerin et al., 2009). Moreover, AW has also been observed close to the Egyptian coast, as a result of a western re-circulation, either of the MMJ or of a current flowing eastward and closer to the Egyptian coast (Zodiatis et al., 2007). The Cyprus warm core eddy, the Shikmona gyre (when it appears), the smaller-scale non permanent cyclonic and anticyclonic eddies in the region, thus significantly increase the complexity of the surface circulation and AW transport in the southeastern Levantine. A high-spatial resolution survey of this area, using gliders and CTD profiles (from March 2009 to March 2010), made it possible to resolve the variability of the Cyprus warm core eddy, the AW and its flow path (Hayes et al., 2010), showing the spatial fluctuation of the eddy and the AW along the northern periphery of this structure, in agreement with what found during the CYBO cruises.

On the other hand, based on the reanalysis of the in-situ POEM data, on the results of 1-year monthly XBT transects (Fusco et al., 2003; Zervakis et al., 2003) and on the analysis of satellite images, Hamad et al. (2005, 2006) and Millot and Taupier-Letage (2005a) proposed a different view, showing that the AW flow along the Libyan and Egyptian slopes is unstable, in a way similar to the Algerian Current (see Fig. 4.1a). What has been called the Libyo-Egyptian Current generates eddies that propagate or become trapped by the bathymetry (over the Herodotus trough, especially), spreading AW offshore: in this view there are no permanent eddies, but a permanent presence of eddies. Recent observations, also supported by the analysis of surface drifters trajectories, indicate that the offshore AW flow is associated with the Libyo-Egyptian eddies (Taupier-Letage, 2008; Gerin et al., 2009; Millot and Gerin, 2010). Moored currentmeter time series also indicate that Libyo-Egyptian eddies can reach the bottom and perturb the deeper circulation (Taupier-Letage and Millot, 2010).

Mesoscale flows are mainly horizontal, being dominated by quasi-geostrophic balances (e.g. Gill, 1982), but small deviations from geostrophy may induce significant vertical exchanges. Sparse in-situ surveys in different regions of the Mediterranean using standard instruments (as CTD and XBT) or more advanced instruments (such as the SeaSoar and gliders), have demonstrated that such upwelling and downwelling events can be strong enough (tens of m day^{-1}) and last long enough (several days) to affect the biological processes. Van Haren et al. (2006) observed extremely fast deep sinking in Algerian eddies with moored ADCP, though in this case the quasi-geostrophic assumption clearly does not apply (vertical velocities being comparable to the horizontal components). Investigations on the quasi-geostrophic dynamics of small mesoscale features (~30-40 km of radius) in the Alboran were conducted by Viudez et al. (1996a, b). They found peak vertical velocities in the range of 10-20 m day^{-1}, that correspond mainly to the smaller mesoscale features observed in the western Alboran. Analogous techniques have been applied also to successive measurements collected in the Alboran subbasin, as described by Allen et al. (2001), Fielding et al. (2001), Sanz and Viudez (2005) and Ruiz et al. (2009). The ageostrophic 3D flow associated to a small mesoscale instability (~15 km of radius) of the Atlantic-Ionian Stream in the western Ionian Sea has been analysed by Buongiorno Nardelli et al. (2001). It is worth noting that new technologies (coupling traditional CTD/XBT/XCTD sampling with gliders and satellite measurements) have been recently applied to test the possibility of sampling mesoscale features at much higher resolution and relatively lower costs (Ruiz et al., 2009; Hayes et al., 2010).

However, the complexity of the mesoscale phenomena in the Mediterranean, and their continuous interplay and interaction with the general circulation, associated with the rapid evolution that characterizes these processes, makes a full understanding and a realistic modeling of the Mediterranean dynamics a challenge. Even assimilating all the available observations from in-situ and satellite instruments in numerical models, the smaller scale processes cannot be adequately reproduced, so that additional efforts will be required to fully understand the dynamics and role of mesoscale variability (in particular at the smaller scales) in the Mediterranean.

2.3. Water mass variability

Because of the net evaporation and heat loss over the region, the Mediterranean, is an engine that transforms fresh and warm AW into saltier and cooler MWs, which eventually outflow to the Atlantic at Gibraltar. The variability of water mass characteristics is addressed by means of time series of their temperature and salinity (TS) properties, heat and salt advection and atmospheric forcing. These time series are far from stationary and exhibit continuous fluctuations around the mean values. For long periods (about 30 years) these means define the climatological TS values, as well as the climatological forcing. It is assumed that they are balanced when the equations for heat and salt budgets are considered. Nevertheless, small imbalances would account for slow changes occurring on a time scale longer than several decades.

2.3.1 The climatological characteristics of water masses

The AW can be identified by a subsurface salinity minimum between 36.2 at Gibraltar and 38.9 in the Levantine subbasin. Close to Rhodes it is transformed by convection into LIW (~15.5 ºC, ~39.1; Wüst, 1961; Hopkins, 1978), but its formation area may be extended to the whole Levantine (Nittis and Lascaratos, 1998; POEM Group, 1992). Both, AW and LIW flow into the Adriatic, where they are involved in the formation of the AdDW (~13.0 ºC, ~38.58), a dense water mass that outflows through the Strait of Otranto and sinks to the deep EMED. There, by mixing with surrounding waters, it reaches its final TS values and forms the EMDW (~13.3 ºC, ~38.67; Zore-Armada and Pucher-Petkovic, 1977; Hopkins, 1978; Roether and Schlitzer, 1991; Manca et al., 2002).

The LIW flows westward through the Sicily Channel (~14.2 ºC, ~38.75) and reaches the Tyrrhenian, where its salinity decreases to ~38.6. Sparnocchia et al. (1999) evidenced the cascading of waters from the eastern basin down to ~2000 m in the Tyrrhenian subbasin (see also Section 3.5). Millot (1999) argued that the LIW flowing into the Tyrrhenian could be identified in this subbasin and in the rest of the WMED, while EMDW loses its identity after cascading and mixing within the Tyrrhenian (with both LIW and WMDW), forming the Tyrrhenian Dense Water (TDW, 12.85 ºC, 38.46). Once in the Provençal subbasin the AW can reach salinities between 38.0 and 38.3 and after mixing with LIW and intense winter cooling, WMDW is formed by deep convection. In the same areas intermediate convection might occur, and in these cases only AW is involved, the resulting water mass being WIW (12 -13 ºC, 38.0-38.3; Salat and Font, 1987).

2.3.2.Interannual variability

Changes in water masses can be caused by long-term alterations in the atmospheric patterns. For instance, the positive North Atlantic Oscillation (NAO) anomaly between the 60s and mid 90s could have reduced precipitation and enhanced evaporation in the Mediterranean (Tsimplis and Baker, 2000). Rixen et al. (2005), Tsimplis and Rixen (2002) and Tsimplis and Josey (2001) have argued that this could have induced higher salinities in the upper layers and cooling in the EMED. Also Krahmann and Schott (1998) attributed the increasing salinities of the AW in the WMED to the positive NAO phase. Some changes may be abrupt, as the freshwater reduction in the EMED due to the damming of the Nile and Black Sea rivers (Rohling and Bryden, 1992, see also Section 3.2), while other changes are linked to internal dynamics of the sea and to feedback mechanisms. According to Pinot et al. (2002), the absence of WIW formation in mild winters favours the northward progression of AW through the Balearic channels, increasing the vertical stratification and preventing the intermediate convection in following years. Brankart and Pinardi (2001) show an abrupt cooling of the LIW (~0.4 ºC) from the late 70s to the early 80s linked to exceptional heat losses in the Levantine and Vargas-Yáñez et al. (2010) show that this anomaly is transmitted to the WMED with almost no delay. During 1995-2009 satellite imagery shows that the surface waters in the Levantine have warmed at a fast rate of 0.39 ºC decade^{-1} (Samuel-Rhoads et al., 2010). Zodiatis et al. (2010a) have found that AW and LIW have warmed in the southern Levantine, while the layer 0-10 m (in summer) have become warmer and saltier at a rate of about 0.53 ºC decade^{-1} and 0.25 decade^{-1}, respectively.

One of the most striking changes that occurred in the sea is the Eastern Mediterranean Transient (EMT, see also Sections 2.1, 2.4 and 3.5), when the DWF in the EMED shifted from the Adriatic to the Aegean. Klein et al. (1999) showed that between 1987 and 1995 the Cretan Deep Water (CDW) became warmer, saltier and denser (> 29.2 kg m^{-3}) than EMDW, and overflowed above the sills in the Cretan Arc into the Levantine and the Ionian. Theocharis (1999) shows that the EMT can be divided into two different phases: a first until 1992 dominated by salinity increase, and a second from the winters 1992 and 1993 dominated by an intense cooling. Changes linked to the EMT have been transmitted to the WMED and Fuda et al. (2002) found significant increasing TS trends in the deep Tyrrhenian (0.029 ºC yr^{-1} and 0.01 yr^{-1}, between 1996 and 2000; see also Section 3.5). As discussed also in Section 2.4, the EMT could also have influenced the WMDW production. Schroeder et al. (2006, 2010) found anomalously high TS values in the bottom waters of the WMED after the severe 2004/05 winter. They hypothesized that the anomaly has been induced by a long-lasting increasing import of salt and heat from the EMED. Hermann et al. (2010) and Grignon et al. (2010) confirmed that the preconditioning of the water column had been the main cause of the anomalous WMDW production. On the other hand, Salat et al. (2009) proposed a mechanism linked to changes in the circulation of the slope current flowing southward along the Catalonian slope.

The Strait of Gibraltar is the place where the heat and salt budget of the Mediterranean Sea is closed. Millot et al. (2006) described a warming and salinification of the outflowing MWs, which in the early 2000s were 0.3 °C warmer and 0.06 saltier than in the early 80s. In the inflowing water Millot (2007) reported a huge S increase of ~0.05 yr^{-1} between 2003 and 2007. Such an increase was accompanied by a densification trend of 0.03 kg m^{-3} yr^{-1}. Those values are calculated for a limited period only and cannot be extrapolated to decades, but they at least show the large interannual variability of the inflow, certainly related to some significant changes in the nearby Atlantic (Millot, 2007; Reverdin et al., 2007; see also Section 3.3).

2.3.3 Long-term changes

On the long-term, many studies have reported warming and salting trends in the deep layers of both basins (Bethoux et al., 1990, 1998; Rohling and Bryden, 1992; Leaman and Schott, 1991; Tsimplis and Baker, 2000; Bethoux and Gentili, 1996; Zodiatis and Gasparini, 1996). Concerning the intermediate layer there are some studies which reported positive salinity trends in the WMED while Krahmann and Schott (1998) concluded that it had not increased its salinity. As shown in Fig. 4.6, Rixen et al. (2005) found a positive salinity trend in the western basin and a net increase superimposed on decadal variability for the eastern one. Surprisingly the decadal variability observed in the EMED was not observed in the WMED. Krahmann and Schott (1998) found no signs of warming in this layer while Bethoux and Gentilli (1996) and Sparnocchia et al. (1994) reported positive trends in the Algero-Provençal and Ligurian subbasins. Similar discrepancies can be found in the upper layer. Vargas-Yáñez et al. (2009) reviewed the different trend estimations obtained in different studies, evidencing the above mentioned discrepancies. Painter and Tsimplis (2003) showed cooling in the upper layer of the EMED and no signs of warming in the WMED. Nevertheless, Salat and Pascual (2006) have reported very intense warming trends in the Catalonian continental shelf (~0.02 ºC yr^{-1}) and similar results have been found in the northern Adriatic continental shelf (Russo et al., 2002).

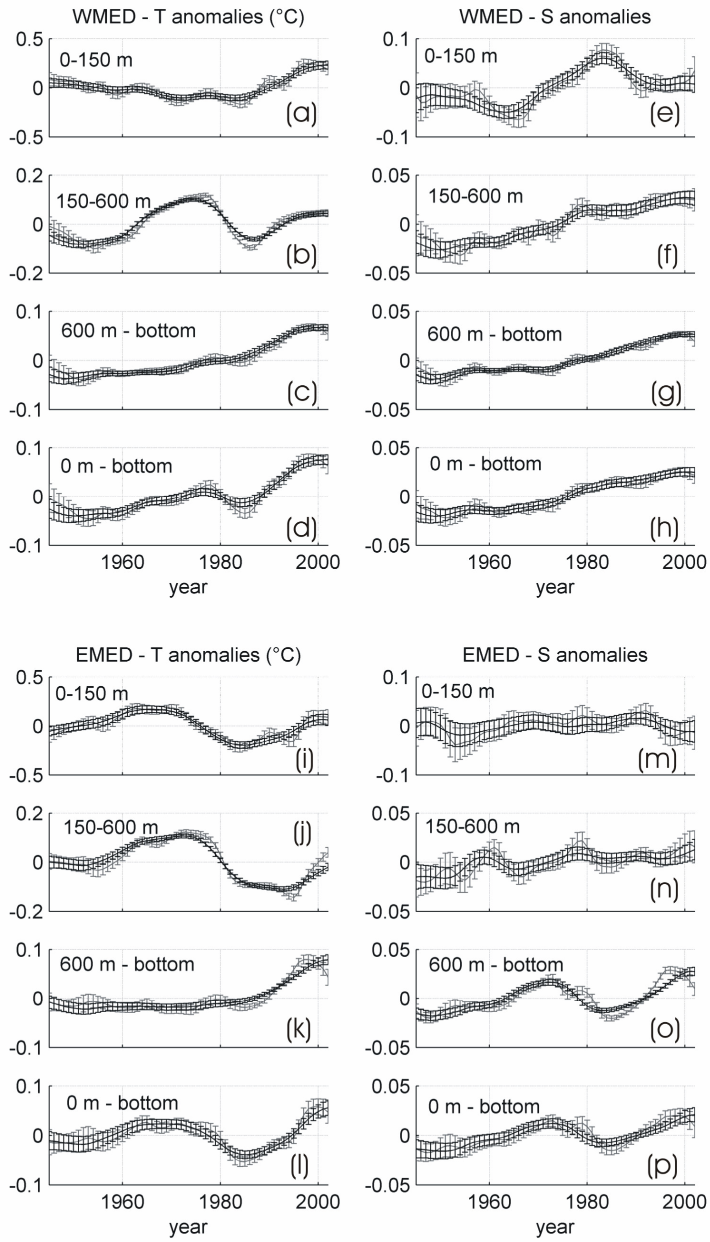

Figure 4.6: Pentadal (gray) and decadal (black) variability (1945-2002) in different layers of (a-d) WMED temperature anomalies,(e-h) WMED salinity anomalies, (i-l) EMED temperature anomalies and (m-p) EMED salinity anomalies. Vertical bars for each yearly estimate represent ±1 error standard deviation (redrawn from Rixen et al., 2005).

Several points are not clear enough yet. The temperature and salinity in the deep layer has increased in both the EMED and WMED while no conclusive results are obtained for the upper and intermediate, layers which contribute to the deep layer formation. In addition, the upper layer of the WMED receives the surface AW which has warmed during the second half of the 20th century (Levitus et al., 2009). As pointed out by Millot (2007), the Mediterranean could simply show the changes happening in the nearby Atlantic, with the local changes being of secondary order. And according to Ruiz et al. (2008), the heat losses through the sea surface do not balance the heat transport through Gibraltar. This imbalance would produce an increase in the heat content of the Mediterranean at a rate of a few W m^{-2} during the last decades, in agreement with the increment of deep water temperature reported by different authors (Font et al., 2007; Schroeder et al., 2006). Finally, numerical models considering IPCC scenarios predict the warming of the upper layers (Marcos and Tsimplis, 2008; Hermann et al., 2008a; see also Chapter 8).

2.4. Changes in water mass formation

The semi-enclosed Mediterranean Sea is one of the few places worldwide where wintertime dense water formation (DWF) occurs, by cooling and evaporation, induced by cold and dry winds. DWF can occur either in the open sea (by offshore convection) or on the shelf (by dense shelf water cascading, or DSWC). As already discussed, both the EMED and the WMED form important water masses. Their properties are mainly determined by the conditions at the sea surface, in terms of AW characteristics (that are gradually modified along its path through the sea) and air-sea exchanges, as well as by the hydrographic conditions of subsurface water masses. Changes in air-sea fluxes (see Section 3.1), interior ocean circulation and mixing can all alter the signature of a water mass in terms of temperature, salinity, equilibrium depth and volume or layer thickness. Since the late 60s DWF processes and their impact on the overall circulation have been studied in both basins. Intermediate and deep water formation takes place in several areas of the sea and in particular in some of the subbasins such as the Provençal (Stommel, 1972; Mertens and Schott, 1998), the Adriatic (Schlitzer et al., 1991; Malanotte-Rizzoli et al., 1997), the Aegean (Roether et al., 1996), and the Levantine (Nielsen, 1912; Lacombe and Tchernia, 1960; Ovchinnikov, 1984). In addition, DSWC occurs almost every year in the Gulf of Lions, in the southern Adriatic and on several Aegean shelves (Durrieu de Madron et al., 2005). These areas are regionally linked and influenced by the same atmospheric forcing that operates in the open-sea convection sites. Recently another site of DSWC has been proposed in the south too: Gasparini et al. (2008) claim that observations of dense water in the Libyan Gulf of Syrte might be attributed to DSWC occurring on the continental margin between Tunisia and Libya. Given the close link with the atmospheric forcings, DWF displays a large variability, from the interannual to the decadal scale.

2.4.1. The eastern basin

The EMED hosts several intermediate and deep water formation sites. Until the findings of Roether et al. (1996), the functioning of the eastern branch of the MTHC was thought to be in a steady state, as all observations agreed with the early work by Pollak in 1951 (e.g. Wüst, 1961; Lacombe and Tchernia, 1958, 1960; Lacombe et al., 1958; Ovchinnikov, 1966; Ovchinnikov et al., 1976; Miller, 1974; Hopkins, 1978; El Gindy and El Din, 1986; Theocharis et al., 1993; Zodiatis, 1992; Zodiatis, 1993b, Malanotte-Rizzoli et al., 1997). This "classical" functioning is hereafter described, while the changes found by Roether et al. (1996) are described later on.

The most voluminous water type of the Mediterranean, the LIW (Millot and Taupier-Letage, 2005a), is formed through open-sea convection in the northern part of the Levantine subbasin, and then it circulates alongslope throughout the whole Mediterranean, occupying intermediate depths (100-500 m). The formation takes place in winter in the Rhodes cyclonic gyre (Nielsen, 1912; Wüst, 1961; Lacombe and Tchernia, 1960; Ovchinnikov, 1984). In a study of this process, Nittis and Lascaratos (1998) have shown that the intensity of the cyclonic circulation plays a preconditioning role by controlling the isopycnal upwelling. The annual rate of LIW formation has been estimated to range between 0.7 and 1 Sv (Nittis and Lascaratos, 1998, and references therein). LIW was found also to be formed locally in the north-western Levantine, cascading along isopycnals from shelf regions (Zodiatis et al., 1998). Other studies (e.g. POEM Group, 1992) reported that formation of LIW is not localized but rather is ubiquitous in the whole Levantine. During severe winters convection may reach the bottom, forming the Levantine Deep Water, LDW (Gertman et al., 1994).

The Adriatic was traditionally considered the source of the deep waters for the eastern basin, the EMDW (Nielsen, 1912; Pollak, 1951; Wüst, 1961; Schlitzer et al., 1991). The main component of the EMDW is the Adriatic Deep Water (AdDW), formed to a major extent through open-sea convection in the southern pit of the Adriatic, with an important role played by LIW or Cretan Intermediate Water (CIW) that precondition the water column. Northern Adriatic Dense Water (NAdDW) formed through shallow water winter mixing over the northern Adriatic shelf (via DSWC), contributes importantly in ventilating the bottom layer of the South Adriatic Pit. It also mixes with the water formed locally through deep convection. The formation rate of Adriatic-originated EMDW has been estimated to about 0.3 Sv (e.g. Lascaratos, 1993), a value comparable to measurements of 0.1-0.4 Sv AdDW exported through Otranto in the period between 1997 and 1999 (Manca et al., 2002).

Also the Aegean was recognized as a source of dense waters (Nielsen, 1912), but not dense enough to contribute to the EMDW (Pollak, 1951; Wüst, 1961; Schlitzer et al., 1991). Even though the Black Sea Water (BSW) entering the Mediterranean through the Dardanelles Strait was shown to form a relative thin surface fresh layer (see also Section 3.4), of highly stable buoyancy, hindering it (Plakhin, 1971, 1972; Zodiatis, 1994), DWF was observed on the North Aegean shelves (Theocharis and Georgopoulos, 1993). The major sites of DWF were considered to be the Cyclades plateau (for shelf formation) and the Cretan Sea (for open-sea deep convection) (Miller, 1963; Lascaratos, 1992, 1993; Zodiatis, 1991). Dense waters originated in the South Aegean outflow through the Cretan Straits (Zodiatis 1992, 1993a, b) and periodically form lenses of CIW, lying below LIW in the eastern basin (Schlitzer et al., 1991; Theocharis et al., 1993).

The above-described traditional view of the DWF processes and sites in the EMED, changed drastically after a comparison between hydrographic transects performed south of Crete in 1987 and 1995 (Roether et al., 1996). During the already mentioned EMT period, high amounts of warmer and saltier water, the Cretan Deep Water (CDW), denser than the previous Adriatic-originated EMDW, had filled the deep layer south of the Cretan Straits, lifting the previous EMDW to shallower depths. While massive DWF in the Aegean first took place in 1987, homogenising the water column down to 700-800 m depth (Zodiatis, 1991), and then in 1992 and 1993, possibly accelerating the local branch of the thermohaline cell (Zervakis et al., 2000, 2004), the export of very dense CDW to the Ionian and Levantine started in 1990 and possibly continued until 2002 (Theocharis et al., 1999, 2002; Roether et al., 2007). The intensity of the DWF in the Aegean was remarkable: it was estimated that 75% of the Aegean outflow took place between mid-1992 and late 1994, at a rate of 3 Sv (Roether et al., 2007). The phenomenon was triggered by the massive formation of dense waters in the North Aegean Sea (NAeDW), which "spilled" into the South Aegean (Zervakis et al., 2000; Gertman et al., 2006). A controversy between the observation studies and several modeling efforts (e.g. Nittis et al., 2003; Bozec et al., 2006) has arisen, where the former argue that most of the CDW is a water mass formed by the mixture of upwelled and propagated NAeDW and LIW, while the latter suggest that CDW is a local water type. The DWF in the North Aegean would require a significant reduction of the isolating role of the surface

BSW in that region, thus a mechanism connecting the rate of the Dardanelles outflow to the formation of NAeDW was proposed (Zervakis et al., 2000). In order to determine which factors triggered the EMT, Beuvier et al. (2010) performed long-term simulations of the Mediterranean circulation. They examined the respective contributions of the atmospheric oceanic forcings during the late 80s and early 90s, namely the atmospheric buoyancy loss, the change of AW circulation in the Levantine, the occurrence of convection events in the Aegean before 1992 and the Black Sea freshwater discharge. Their results suggest that the key triggering factors of the EMT were the surface heat and water losses, hence buoyancy loss, that occurred during the severe winters 1991/92 and 1992/93, as already suggested by Josey (2003).

Since 1993 there has been a stagnation period regarding the formation of NAeDW (Zervakis et al., 2003; Velaoras and Lascaratos, 2005), resulting in a gradual stop of the CDW export to the EMED (Theocharis et al., 2002; Roether et al., 2007). At the same time, the Adriatic has recovered its role in exporting dense waters to the EMED, at rates similar to pre-1987 values (Klein et al., 2000; Manca et al., 2002; Roether et al., 2007; Budillon et al., 2010). Concomitantly, the Ionian upper-layer circulation shows decadal reversals from anticyclonic to cyclonic patterns, that are closely related to this recovery (Borzelli et al., 2009): the northern Ionian and the Adriatic can interplay as a bi-modal oscillating system (BiOS), described by Gačić et al. (2010) and in Section 2.1. In the period characterized by the anticyclonic pattern, as was the case in the early 90s, the northern Ionian and the Adriatic were invaded by fresher water of Atlantic origin that reduced either the density and/or the formation rate of the AdDW. The reversal to a cyclonic pattern took place in 1997: it was then possible again for high salinity water from the east (LIW and/or CIW) to enter the Adriatic, enabling its return as the main source of EMDW. However, the newly formed EMDW is now warmer, saltier and denser than the EMDW observed during and before the EMT (Rubino and Hainbucher, 2007; CIESM, 2009).

2.4.2 The western basin

In the WMED the main DWF region is the area off the Gulf of Lions. During fall and early winter, repeated intense wind events gradually destroy the mixed layer, in a preconditioning phase. In winter, dry and cold winds, such as Mistral and Tramontane, dominate. If this forcing is moderate, AW is simply cooled: its increase in density is weak and the water formed, the WIW, settles to the intermediate layer at around 200 m depth. Long-lasting and repeated intense wind events eventually mix AW with the underlying warmer and saltier LIW. Any further heat loss is then likely to induce deep convection, which leads to the formation of WMDW, reaching the seafloor at around 2500 m depth during the most severe winters (e.g. Stommel, 1972; Rhein, 1995; Mertens and Schott, 1998; Send et al., 1999). Finally the deep water formed exits the convective region and starts spreading south- and westward (e.g. Millot, 1999).

During the past few years (since 2005), the northern part of the WMED seems to have become a very active DWF site. Very intense events have been reported in winter 2004/05 as well as in winter 2005/06 (Schroeder et al., 2008b; Smith et al., 2008; Canals et al., 2006), involving both open-sea convection and DSWC. There are new indications of DWF also in winter 2008/09 (Fuda et al., 2009). The consequence is that since winter 2004/05 the deep waters of the WMED have experienced significant physical changes (Lopez-Jurado et al., 2005; Schroeder et al., 2006, 2008b; Smith et al., 2008), which are comparable to the ones that occurred in the 90s in the EMED, during the EMT, both in terms of intensity and observed effects. The major changes observed in the WMED include an abrupt increase in the deep heat and salt contents (see Fig. 4.7), and a change in the deep stratification, with the appearance of a sharp inversion in the temperature-salinity diagrams. These changes started in winter 2004/05 with the production of an anomalously warm, salty and denser new deep water, which uplifted the old one by several hundreds of meters, over almost the whole WMED. This anomaly has been significantly enhanced by the huge amount of new deep water formed in winters 2004/05 and 2005/06, which induced a basin-wide propagation of the new WMDW and thus of the abrupt increase in deep heat/salt contents (Schroeder et al., 2008b). Data collected between 2004 and 2006 showed that in this period the deep layer of the WMED experienced a temperature increase of about 0.038 °C and a salinity increase of 0.016. These increases are five to seven times greater than the increasing trends indicated by Béthoux and Gentili (1999) and about four times greater than the estimates given by Rixen et al. (2005) for the 1985-2000 period (shown in Figs. 4.6c and 4.6g; see also Schroeder et al., 2008b). Evidences of the presence of the new deep water has also been found close to Gibraltar, in the shallower Alboran subbasin. Indirect evidences have been reported in García-Lafuente et al. (2007) who identified pulses of cold water flowing out of the Mediterranean at Espartel sill in the Strait of Gibraltar in early spring 2005 and 2006, as the result of uplifting of old WMDW (see Section 3.3). In addition, in the analysis of time series at the Camarinal sill and on the Moroccan shelf in the Strait of Gibraltar, Millot (2009) reported dramatic changes in spring 2005: from the beginning of the time series in 2003, it was the first time that no LIW was recorded in the outflow and WMDW was present at both locations, which indicates an outflow mainly of western origin. Those observations were attributed by Millot (2009) to the large amount of WMDW formed during winter 2004/05 in the Provençal subbasin.

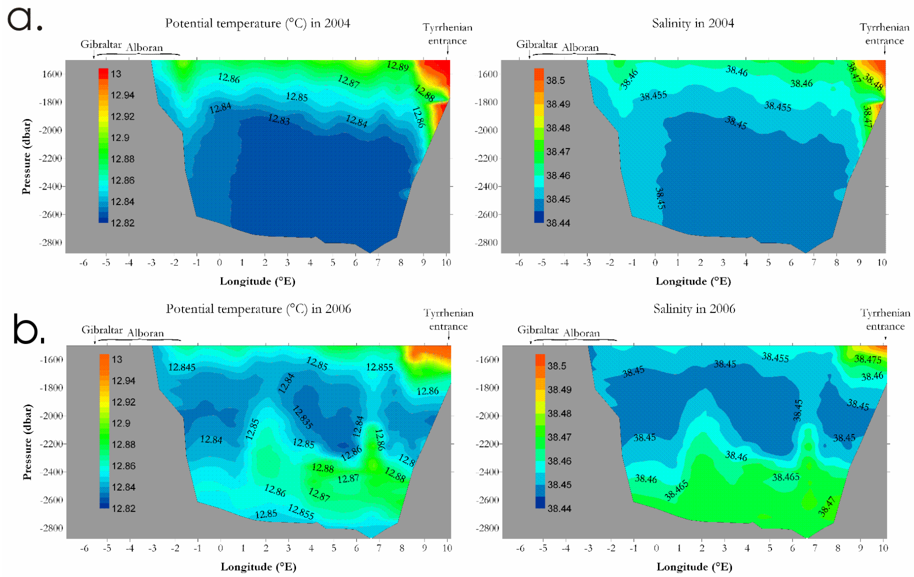

Figure 4.7: Temperature and salinity below 1500 m between the Sardinian Channel and Gibraltar (west is on the left) in (a) October 2004, and (b) October 2006 (from Schroeder et al., 2008b).

Given that winter 2004/05 set the beginning of a changed situation in the deep layers of almost the whole WMED, in CIESM (2009) it was proposed to refer to it as the Western Mediterranean Transition (WMT), to distinguish between the present and the previous situation. Schroeder et al. (2006) related the new deep properties to a progressive increase of heat and salt content in the intermediate layer, due to the arrival of water of eastern origin which has been affected by the EMT. Other authors (Font et al., 2007; Lopez-Jurado et al., 2005), attributed it to the extremely strong winter forcing in 2004/05. In terms of air-sea heat exchange, Lopez-Jurado et al. (2005) showed that the heat loss for this winter was 70% above the winter average, with the highest values since 1948, using the NCEP/NCAR reanalysis. Herrmann et al. (2010) and Schroeder et al. (2010) argue that the new anomalous WMDW characteristics are mainly related to the autumnal heat and salt contents of the water column in the convection region before the convection event. These authors also claim that the EMT had a role in the high volume of WMDW formed in 2005, by deepening the heat and salt maxima, which weakened the pre-convection stratification. Also Grignon et al. (2010) showed that even a normal winter would have led to deep convection in

2004/05 due to low pre-winter stratification. The severe winter thus led to the formation of a massive amount of new deep water.

3. The Forcings of the Mediterranean Sea

In this section we consider the forcings of the Mediterranean Sea, that drive the circulation and determine the water mass properties, as described in Section 2. Besides wind (which is only briefly described in Chapter 0), the main drivers are the surface heat and freshwater exchanges between the sea and the atmosphere (Section 3.1). Other fundamental forcings are considered, such as the river influx (Section 3.2), the exchanges through the Strait of Gibraltar (Section 3.3) and the exchanges with the Black Sea (Section 3.4). In addition in Section 3.5 we included the exchanges between the eastern and the western basins, as it has been shown that the natural decadal variability of the Mediterranean Sea thermohaline cell is related to the amount of water mass that flows through the Sicily Channel (see discussion in Section 4).

3.1. The surface heat and freshwater exchanges

3.1.1 Heat and freshwater budgets

The availability of estimates of the heat and freshwater transports at the Strait of Gibraltar and the semi-enclosed nature of the basin place strong constraints on the Mediterranean Sea budgets of these fields and allow them to be used to some extent as a test bed for evaluation of the accuracy of air-sea flux datasets for this region. The caveat here is that the radiative flux formulae may not be applicable to other regions of the global ocean. Thus, conclusions regarding the accuracy of different flux products for the Mediterranean may not hold elsewhere.

The net heat flux (Q_{NET}) is the sum of four terms,

$$Q_{NET} = Q_{SW} + Q_{LW} + Q_{LH} + Q_{SH}$$

where Q_{SW}, is the net shortwave flux; Q_{LW}, the net longwave flux; Q_{LH}, the latent heat flux and Q_{SH}, the sensible heat flux. Heat budget closure requires that the basin mean net air-sea heat flux should equal the corresponding value determined from the Strait of Gibraltar transport when averaged over sufficiently long time scales that heat storage is not a major term. Mooring based measurements have revealed a net heat transport into the Mediterranean through the Strait of Gibraltar (see Section 3.3), requiring a small net heat loss over the basin if closure is to be obtained, a value of -5 W m^{-2} being obtained by MacDonald et al. (1994). In contrast, it has long been recognised that observation based air-sea flux datasets typically exhibit a mean net heat gain over the Mediterranean of 20-30 W m^{-2} (Bunker et al., 1982; Garrett et al., 1993; Gilman and Garrett, 1994). This bias probably reflects, to some extent, the large-scale global ocean heat budget closure problem which is similar in magnitude and remains to be resolved (Josey et al., 1999; Gulev et al., 2010). However, some aspects of the Mediterranean closure problem are likely due to more specific issues, in particular estimates of the radiative fluxes. Bignami et al. (1995) developed an empirical longwave flux formula specifically for the Mediterranean which results in stronger net longwave loss compared to formulae developed for the North Atlantic (Josey et al., 2003). Gilman and Garrett (1994) note that estimates of the shortwave flux need to be corrected for the effects of aerosols.

	Q_{SW}	Q_{LW}	Q_{SH}	Q_{LH}	Q_{NET}
In situ (NOCS)	185	-84	-7	-89	+5
Satellite (ISCCP+ HOAPS)	187	-76	-14	-90	+7
Sanchez-Gomez et al., 2011	185	-84	-14	-90	-3
ARPERA	188	-83	-12	-108	-15
Corrected-ERA40	178	-79	-14	-92	-7
ENSEMBLES RCMs (ensemble average)	181	-75	-100	-13	-9
ENSEMBLES RCMs (intermodel ranges)	154÷214	-70÷ -100	-8÷ -22	-85÷ -128	+21÷ -40

Table 4.2: Net heat budget (in W m^{-2}) of the Mediterranean from different sources, in-situ data (NOCS, Mediterranean version, Sanchez-Gomez et al., 2011), satellite products (ISCCP-FD for Q_{SW} and Q_{LW}, HOAPS for Q_{LH} and Q_{SH}, computed by Dubois et al., 2010), the best estimate obtained by Sanchez-Gomez et al. (2011) combining in-situ and satellite products, the ARPERA DDS, a corrected method applied to the ERA40 reanalysis (Pettenuzzo et al., 2010), the ENSEMBLES project ERA40-driven RCMs average and ranges (without spectral nudging, 12 models at 25 km, from Sanchez-Gomez et al., 2011, period 1958-2001).

These issues have been addressed in a modified version of the ship-based National Oceanography Centre (NOC) flux dataset produced by Josey et al. (1999) and the resulting heat budget discussed in Sanchez-Gomez et al. (2011). Individual components are listed in Table 4.2, giving a basin mean net heat flux, Q_{NET}, of 5 W m^{-2}; thus, the discrepancy with the Gibraltar transport has been reduced to about 10 W m^{-2}. This value is still too large but it is difficult to see how further significant changes can be made to the radiative fluxes, and it is likely that corrections to the latent and sensible heat flux will be required. One of the issues here may be that small scale, intense heat loss processes are not well represented in products based on ship observation. A recent evaluation of an ensemble of regional climate models, with a better representation of these processes reveals an ensemble mean value for the net heat flux of -9 W m^{-2} which is within 4 W m^{-2} of the transport derived value (Sanchez-Gomez et al., 2011).

Another source of higher-resolution air-sea flux estimates are satellite-derived products. The highest resolution available for the latent and sensible heat flux is the HOAPS-G (www.hoaps.org) datasets with a 0.5°x0.5° resolution (1987-2005). This product covers only 100% sea points, that are not affected by land values during the satellite data retrieval. Consequently, HOAPS does not give information on areas too close to the coast line or tho the islands and finally itonly gives an estimate covering a total sea surface of 1.15 x 10^{12} m^2, that is to say less than 50% of the total sea surface (see for example Romanou et al., 2010). In addition, it is not yet possible to obtain reliable retrievals of the near surface air temperature from satellites and some concerns remain over the accuracy of near surface humidity (Gulev et al., 2010). In the absence of air temperature measurements, for HOAPS it has been necessary to infer a value from the specific humidity, assuming that the relative humidity is constant (80% is used by Grassl et al., 2000). This approach may introduce biases in the air temperature which then impact on the sensible heat flux, which is critically dependent on the sea-air temperature difference. In particular, if a value of 80% is too high, the inferred air temperature will be too low, and thus the sensible heat flux will be overestimated. With these limits in mind, the spatial average values obtained from HOAPS are slightly higher than NOC for Q_{LH} (-90 ± 4 W m^{-2}) and twice as strong for Q_{SH} (-14 ± 1 W m^{-2}). Adding these turbulent fluxes to the radiative values estimates from the NOC dataset, Sanchez-Gomez et al. (2011) obtain Q_{NET}=-3 W m^{-2} which is more in agreement with the net Gibraltar heat transport, even if it should be viewed with caution. A review of satellite and in-situ datasets to compute surface heat budget is available in Dubois et al. (2010).

Recently, Pettenuzzo et al. (2010) tried to solve the heat budget closure, modifying the atmosphere and ocean variables of ERA40 and applying bulk formulae to compute the fluxes. The modified version of ERA40 is based on reliable in-situ and satellite datasets and it allows to close the heat budget with Q_{NET}=-7 W m^{-2} (see Table 4.2 for the components). The weaknesses of this correction method stands in the uncertainty of the calibration coefficient and in the final spatial resolution of the modified product (still 125 km as in ERA40).

Closure of the basin mean freshwater budget provides an additional constraint on the magnitude of the latent heat flux (Gilman and Garrett, 1994). However, precipitation data contain large errors and consequently this field is known with insufficient accuracy to allow the freshwater constraint to be usefully applied as an evaluation tool at present (Sanchez-Gomez et al., 2011). Indeed a more than 100% error still remains for example between the satellite-based GPCP estimates

(Adler et al., 2003) with a mean value of 1.6 ± 0.1 mm day^{-1} (1979-2008) and the satellite-based HOAPS estimates with a mean value of 0.7 ± 0.1 mm day^{-1} (1988-2005) following Dubois et al. (2010). Those authors took into account the HOAPS evaporation (-3.1 mm day^{-1}) and precipitation (0.7 mm day^{-1}) estimates, the river runoff estimate from Ludwig et al., 2009, (0.4 mm day^{-1}) and the Black Sea freshwater input from Stanev et al., 2000, (0.2 mm day^{-1}), to reach a net surface freshwater budget of -1.8 mm/d that is equivalent to about +0.05 Sv for the Gibraltar net water transport, in agreement with recent estimates (see also Sections 3.2 and 3.3 on related issues). Although, unfortunately also for evaporation estimates large errors still remain and thus it is not possible to draw reliable conclusions about trends in this variable. Consequently, we cannot state whether E-P-R has increased significantly in recent years (see also Section 3.2 for R and P).

3.1.2. Climatological mean air-sea flux fields

Climatological mean fields of the air-sea flux terms are available from a variety of datasets (see e.g. Josey, 2003 for heat flux; Myers et al., 1998 for wind stress and Aznar et al., 2010 or Sanchez-Gomez et al., 2011 for precipitation). Here, we show the components and the net heat flux from the ARPERA model (Herrmann and Somot, 2008; Tsimplis et al., 2009; Aznar et al., 2010; Beuvier et al., 2010; Herrmann et al., 2010; Josey et al., 2011; see also Table 4.2) to highlight the main features (Fig. 4.8). We choose to show these fields as they are similar to observational datasets at large scales but also reveal small scale features, which we anticipate would be present in the observations if sufficient data were available. The ARPERA fields have been obtained by a dynamical downscaling of the ERA40 reanalysis using the regional climate model ARPEGE-Climate, at a resolution of 0.5° x 0.5°, while observation based products are typically at 1°x1° or greater. has been extended recently to cover the period 1958-2008 (using ECMWF analysis after year 2001). Fig. 4.8 reveals that the net heat flux field is largely determined by the balance between Q_{SW} and Q_{LH}. The Q_{SW} field has a primarily north-south variation while Q_{LH} shows particularly strong heat loss in the Gulf of Lions and Aegean. Note the jet like structure of the most intense latent heat loss in the EMED which probably reflects orographic control of the wind. Q_{SH} is typically much weaker than Q_{LH} (note the difference in scales) and Q_{LW} is fairly uniform over the basin. There is a strong seasonal cycle in the components, particularly in Q_{SW} and Q_{LH} (see Sanchez-Gomez et al., 2011, for further details).

The relative importance of the different terms for ocean processes, in particular DWF, has been the subject of much research. Both the heat and freshwater fluxes have the potential to contribute to the buoyancy flux, but it appears that during wintertime heat term is an order of magnitude more important than the freshwater one for buoyancy flux anomalies associated with extreme events such as the WMDW formation (Herrmann and Somot, 2008; Schroeder et al., 2010; Herrmann et al., 2010) or the EMT (Josey, 2003; Beuvier et al., 2010).

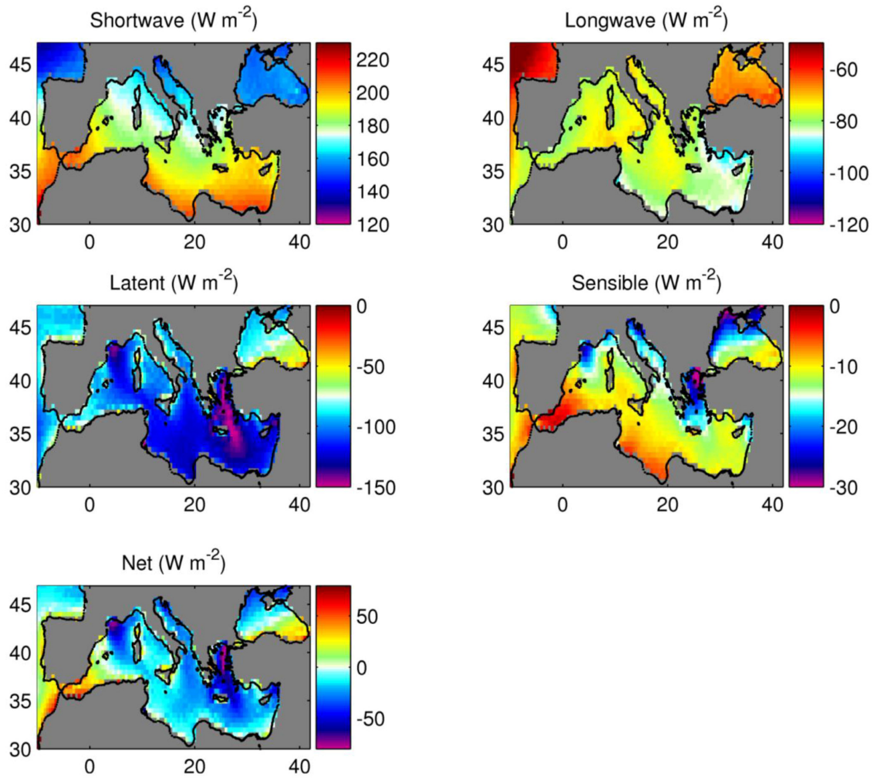

Figure 4.8: Annual mean fields of the heat flux components and the net heat flux from the ARPERA model averaged over the period 1958-2006.

3.1.3. Influence of large-scale modes of atmospheric variability

Large-scale modes of atmospheric variability have been the subject of extensive research over the past few decades. In particular, impacts of the NAO have been recognised in many physical and biological fields over the North Atlantic, Europe and further afield (see Hurrell et al., 2003) and on many variables within the Mediterranean (e.g. sea-level, see Tsimplis and Josey, 2001; Gomis et al., 2006, and Chapter 5). A range of other modes have been determined in various studies. In addition to the NAO, the modes of relevance for the Mediterranean region are the East Atlantic pattern (EAP), the Scandinavian pattern (SCAN) and the East Atlantic/West Russian pattern (EA/WR).

The EAP is less well known than the NAO but its importance is becoming recognised, for example through its influence on the WMED and at larger scales in controlling the freshwater flux to the North-East Atlantic (Josey and Marsh, 2005). The WMT (see Section 2.4) has been linked by Schroeder et al. (2010) to the EAP. The relative contributions of the atmospheric modes to the heat budgets of the Mediterranean, and its basins, has been recently determined by Josey et al. (2011) for both winter and summer using NCEP/NCAR and ARPERA. For each mode, winter anomalies dominate the annual mean heat budget. The leading mode, the NAO, has a surprisingly small impact on the full basin winter mean heat budget, < 5 W m^{-2}. In contrast, the EAP has a major effect, 25-30 W m^{-2}, with a slightly stronger impact on the WMED. The SCAN mode has the weakest influence of those considered, while the EA/WR mode plays a significant role generating a dipole in the heat exchange with an approximately equal and opposite signal of 15-20 W m^{-2} on the EMED and WMED. Josey et al. (2011) also find that extreme winter surface heat loss at the time of the EMT is primarily related to the EA/WR pattern. In addition to its impact on the heat flux, this mode has been recognised as having an impact on rainfall (Krichak and Alpert, 2005).

Further research is needed with regard to other specific patterns which may also prove to be significant for the region. Hatzaki et al. (2007, 2009) have defined an Eastern Mediterranean Teleconnection Pattern with poles over the NW Atlantic and EMED, which might influence temperature and precipitation in the EMED. Likewise, a North Sea - Caspian pattern has been defined by Kutiel et al. (2002) and also shown to influence EMED temperature.

In a regional model study (1961-1999 period), Somot (2005) found significant negative correlations between the winter NAO index (based on the difference of normalized sea-level pressure between Lisbon and Stykkisholmur/Reykjavik) and the winter-averaged heat and buoyancy loss over the Gulf of Lions and the associated WMDW formation rate, confirming the results by Vignudelli et al. (1999) and Rixen et al. (2005). However, despite the statistically significant correlations, the NAO explains less than half of the interannual variance of the processes, 17% for heat loss, 32% for wind stress and 30% for DWF rate. Contrary to the Gulf of Lions case, it has been shown that this correlation, though negative, is very weak at the basin scale (Pettenuzzo et al., 2010).

3.1.4. Regional modeling/dynamical downscaling perspective

Forcing 3D models with outputs of low-resolution reanalyses do not allow a good representation of the various water mass formation processes and some key elements of its surface circulation. For example, the WMDW formation and the EMT event cannot be simulated using ERA40 forcings without ad-hoc corrections (Herrmann et al., 2008b; Herrmann and Somot, 2008; Somot and Colin 2008; Sannino et al., 2009b). The ERA40 weaknesses seem to be too low shortwave and latent heat flux (Pettenuzzo et al., 2010) mainly due to underestimation of the surface wind (Ruti et al., 2007; Herrmann and Somot, 2008; Pettenuzzo et al., 2010) and underestimation of extreme windy events (Herrmann and Somot, 2008; Herrmann and Somot, 2011). The idea of performing Dynamical DownScaling (DDS) of the reanalyses consequently emerged, targeting a resolution of 50 km for the whole sea and 10 km for some specific regions (Langlais et al., 2009; Lebeaupin-Brossier et al., 2011; Herrmann and Somot, 2011). The impact of increasing the resolution is seen in the mean wind field and in extreme wind events, where it leads to more extreme values of momentum, heat and water fluxes (Herrmann and Somot, 2008; Josey et al., 2011), with strong impacts on DWF, as demonstrated in the Gulf of Lions (Herrmann and Somot, 2008), for long-term WMDW formation (Herrmann et al., 2010) and for the EMT (Somot and Colin, 2008; Beuvier et al., 2010).

The added value of the DDS has been demonstrated for the representation of extreme wind and air-sea fluxes and for simulating DWF, but large uncertainties remain regarding the choice of the regional model used for downscaling. Comparison of different downscalings of a given reanalysis still leads to a wide range of uncertainty as shown by Sanchez-Gomez et al. (2009) and Sanchez-Gomez et al. (2011). For example, the state-of-the-art European ERA40-driven RCMs compared within the FP6 ENSEMBLES project (http://ensembles-eu.metoffice.com/) give results between 420 and 720 mm/yr for the freshwater budget and +21 and –40 W m^{-2} for the heat budget (see Table 4.2). Another approach under development is the use of the coupled atmosphere-ocean DDS (Somot et al., 2008; Artale et al., 2009; FP6 CIRCE project) or the Regional Climate System DDS, including the feedback of rivers. Both techniques have the potential to ensure a better consistency of the budgets at the air-sea interface.

The basin mean heat budgets for the various datasets discussed previously together with results from various RCM ensembles are summarised in Table 4.2 (see also Chapter 8). Assuming that the sea is not warming or cooling over a long period of time (over the 1950-2000 period, the warming rate is equivalent to less than 0.5 W m^{-2} for the whole Mediterranean Sea, see Rixen et al., 2005), the surface heat budget that should compensate the Gibraltar net heat transport, discussed in Section 3.3, is estimated to be -5 W m^{-2} (MacDonald et al., 1994).

Recall from 3.1.1, that Sanchez-Gomez et al. (2011) showed that by combining the Q_{SW} and Q_{LW} from NOCS and the Q_{LH} and Q_{SH} from HOAPS the net heat flux becomes -3 W m^{-2} in agreement with the Gibraltar Strait estimate. We now consider the model based values. ARPERA shows a nearly balanced heat budget with slightly too much heat loss, mainly due to overestimated latent heat loss. The 12 ENSEMBLES RCMs driven by ERA40 at 25 km have a huge spread for the various components, showing that the physical parameterizations that are different from one model to another play a major role in determining the air-sea fluxes over the Mediterranean area. It is worth noting that the basin mean heat budget ranges from +21 W m^{-2} to -40 W m^{-2} for the non coupled RCMs in ENSEMBLES and this could lead to very different behaviour if an ocean model is forced by such fluxes. This means that the choice of the RCM is a key element when performing a DDS to force a Mediterranean Sea model. If a DDS can bring an added value in the representation of wind and extreme air-sea fluxes, it can also retain value with respect to the reanalysis.

3.2. The river runoff

Freshwater inputs contribute to drive the thermohaline circulation of the Mediterranean Sea. In particular, river runoff links the continental climate to the circulation of the sea, which is at the same time affected by changes in the anthropogenic use of freshwater.

Signatures of important past changes in hydrology and global climate over the last half million years can be found in the sapropel layers of the eastern basin sediments, thus witnessing past variability in DWF processes due to variations in freshwater inputs (Bethoux and Gentili, 1999). But also during more recent times, changes in the river inputs could have impacted the circulation patterns in the Mediterranean Sea. Skliris et al. (2007) demonstrated by modeling that reductions in the riverine freshwater supply can cause greater DWF rates. These authors focused on the reductions of the river inputs due to the damming of large rivers, such as the Nile and the Ebro. On the other hand, Somot et al. (2006) showed in a transient climate change simulation that increasing surface salinities related to reduced freshwater inputs could be counteracted by thermal induced lowering of the surface densities, which, in combination, could even provoke a decrease of the DWF rates towards the end of the 21st century (see Chapter 8). Further research is therefore needed to quantify accurately the past and to foresee the possible future changes in the riverine freshwater inputs in order to assess their impacts on the circulation patterns in the Mediterranean Sea. As a consequence, any attempt of detecting changes in river runoff must take into account the complex interconnections between human activities, environmental driving forces and climatic factors. In particular the damming of rivers received considerable attention because of the sudden reductions of river runoff this can induce. Skliris et al. (2007), in their study, quantified the runoff reductions related to damming of the Nile and Ebro to more than 100 km^3 yr^{-1}, which represents a considerable part of the total Mediterranean freshwater budget from rivers (see below). But this value is likely to be exaggerated. In particular the effect of the Aswan High Dam on the Nile discharge has been overestimated, as the authors compared its present-day runoff at the mouth (< 2.5 km^3 yr^{-1}) with the natural long-term discharge at Aswan (about 83 km^3 yr^{-1}). The water is here still far away from the sea and anthropogenic water use in the lower Nile has a long history. Moreover, according to Nixon (2003) by far most of the Nile water now reaches the sea through the numerous drainage canals in the Nile delta (about 12.5 km^3 yr^{-1}) and not directly through the river mouth. The same author reports that the reduction of the Nile discharge after the commissioning of the Aswan High Dam may be estimated to less than 30 km^3 yr^{-1} (see Fig. 4.9).

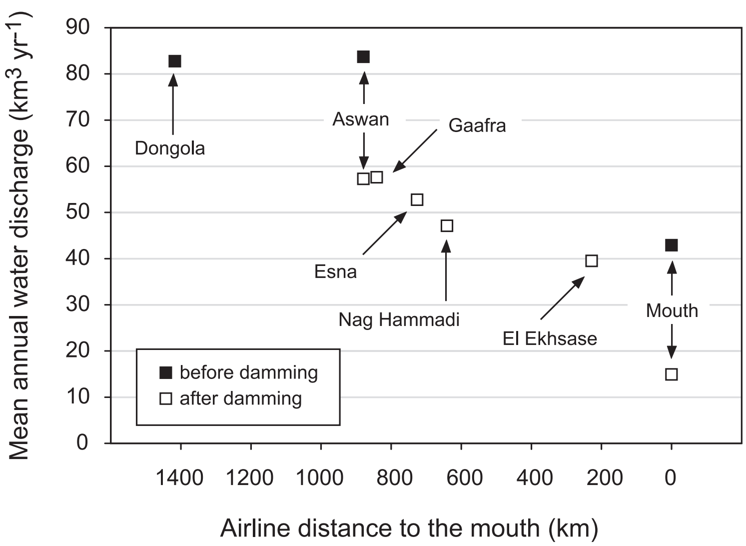

Figure 4.9: Average water discharge at different gauging stations along the Nile River before and after commissioning of the Aswan High Dam. Data are from Vörösmarty et al. (1998) except those for the river mouth, which come from Nixon (2003).

Climate change, on the other hand, may also have had a considerable impact on freshwater discharges from rivers. Recent works have focused on the detection of climate change induced trends in the Mediterranean area, including river runoff. Ludwig et al. (2003, 2009) performed trend analyses on a series of 37 Mediterranean and Black Sea rivers for which at least 20 years of observed river discharge data were available. Beside the two largest rivers in the north (Rhone and Po), for which the discharge remained constant, most of the Mediterranean rivers reveal strong negative trends since the early 60s, indicating that the decrease in freshwater discharges is a general phenomenon in the Mediterranean drainage basin. Strongest negative trends appear for rivers that were affected by the construction of dams, such as the Ebro River in Spain and the Moulouya River in Morocco. However, in most cases when runoff declined, also the corresponding precipitation values follow a significant negative trend (Ludwig et al., 2010). Decreasing precipitation trends during the second half of the last century have been detected as a general pattern in the Mediterranean region (e.g. Xoplaki et al., 2004). They are consistent with a clear positive trend of the NAO index in winter from the 60s to the end of the last century. NAO is generally known for its anti-correlation with river discharge in the Mediterranean area (Shorthouse and Arnell, 1997; Struglia et al., 2004) and the considered period spans from years characterized by a strong negative value of the index to years when the greatest positive values have been recorded. Similar results have been obtained by Mariotti et al. (2008), who compared precipitation anomalies, discharge anomalies and the Palmer Drought Severity Index (PDSI) over the Mediterranean area. A weak negative trend was observed in two different precipitation datasets while the CRU/PRECL data shows no trend. A more evident negative trend appeared in the PDSI due to the combination of changes in precipitation and surface temperature. The most evident changes have been found in the river discharge anomalies relative to the period 1960-1980, which is likely characterized by intensification of anthropogenic water use as well.

Unfortunately, an exhaustive data analysis of the Mediterranean river discharge is impaired by the lack of data, mainly from rivers in the south-eastern parts of the basin. This fact, together with the necessities of both climate change and impact studies, has fostered the development of alternative methods of estimating large-scale budgets for present and future climate conditions. Some are based on empirical relations between runoff, precipitation and temperature fields, while others focused on the surface integration of the runoff fields produced by climate models or on the development of macro-scale hydrological models. Ludwig et al. (2009) proposed an extrapolation of the runoff evolution during the 1960-2000 period for the major regional drainage basins of the Mediterranean and Black Sea by combining observations and empirical modeling. For all river basins and years for which observations were missing, the corresponding water discharge was estimated via the empirical formula of Pike (1964). The latter was originally developed to predict annual runoff for large catchments in Malawi on the basis of annual precipitation and temperature data, but was also found to provide realistic estimates in many river basins of the Mediterranean climate type. This approach resulted in an estimated reduction of the total freshwater discharge to the Mediterranean Sea of almost 90 km^3 yr^{-1} between 1960 and 2000 (from about 390 to 305 km^3 yr^{-1}). This reduction is rather a minimal estimate, as it does not account for additional reductions in many ungauged rivers related to damming and anthropogenic water extractions. Greatest reductions appeared for the drainage basins of the Alboran, the south-western Mediterranean, the southern Levantine and Aegean subbasins. In the latter, the strongest reductions were observed from the early 80s to the early 90s (see Fig. 4.10) and may hence also have contributed to the preconditioning of the Aegean surface waters that eventually triggered the EMT in this area.

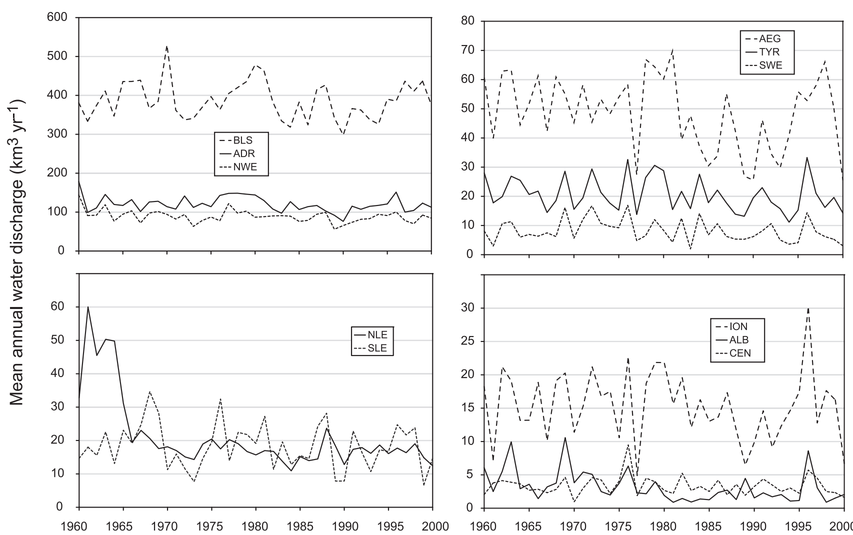

Figure 4.10: Evolution of freshwater inputs from rivers to major subbasins of the Mediterranean and the Black Sea according to Ludwig et al. (2009): Alboran (ALB), south-western Mediterranean (SWE), north-western Mediterranean (NWE), Tyrrhenian (TYR), Adriatic (ADR), Ionian (ION), Central Mediterranean (CEN), Aegean (AEG), northern Levantine (NLE), southern Levantine (SLE), Black Sea (BLS).

Alternatively, general circulation models (GCM) currently produce river runoff as an output of their soil-vegetation parameterization. The appropriate integration of such field over the catchment area of interest allows an estimate of the discharge at the river mouth. Lucarini et al. (2007, 2008) analyzed this way the discharge of the Danube river both under present climate conditions and future scenarios on the basis of different regional and global climate models. The simulated discharges were of the same order of magnitude as observations, with the true value lying in the spread of the models, even if the ensemble mean value underestimated the observed value by 11% (Lucarini et al., 2008). Elguindi et al. (2009) used the ARPEGE model to evaluate the hydrological balance of the Mediterranean Sea and to estimate the discharge of the major Mediterranean and Black Sea rivers (Ebro, Po, Rhone and Danube) through integration of the modeled runoff fields. Their estimates reproduced the observed mean annual discharge in the large rivers with an accuracy spanning from 1% (Danube) to 25% (Po). But they also demonstrated that in the Mediterranean region, accurate runoff estimations from GCMs still suffer from their coarse spatial resolutions.

Finally, also macro scale hydrological models have been developed to link GCMs to the hydrological cycle on land. They generally simulate the stream flow through partitioning of the incoming precipitation and snow melt into evapo-transpiration, soil moisture, surface flow and deep flow, according to the assumed vegetation and soil characteristics. They can be calibrated against measurements or not (Nijssen et al., 2001; Arnell, 2003), and may be coupled to both reservoir models and routing models (Hamlet and Lettenmaier, 1999). However the use of a routing scheme is not mandatory unless it is necessary to detect changes in streamflow at definite locations along the river network. It appears to be necessary when the relevant time scales for the climatic studies (i.e. monthly means) are shorter than those typical of water transport in the catchment, that is for huge catchment areas. Mediterranean rivers have medium size catchments, so that a routing scheme is redundant for many climatic applications, whereas it might prove useful for the prescription of freshwater fluxes to ocean models, depending on the model sensitivity to such forcing. A routing scheme is obviously necessary in any attempt to disaggregate the river discharge signal into a reliable runoff field, as done in Fekete et al. (2002).

Unfortunately, the application of these models suffers from the difficulty of defining the model parameters that allows them to be spread at large spatial scales without specific calibrations, in particular in complex drainage basins such as those of the Mediterranean. Their application has so far been limited either to global studies or to large catchment areas, largely excluding the Mediterranean region as a specific study region for this type of modeling approach.

3.3. The exchanges through the Strait of Gibraltar

The Strait of Gibraltar, the beginning and end of the open MTHC cell, has a tortuous bottom topography that propitiates a quite complex internal dynamics. Its strategic position makes it a very suitable place for monitoring the widely reported changes in the properties of MWs inside the sea (Millot et al., 2006; García-Lafuente et al., 2007, 2009) and, recently, also changes in those of AW (Millot, 2007) that could influence the DWF in the next future. As already mentioned, the topography of the strait is a key point in the functioning of the Mediterranean; of particular importance is the presence of Camarinal sill (CS, Fig. 4.11), very shallow (297 m) when compared with the several hundred meters thickness of the intermediate MWs layers circulating in the Alboran subbasin and the maximum depths in the western basin (nearly 4000 m). Obviously, it hampers the ventilation of the deeper MWs that reside well below the sill depth.

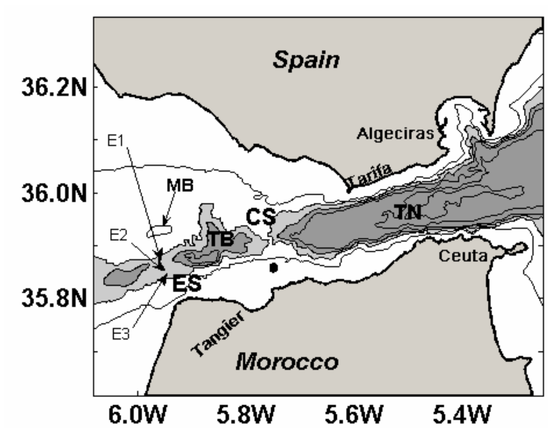

Figure 4.11: Map of the Strait of Gibraltar showing the main topographic features: TN is Tarifa narrows, the narrowest section (14 km), CS and ES indicate the sills of Camarinal (297 m) and Espartel (360 m). TB is the Tangier basin and MB indicates a seamount (Majuan Bank) that rises to 60 m depth. Isobath-depths are 100 m, 290 m (light-shaded area to highlight the maximum depth of 297 in CS), 400 m (medium-dashed contour), and 500 m, 700 m and 900 m, which are not labeled for the sake of clearness. Arrows point at mooring positions commented in the text. Black dot in CS south indicates a specific monitoring site on the Moroccan shelf.

A second key point is the existence of tides that change dramatically the picture of a steady two-way exchange. For instance, the amplitude of the M2 flow is ~3 Sv (Bryden et al., 1994; García-Lafuente et al., 2000), four times greater than the mean flow, and it produces generalized flow reversals (Sannino et al., 2004). The actual exchange is pulsating: large volumes of MWs cross CS towards the Atlantic during the flood tide that accumulates in the Tangier basin (TB, Fig. 4.11) because the rate of drainage through Espartel sill (ES, Fig. 4.11) is lower than at CS. Recently (Sannino et al., 2007, 2009a; Sánchez-Román et al., 2009) ES has been recognized as a fundamental topographic feature because hydraulic control of the outflow is nearly permanent there. This in turn produces the flooding of the CS control, the outflow reversal during part of the ebb and the release of the large amplitude internal jump formed in the TB nearly twice a day (Armi and Farmer, 1988; Sánchez-Garrido et al., 2008). MWs accumulated in the TB go on flowing through the ES control section rather smoothly but also back to the Mediterranean when the CS control is lost. The next ebb tide carries AW over CS to the east that remains controlled at the hydraulic control of Tarifa Narrows (TN, Fig. 4.11) (García-Lafuente et al., 2000; Sannino et al., 2004), that plays a similar role with the inflow as ES with the outflow. According to results presentd by Bryden et al. (1994), García-Lafuente et al. (2000) and Sánchez-Román et al. (2009), hydraulic controls reduce the tidal signal at the two effective ends of the strait to around 20% of CS value in the inflow at the east and to 27% of CS value in the outflow at ES, so that the strong pulsating nature of the exchange found at CS is quickly smoothed within the dimensions of the strait. Controls not only damp tidal signals but also enhance mixing within the internal hydraulic jump in the TB during the flood and in the large amplitude internal waves propagating towards the Mediterranean at the other half of the strait (Sannino et al., 2004). Further, as more deeply discussed in Chapter 5 (Section 5.7) the sea-level slope along and across the Strait of Gibraltar is linked with the type of exchange, in particular with whether it is maximal or submaximal.

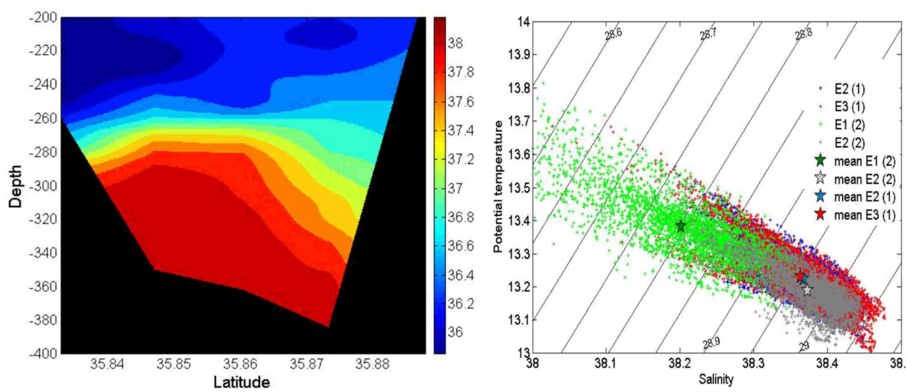

Figure 4.12: (Left panel) Salinity cross-section at 5.98ºW, 2 km to the west of the monitoring section indicated by the three arrows labeled E1, E2 and E3 in Fig. 4.11, for depths greater than 200 m. (Right panel) θ-S diagram of observations collected at E1 (350 m) and E2 (345 m) in March-June 2008 (number 2 within brackets in the legend) and E2 (345 m) and E3 (312 m) in November 2007-February 2008 (number 1 within brackets). Stars indicate mean values.

Strong tidal currents over CS are a source of potential energy available for uplifting MWs from depths as large as 800-1000 m by Bernoulli aspiration, (Bryden and Stommel, 1982; Whitehead, 1985; Kinder and Bryden, 1990). The bottom depth of the strait at its Mediterranean side is around 900 m (Fig. 4.11) so that the whole layer of MWs in its eastern approach can be effectively ventilated by Bernoulli aspiration over CS. The suction is obviously coupled to tidal dynamics so that a parcel of MW at the eastern end of the strait prone to leave the sea moves back and forth for two or three tidal cycles before surpassing CS and entering the TB where it can spend two more cycles before eventually flowing out through ES to the open ocean.

Several MWs are distinguished in the eastern part of the strait. A reanalysis of the Gibraltar Experiment data carried out by Millot (2009) shows the presence of different MWs close to the strait in the Alboran: WIW, LIW, TDW and WMDW. In the northern part of the section, the WIW core (at 150-200 m) is above the LIW one (at around 450 m). Deep waters beneath showed preference to be banked against the African slope (Bryden and Stommel, 1982; Parrilla et al., 1986) at depths lower than 700 m and even just below AW (Millot, 2009). A very similar latitudinal differentiation with only minor changes in the properties of each of the MWs is maintained to the west inside the strait (Millot, 2009), suggesting very reduced mixing among them during their initial phase of progression to the west. The spatial cross-strait distribution appears to be maintained until the CS section at least (Millot et al., 2006; Millot, 2009). The periodic formation of internal hydraulic jumps (Armi and Farmer, 1988; Sannino et al., 2004, 2007, 2009a) or other energetic features such as lee waves (Bruno et al., 2002) in the TB drives intense diapycnal vertical mixing that entrains AW into the Mediterranean layer and erodes largely the specific properties of the different MWs. For instance, the proportion of AW in the near-bottom layer of the outflow increases from 2% at CS to 5-6 % at ES due to the tidally driven mixing and entrainment in the TB (García-Lafuente et al., 2007). The left panel of Fig. 4.12 shows that salinity below 260 m depth increases southwards in ES, in contrast with the spatial pattern east of CS where LIW leaves a local salinity maximum along the northern shelf (Millot, 2009). LIW signature in ES has been eroded by mixing that appears to be enhanced in the northern part judging from the vertical spreading of isohalines visible at the right side of Fig. 4.12 (left panel). The right panel of Fig. 4.12 confirms that waters north of ES but still south of the MB ridge (site E1, see Fig. 4.11) are fresher than in the center or south (sites E2 and E3), a freshening that Millot (2009) ascribes to an important presence of WIW, and that exhibit larger fluctuations. The TB seems to be the first site where MWs experience relevant transformations, cancelling out their hydrological differences, although, according to Millot (2009) they still preserve differences at 6.25ºW, 27 km west of ES, where they lead to a splitting of the outflow into veins.

While intermediate MWs in the Alboran lay at depths from which they can flow relatively easily over CS, deep MWs take advantage of the primary source of energy provided by tides to be uplifted and advected over the sill. However, Millot (2009) points out that intermediate MWs in the Alboran flow faster than deep ones, which makes the interface between them sloping up southwards, hence uplifting the latter up close to the CS. There are processes such as the winter formation of WMDW that periodically raises the interface between deep and intermediate waters making the former more easily available for either suction (García-Lafuente et al., 2007, 2009) or lifting. There are also mechanisms that modulate tidal energy and modify the maximum depth from which deep waters can be aspired, the most obvious one being the spring-neap tidal cycle that uplift deeper waters during spring tides (Kinder and Bryden, 1990) and induce variations in the properties of the outflow. Another mechanism acting on the same time scale of a few days is the meteorological forcing over the Mediterranean basin (Candela et al., 1989) that modifies the exchanged volumes substantially on the short term (García-Lafuente et al., 2002) as well as the properties of inflow (NACW vs. ASW) and outflow due to mixing, as illustrated by Millot (2008). The outflow increase that follows the rise of atmospheric pressure over the WMED is achieved by the increase of the averaged outflowing velocity and the upwards motion of the interface (García-Lafuente et al., 2002). The former enhances flood tidal currents that now are able to aspire deeper waters from the eastern approach of the strait. García-Lafuente et al (2009) found significant positive correlations between near-bottom temperature in ES and the meteorologically forced fluctuations of the outflowing velocity in the same location. The effect of the WMED replenishment by deep convection of WMDW on the properties of the outflow of MWs at Gibraltar has been illustrated in García-Lafuente et al. (2007) for winters 2004/05 and 2005/06 when not only large volumes but also high-density newly formed WMDW filled the deepest part of the basin (Lopez-Jurado et al., 2005; Schroeder et al., 2006, 2008b; Smith et al., 2008; see also Section 2.4). Old resident WMDW-TDW waters were uplifted to depths from which they could be drained away leaving clear cold signatures in the outflow shortly after the time of deep convection. Another mechanism invoked in García-Lafuente et al. (2009) to induce variability of the outflow properties is the existence of a well developed western Alboran gyre that would favour the motion of deep waters towards the eastern entrance of the strait in the southern part of the Alboran (where WMDW prevails) but hamper the advance of LIW in the north. Vargas-Yáñez et al. (2002) showed that summer is the most favorable season for well-developed gyres and, hence, for a better ventilation of deep MWs if this mechanism is actually working.

According to Criado-Aldeanueva et al. (2006) and Peliz et al. (2009) the AW inflow comes from the northern half of the Gulf of Cadiz following two different paths, one along the continental Iberian slope, probably the main contributor of ASW, and a second one offshore that carries water from the middle of the gulf, which would be the main source of NACW in the inflow. The likely presence of hydraulic control in TN (Sannino et al., 2004, 2007, 2009a) limits the size of the inflow and propitiates mixing with the MWs countercurrent, which originates the first important modification of AW along its path in the upper branch of the Mediterranean open thermohaline cell. In the vicinity of CS (see black dot in Fig. 4.11) Millot (2007) showed a notable salinity increase of 0.2 in the AW between 2003 and 2007, superimposed on a seasonal signal of ~0.1 amplitude. The site was chosen to monitor AW since the Atlantic layer is thicker there and, additionally, diapycnal mixing seems to be less intense than in the north (Fig. 4.12, right panel). The increase corresponds to a trend of 0.05 yr^{-1} that must be ascribed to changes in the source of AW rather than to the internal hydraulics of the strait. The observed short-term trend is more than one order of magnitude greater than the trend observed in the MWs (Rixen et al., 2005), suggesting that it cannot be a long-term sustained trend but rather the result of a interannual-decadal fluctuations of the inflow properties (Millot, 2007). A recent paper by Grignon et al. (2010) shows a considerable increase of the surface layer salinity in the Ligurian subbasin, which is strikingly similar to that observed in the strait. The trend is more apparent from 2004 onwards, a year later than in the strait, which would reinforce the common origin of both signals taking into account the time a parcel of AW crossing the strait would take to arrive at the northern Ligurian. If so and judging from the pre-2003 evolution at the Ligurian site, the change observed in CS would be the result of a multi-year cycle whose rising phase started the same year as the observations in Millot’s (2007) paper. The origin of this fluctuation is not clear; it could be linked to changes in the pattern of large-scale features in North Atlantic such as the position of the North Atlantic subtropical gyre or that of the Canary current, or to more local phenomena in the Gulf of Cadiz such as a thickening of the surface layer. For instance, if the depth of the interface at ES (around 200 m, Sánchez-Román et al., 2009) is taken as representative of the depth from which NACW in the Gulf of Cadiz feeds the inflow, a thickening of the ASW layer accompanied by an eventual sinking of NACW in this source region would leave slightly saltier NACW at this depth that would participate in the observed salinity change on the Moroccan shelf station in CS. The reasoning is quite speculative and further research is obviously required to explain the origin of this noticeable short term salinity change.

The outflow at Gibraltar has been monitored since 2004 by means of an uplooking ADCP located at ES. The long time series of horizontal velocity at different levels allows for new computations of the outflow (Sánchez-Román et al., 2009). These authors indicate a mean outflow of –0.78 Sv after carrying out some corrections arising from experimental limitations and the splitting of the ES section bathymetry into two channels north and south of MB (Fig. 4.11). The error estimate of this value is somewhat meaningless due to the large fluctuations at different time scales; as a reference, Sánchez-Roman et al. (2009) estimate a standard deviation of 0.37 Sv in the time series of instantaneous outflow that reduces to 0.13 Sv if tides are removed (meteorological variability). Soto-Navarro et al. (2010) using the same set of observations along with atmospheric data over the Mediterranean from reanalysis give the mean values of 0.81±0.06 Sv and –0.78±0.05 Sv for the inflow and outflow, respectively. A final remark to these figures must be done concerning the entrainment of AW by the fast-flowing MW west of CS that makes salinity at ES be slightly lower than at CS. It was already pointed out that AW proportion found at ES is around 3 to 4 % greater than at CS, which in turn implies an outflow at CS smaller than at ES by the same proportion if the outflow salinity transport is to be preserved. As most of the historical, observation-based estimates of the outflow have been computed at CS, the former figures must be reduced by this amount to give a mean of +0.78 Sv and –0.75 Sv for the inflow and outflow, respectively.

3.4. The exchanges with the Black Sea

2.4.1 The Region

The Turkish Straits System (TSS) is a relatively small interior sea (Fig. 4.13) where Asia and Europe embrace the Sea of Marmara (70 x 250 km), opening to the Black Sea and the Aegean through the Bosphorus (length 35 km, minimum width 0.7 km) and the Dardanelles (length 75 km, minimun width 1.3 km) straits, respectively. The Sea of Marmara is a deep basin with three elongated depressions (maximum depth ~1350 m) interconnected by sills (depth ~600 m) and flanked by continental shelves, of 40 and 10 km width, respectively on the south and the north.

2.4.2 Interbasin Coupling and Contrasts

During 1679-1680 Luigi Ferdinando Marsili (1658-1730) made the first quantitative measurements of seawater density en route to Constantinople (İstanbul) from Venice, as well as of density, currents and sea-level in the

Bosphorus, proving the existence of a countercurrent transporting Mediterranean water below the surface current of Black Sea Water (Marsili, 1681).

The contrast in the annual net water budget Q = E – P – R (evaporation – precipitation – river inflow) of the coupled basins results in different water regimes in the Mediterranean (Q > 0) and the Black Sea (Q < 0). Marsili (1681) showed that the resulting density (and hence pressure) differences between the two basins are enough to drive and maintain the exchange through the Bosphorus. However, additional pressure gradients may exist as a response to atmospheric pressure and wind effects in the adjacent basins (Özsoy et al., 1998).

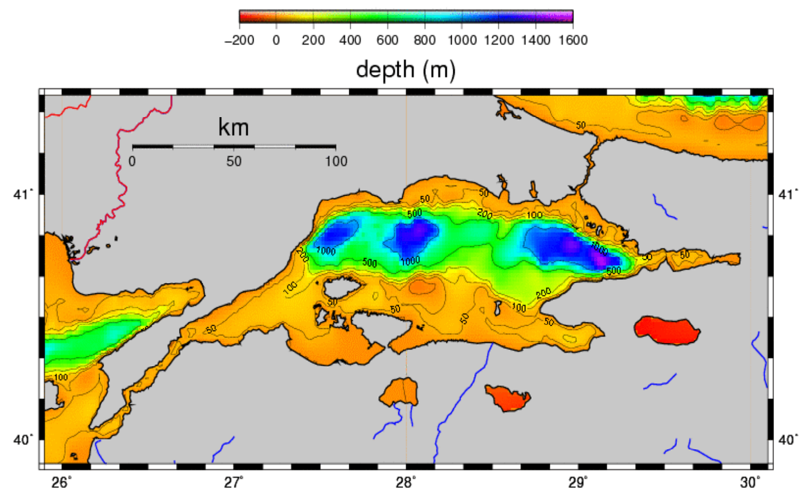

Figure 4.13: Location and bathymetry of the Turkish Straits System.

The TSS is a highly stratified two-layer system, where the sharp pycnocline confines wind-mixing to the upper layer, and restricts ventilation in the lower layer (Andersen and Carmack, 1984). The oxygen supplied to the lower layer by dense water entering from the Dardanelles Strait is just sufficient to prevent the development of anoxia in the deep basins (Beşiktepe et al., 1993, 1994).

Turbulent entrainment and interfacial mixing in the two straits dominate the evolution of the waters in transit (Beşiktepe, et al., 1993, 1994; Gregg and Özsoy, 1999; Gregg et al., 1999; Özsoy et al., 2001). The rate of salinity increase in the upper layer and the slope of the interface are largest in the southern Bosphorus area continuing through the exit to the Marmara Sea, and also in the western part of the Dardanelles Strait. The cold intermediate water of the Black Sea reaches the surface past a hydraulic transition in the southern Bosphorus and partially contributes to the cold-water tongue above the sharp pycnocline formed by winter cooling in the Marmara Sea.

2.4.3 Water Fluxes

Steady state mass balance, making use of average salinity measured at the straits and of water fluxes in the Black and Marmara Seas enables computation of the annual average fluxes from a box model of the TSS (Ünlüata et al., 1990; Beşiktepe et al., 1993, 1994), with an updated seasonal version (Fig. 4.14a) provided by Beşiktepe (2003). In the Black Sea the total freshwater input (P=300 $km^3\ yr^{-1}$ and R=350 $km^3\ yr^{-1}$) is twice as large as the loss term (E=350 $km^3\ yr^{-1}$). The exchange through the TSS increases in the spring-early summer, and weakens markedly in autumn (within a margin of about ±40% of the annual mean) in response to the freshwater input to the Black Sea (Beşiktepe, 2003).

Indirect estimates of the net transport via Bosphorus based on long-term water fluxes and sea-level variations in the Black Sea (Stanev and Peneva, 2002) indicate seasonal anomalies (Fig. 4.14b), with variations of the order of ±75% of the mean, that is considerably larger than the ±40 % estimated by Beşiktepe (2003) from the seasonal based mass budget. These differences arise from data uncertainties as well as differences in the averaging (monthly versus seasonal) applied to the data. However, both methods yield the same general pattern of seasonal variability.

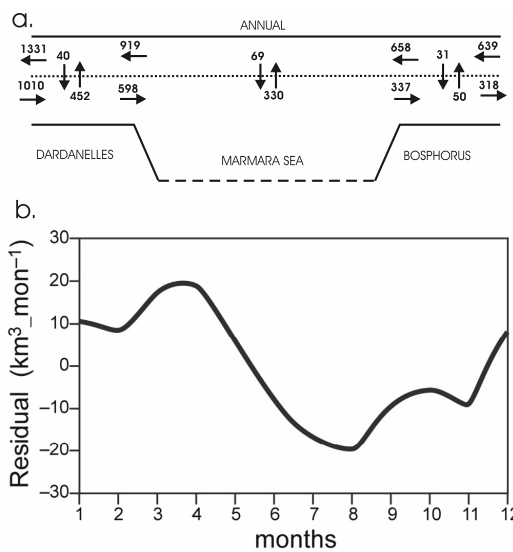

Figure 4.14: (a) Steady-state annual mean fluxes ($km^3\ yr^{-1}$) through the TSS and between its individual compartments (after Beşiktepe, 2003); (b) seasonal anomalies of the net transport through the Bosphorus Strait based on data from 1923-1997 (redrawn from Peneva et al., 2001).

Because runoff estimates consistent with observations could not be obtained from atmospheric models, their use to estimate the Bosphorus transport as a residual of the water budget has had limited success (Georgievski and Stanev, 2006). On the other hand, Grayek et al. (2010), making use of an atmospheric model to force a Black Sea circulation model, obtained consistent reconstructions of seasonal water fluxes and demonstrated a significant negative correlation between basin mean salinity and mean sea-level.

Fluxes computed from ADCP data in the Bosphorus (Özsoy et al., 1996, 1998) show the same seasonal behaviour as reviewed above, but reveal maxima of about $Q_{upper} = 1600$ km^3 yr^{-1} and $Q_{lower} = 630$ km^3 yr^{-1} for the upper and lower layers respectively, including blocked cases, indicating instantaneous fluxes 2-3 times larger than the annual mean. Despite large scatter in data due to sampling, overall average values of $Q_{upper} = 540$ km^3 yr^{-1} and $Q_{lower} = 115$ km^3 yr^{-1} were computed, the latter value possibly being underestimated as a result of data loss near the bottom. Oğuz et al. (1990) showed that the upper or lower layer flow is blocked when the net flux exceeds -580 km^3 yr^{-1} or 800 km^3 yr^{-1}, in their respective directions, the latter estimate being consistent with the results of a two-layer model.

The interbasin exchange through the TSS is sensitive to conditions in the adjacent basins (changes in the net water flux entering the Black Sea, as well as sea-water density, atmospheric forcing and sea-level difference), and on average has to balance the net annual water budget of the coupled system. Because the ratio runoff/basin volume is much larger for the Black Sea compared to the Mediterranean, the TSS water exchange is more sensitive to runoff changes in Black Sea rivers. With a catchment area five times as large as the sea surface area, the Black Sea amplifies global climate signals (Stanev and Peneva, 2002).

The mean residence time varies from a few months for the upper layer, to 7 years for the lower layer of the TSS, to about 100 years for the Mediterranean, and increases from a few years above the permanent halocline, to several thousands of years for the deeper Black Sea (Beşiktepe et al., 1993, 1994; Özsoy and Ünlüata, 1997), emphasizing the multi-scale character of the coupled system.

2.4.4 Strait Dynamics

The vertical profile of horizontal density difference between the adjacent basins is the main driver of the stratified two-layer exchanges through the TSS (Marsili, 1681), although the freshwater excess maintains a barotropic flow, with a higher sea-level in the Black Sea. The exchange is driven by local and remote atmospheric forcing affecting the two connected basins, and influenced by complex non-linear processes of hydraulic controls, dense water overflows, buoyant jets, mixing and entrainment. With hydraulic controls operating at a sill outside its Black Sea exit and a contraction and a sill in the southern part, the Bosphorus is the best example of the maximal exchange regime (Farmer and Armi, 1986), operating in the full range of weak to strong transient barotropic component. The Dardanelles Strait flow appears to be in the submaximal regime, subject to a single hydraulic control at the mid-strait contraction (Ünlüata et al., 1990).

Transient blocking of the Bosphorus exchanges in either layer typically lasts a few days (Ünlüata et al., 1990; Latif et al., 1991; Özsoy et al., 1995, 1996, 1998, 2001, 2002; Özsoy and Ünlüata, 1997, 1998). The lower layer is occasionally blocked in spring and summer, with increased Black Sea influx, mostly under the effect of northerly winds. Upper layer blocking events ('Orkoz') occur with reversal of the net flow under the effect of southerly winds in autumn and winter (Gunnerson and Özturgut, 1974; Ünlüata et al., 1990; Latif et al., 1991), often causing a three-layer situation in the Bosphorus. Oğuz et al. (1990) contended that a sea-level difference of more than 50 cm and less than 10 cm would be needed respectively for the lower or the upper layer to be blocked. Blocking conditions have been successfully created in idealized hydrodynamic models of the Bosphorus (Sözer and Özsoy, 2002). However, the forcing required for blocking events is often not so clear: alternative cases of increased pressure or winds are indicated by concurrent currentmeter, sea-level, wind and pressure records (Özsoy et al., 1998). A 3-D description of the flow with fine details has been provided by Gregg and Özsoy (1999) and Gregg et al. (2002), and unpublished data from automated coastal meteorology, sea-level and ADCP stations (http://moma.ims.metu.edu.tr) are currently being evaluated (Özsoy et al., 2009). Among various modeling efforts discussed elsewhere, there exist two-layers 1-D models of Dardanelles (Oğuz and Sur, 1989) and Bosphorus (Oğuz et al., 1990), 2-D models of Dardanelles (Staschuk and Hutter, 2001) and Bosphorus (Staschuk and Hutter, 2003; Ilicak et al., 2009) and 3-D models of Dardanelles (Kanarska and Maderich, 2008) and Bosphorus (Sözer and Özsoy, 2002; Oğuz, 2005b; Sözer, 2010).

Different sets of current measurements in the Bosphorus (Pektaş, 1953; Gregg and Özsoy, 1999; Özsoy et al., 1998, 2009; Güler et al., 2006; SHOD, 2009) provide details on the variability of the complex current system of the Bosphorus, revealing meandering surface currents and recirculating eddies in bays, including the elongated cell west of the channel near the Golden Horn. The surface flow often accelerates past the contraction, and the current velocity frequently exceeds 1 m s^{-1} in the southern Bosphorus often reaching values of 2-3 m s^{-1} at the southern exit. Similarly, the narrows (Nara Pass) of the Dardanelles Strait exhibit surface currents of about 1 m s^{-1} past this point towards the Aegean. Existing time series show many different time-scales of oscillations in the TSS, including diurnal, inertial and semi-diurnal periods of small amplitude as well as those at 2-7 days periods representing the influence of atmospheric and oceanic motions in the adjacent basins (Yüce, 1993a, b; IMS-METU, 1999).

Besides being a good indicator of climatic fluctuations, sea-level is a sensitive measure of climate in enclosed and semi-enclosed seas driven by large rivers. In the Black Sea, sea-level is controlled by the Bosphorus transport, atmospheric pressure and freshwater fluxes (Özsoy and Ünlüata, 1997, Özsoy et al., 1998). Following the earliest attempts (Marsili, 1681; Möller 1928), modern measurements of sea-level in the Bosphorus (Smith, 1942; Bogdanova, 1965; Çeçen et al., 1981; Gunnerson and Özturgut, 1986; Büyükay, 1989; Alpar and Yüce, 1998) found differences of 30-60 cm across the entire TSS, and 20-40 cm across the Bosphorus. Repeated measurements (Özsoy et al., 1998; Gregg and Özsoy, 1999; Yüksel et al., 2008) have shown 20-60 cm differences across the Bosphorus. Gregg and Özsoy (1999) used the zero-velocity surface and the density distribution to compute the free surface gradients in the Bosphorus, and found the sea-level to change most rapidly near the contraction. This has been later verified by 3-D modeling (Sözer, 2010).

2.4.5 Climate Variability

As a result of hydrological changes and the interaction with the Mediterranean, the Black Sea has a history of recurrent transformation between freshwater lake and sea (Ryan et al., 2003; Eriş et al., 2007; Martin et al., 2007). Present-day conditions appear to have been approached about 3 kyr BP and less intense interbasin interactions are evident today. Frequent observations at the Bosphorus entrance reveal interannual/decadal scale variations of salinity (Özsoy, 1991). Cooling events are often connected in the entire region (Özsoy, 1999, 2001).

As discussed earlier, ventilation reaches effectively the intermediate and deep layers in the Mediterranean. On the other hand, in the Black Sea, surface buoyancy added by the major rivers, negative buoyancy added by the Bosphorus inflow and boundary mixing along the continental slope support a sharp permanent pycnocline (Özsoy and Ünlüata, 1997), limiting ventilation in the almost anoxic deep basin. A series of recent ecosystem changes are known to have occurred in the Black Sea as a result of increased nutrient supply and changes in ventilation rates (Özsoy and Ünlüata, 1997; Oğuz, 2005a).

Correlations of the NAO with sea-level variability and thermal state of the Black Sea (Stanev and Peneva, 2002; Tsimplis et al., 2005) reveal pronounced regional responses to global climatic variability (Lionello et al., 2006). Being smaller than the Black Sea, the Aegean is affected by the surface outflows from the TSS, which is evident in the correlation between near surface salinity in the Aegean and at 50-300 m depth in the Black Sea (Tsimplis et al., 2005), and by large-scale atmospheric patterns (Gündüz and Özsoy, 2004).

3.5. The exchanges between the eastern and the western Mediterranean

The connection between the eastern and the western basins is provided by the Sicily Channel, a topographically complex region comprising two sill systems (530-540 m), separated by an internal deep basin (mean depth 800 m), where several trenches can be deeper than 1700 m. The channel reaches its minimum width (about 140 km) at the western sill. Here, on both the Sicilian and Tunisian sides, there are broad shelves less than 100 m deep, but below 200 m the total width of the passages is less than 35 km. In addition the relevance of the Sicily Channel is related to the fact that the natural decadal variability of the MTHC is related to the amount of water mass that flows through the Sicily Channel, as shown by Artale et al. (2006). Dynamically, the channel is a two-layer system: the upper layer (about 200 m thick) is occupied by the AW and flows eastward, while the deeper layer is composed mainly of LIW and upper EMDW, flowing from east to west.

Topography plays an important role in the flow of both layers. In addition the surface layer is dominated by mesoscale processes, while in the subsurface layers topographic steering prevails, maintaining a rather constant direction of the current. The Coriolis effect induces the upper layer of the EMDW (indicated in the following as transitional EMDW, or tEMDW) to cross the channel mainly on the Tunisian side (Millot, 1999), while Astraldi et al. (2001) pointed out that the significant Bernoulli effect associated with the high LIW velocity further favours the tEMDW outflow to reach the western basin. As pointed out by many authors (Moretti et al., 1993; Astraldi et al., 1999; Robinson et al., 1999; Sammari et al., 1999), in the channel the AW follows different routes, mainly entering close to Tunisia (the freshest vein) or crossing the Adventure Bank. In situ measurements (Gasparini et al., 2003), combined with analyses of infrared and altimeter satellite data (Buongiorno Nardelli et al., 2006, 1999) and surface drifters (Poulain and Zambianchi, 2007), show that mesoscale dynamics play a key role. Because of the high variability and the large spread of its paths, the monitoring of the AW is more difficult and critical then that of the LIW and tEMDW.

In the following the analysis of the AW characteristics in the region is focused on the western sill of the channel: the mean salinity has been estimated in the layer between the surface 100 m depth, along the section Cape Bon-Mazara del

Vallo (Gasparini et al., 2005). Its annual evolution (Fig. 4.15, upper panel) indicates that, for the examined period, the AW maintains almost stable salt content. After a large oscillation during the 90s (S = 37.72 in 1990, decreases to 37.24 in 1992 and subsequently increases to 37.68 in 1999), it evolves with small oscillations around a mean value of 37.6. The comparison with the salt content of the LIW (estimated considering the mean salinity along the same section, below the salinity maximum) indicates some correspondences during the 90s, when the evolution of the respective salt contents are almost out of phase with AW (Fig. 4.15, lower panel): to a remarkable increase of salt content in the LIW stream corresponds a significant salt decrease in the surface layer in 1992. During the first years (until approximately 2001), the inverse relation between the salt content of AW and LIW seems to suggest a salt compensation through the channel. Nevertheless, after that period, the two layers seems to have different evolutions: while the AW maintains almost stable characteristics, the LIW experiences a progressive salinity increase, with a maximum reached in 2008.

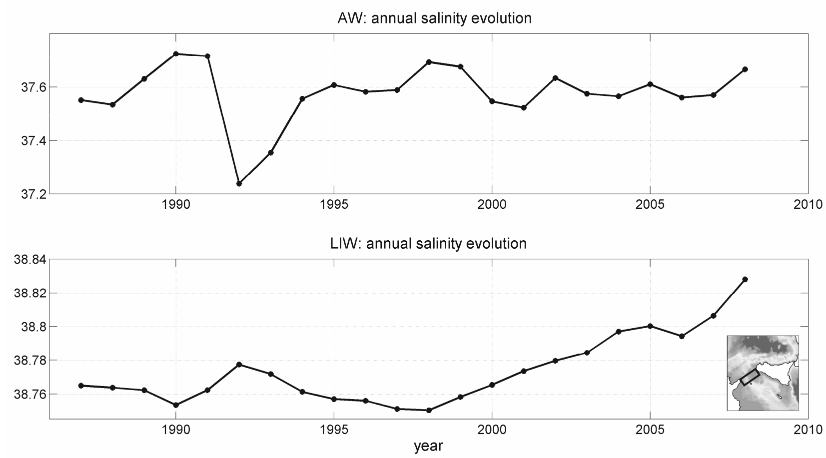

Figure 4.15: Temporal evolution of annual mean salinity in the Sicily Channel, between Cape Bon and Mazara: (upper panel) surface layer (computed as the average value of the first 100 m); (lower panel) LIW core on the Sicilian side of the channel, computed as the average value of a 100 m layer below the salinity maximum (redrawn and updated from Gasparini et al., 2005).

Many studies provide information about flux exchanges (Manzella et al., 1988; Astraldi et al., 1999; Gasparini et al., 2005), indicating an annual mean of the order of 1 Sv within both layers. Of particular relevance is the propagation of the EMT signature from the eastern to the western basin. The exceptionally large volume of new deep waters of Aegean origin (Roether et al., 2007) produced during the EMT modified the thermohaline characteristics of the intermediate layer in the channel (traditionally occupied by LIW) and induced the uplifting of the resident deep waters in the Ionian, significantly increasing the volume of tEMDW crossing the Sicily Channel, towards the Tyrrhenian subbasin.

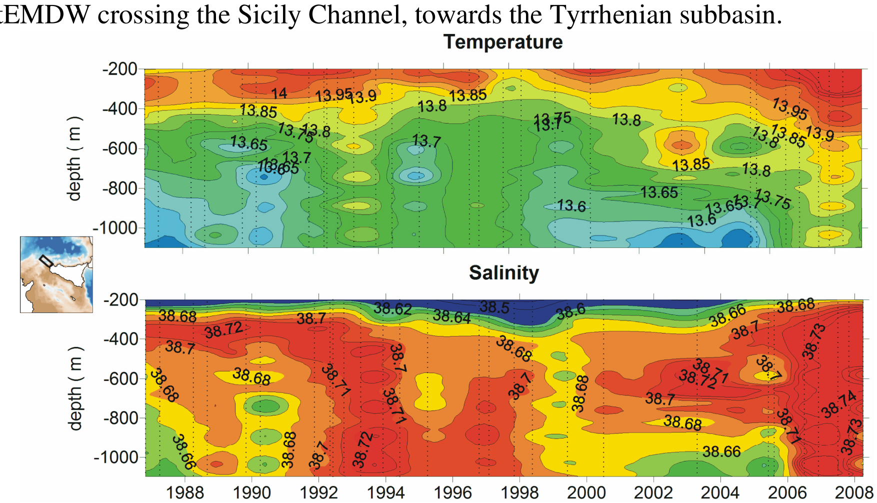

Figure 4.16: Temporal evolution of potential temperature and salinity at the Tyrrhenian entrance, in correspondence of a narrow passage, from 200 to 1200 m depth, using data from periodic hydrographic campaigns (redrawn and updated from Gasparini et al., 2005).

In order to describe the propagation of the EMT from the eastern to the western basin, attention will be addressed to the Eastern Mediterranean Outflow (EMO) at the Tyrrhenian entrance and the interior deep regions of the Tyrrhenian subbasin. This demonstrates the impact of the Sicily outflow on the Tyrrhenian subsurface layers and, consequently, on the western basin. It is well known that the Sicily outflow, at the western exit of the channel, turns right, enters the Tyrrhenian and flows along the Sicilian continental slope (Millot, 1987). This connection between the channel and the Tyrrhenian has been described in detail by Sparnocchia et al. (1999). In Fig. 4.16 the temporal evolution of the water column characteristics (between 200 m and the bottom) at the Tyrrhenian entrance is shown. Following the salinity evolution (Fig. 4.16, lower panel), we observe that the salinity maximum (representative of the EMO) is positioned at about 300–400 m until 1991. Subsequently, an evident sinking can be observed and the salinity maximum reaches the bottom, remaining there for about 6 years (at least until 1998). During the same period potential temperatures of 13.7 °C, or higher, are observed close to the bottom (Fig. 4.16, upper panel). This indicated that for at least 6 years a significant injection of salt and heat extended to the deeper layers. The reason is the remarkable increase of density in the outflow, which became much denser than the resident waters (Gasparini et al., 2005), allowing the EMO to sink deeper. However it is essential to remark that the sinking of the Sicilian outflow was also observed before the EMT period (Guibout, 1987; Garzoli and Maillard, 1976). What distinguishes the EMT is that those episodes became particularly intense and continuous, because of the EMDW uplifting in the Ionian basin. Obviously, the sinking from depths shallower than 400 m down to 2000 m induces a tremendous mixing of the EMO itself and of the EMO with the resident water in the Tyrrhenian (Millot, 1999), giving origin to what has been called the Tyrrhenian Dense Water (TDW). This mixing is clearly shown by the small structures present on the vertical maps in Fig. 4.16. After the EMT period, a restoring tendency became evident and a well-defined saltier vein could be observed at a depth of about 600–700 m during March 2003. A further input of warm and salty water along the entire water column is evident after 2006, which is the most remarkable export of salt and heat from the eastern to the western basin of the last twenty years.

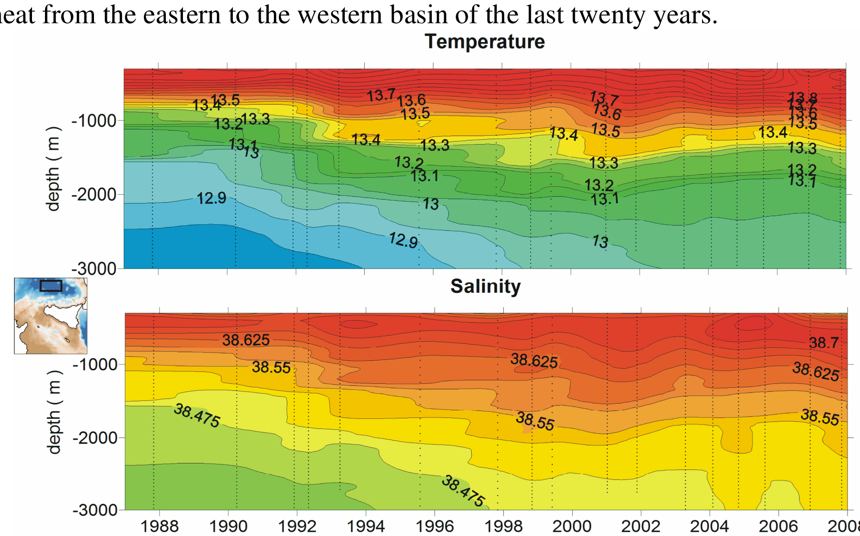

Figure 4.17: Temporal evolution of potential temperature and salinity in the central Tyrrhenian from 300 to 3000 m depth, using data from periodic hydrographic campaigns (redrawn and updated from Gasparini et al., 2005).

The consequences of the changes observed in the outflow are clearly evident in the central part of the Tyrrhenian (Gasparini et al., 2005). The temporal evolution of the hydrographic characteristics in the deep water column (Fig. 4.17) indicates that after 1992 almost the entire water column below 300 m shows the same temporal evolution: the saltier and warmer waters progressively extend their influence in depth. The density field (not shown, see Gasparini et al., 2005) has a more oscillating pattern, without a particular trend, reaching its highest values at depth in the period 1997-2001. During the period 1992–2001, the mean temperature and salinity between 500 and 3000 m increased by 0.024 °C yr^{-1} and 0.008 yr^{-1}, respectively, evidencing that the EMT induced a significant enhancement of mixing related to the sinking of a huge volume of water of eastern origin.

These extended and long-lasting modifications propagated to the entire western basin. More specifically they reached the DWF sites (Schroeder et al., 2006; see also Section 2.4). An important factor controlling the deep water formation in the Provençal subbasin is the salt distribution in the water column and more specifically the LIW salt content (Lacombe et al., 1985). The further enhancement of the salt imported from the eastern to the western basin for a long time makes the western basin more prone to production of warmer and saltier deep waters.

4. Variability in the Heat and Freshwater Characteristics at Interannual to Multi-Decadal Time Scales

The oceanic variability at interannual, interdecadal, and multi-decadal scales plays a key role in climate variability and climate change. Instrumental records of increasing duration and spatial coverage document substantial variability in the path and intensity of ocean currents on time scales of months to decades. While some observed oceanic variability can be clearly related to forcing mechanisms, for other observed variability those mechanisms are less clear. Indeed, even if the external forcing were constant in time, that is, if no systematic changes in insolation or atmospheric forcing, would occur, the climate system would still exhibit variability on various time scales (Dijkstra and Ghil, 2005). Consequently, processes internal to the climate system can give rise to spectral peaks not directly related to the variability of the forcing (see Pisacane et al., 2006, for the Mediterranean and Pierini et al., 2009, for the Kuroshio Extension).

Due to its relatively small dimensions, the Mediterranean Sea promptly responds to atmospheric variability (Demirov and Pinardi, 2002; Stratford and Haines, 2002). Indeed, the variability of DWF and water mass transformations in the Mediterranean has been mainly attributed to interannual changes in the strength of the external atmospheric forcing (Castellari et al., 2000; Mertens and Schott, 1998). Nevertheless, theoretical and idealized as well as realistic modeling studies have shown that feedbacks between the DWF rate and the strength of the overturning circulation are potential sources of internal variability, independently of changes in the atmospheric forcing (Lenderink and Haarsma, 1994; Yin and Sarachik, 1995). Such mechanisms of variability can be effectively studied inside the Mediterranean, where processes are expected to occur on time scales that enable both close experimental monitoring and affordable numerical simulations (Herrmann et al., 2008b; Artale et al., 2002).

From these considerations the following question arises: is it reasonable to consider the Mediterranean as a system in equilibrium over multi-decadal or longer time scales, or, on the contrary, is it more realistic and physical to consider it as a system in a non-equilibrium state, or in a multi-state equilibrium?

Looking at decadal time scales, Marullo et al. (2011) have analyzed the longest time series of the Mediterranean sea surface temperature, ranging from 1854 until now, and found that the Atlantic multidecadal oscillation (AMO), known as a surface manifestation of the 70-year natural oscillation of the North Atlantic thermohaline circulation (THC in the following), is a mode of variability that includes also the Mediterranean region. One of the concluding remark of this paper is that the Mediterranean must be considered as an important component of the internal variability of the North Atlantic THC, not only via feedback mechanisms or teleconnections between the external forcing of the two basins (Huck et al., 1999; Te Raa and Dijkstra, 2002; Li 2006), but more importantly through the spreading of the Mediterranean outflow in the North Atlantic as initially argued by Artale et al. (2006) and Lozier and Stewart (2008).

Whilst if we look at shorter time scales and observations along the entire water column, robust trends are observed in the deep layer of the WMED (Vargas-Yáñez et al., 2010), while remarkable oscillations are observed in the intermediate layer in particular in the EMED (Rixen et al., 2005). Moreover regarding this basin the EMT period (Klein et al., 1999) deserves particular attention. During this event, the change in the vertical water mass distribution is accompanied by a change in the dispersal path of the fresher AW and of the saltier and warmer LIW/CIW, inducing variability on the eastern MTHC. In particular from 1993 to 2001 the whole EMED has shown a dramatic and sudden change in the sea surface features, including the reversal of the Ionian upper layer circulation in 1997 from anticyclonic to cyclonic (Borzelli et al., 2009; see also Sections 2.1. and 2.4.). Borzelli et al. (2009) proposed that such a reversal was principally associated to the internal water movement as a consequence of the EMT, while the wind stress played only a secondary role. Moreover Gačić et al. (2010) generalized this concept hypothesizing that such inversions are possible even without Aegean influence, but are more likely due to the variability of the production of deep water in the southern Adriatic. But more interesting is their proposed feedback mechanism, BiOS (see Section 2.1.), between the production of Adriatic deep water and the Ionian circulation.

The impact of the EMT on the WMED and on deep convection in the Gulf of Lions, was discussed recently in Schroeder et al. (2010), who found that the heat and salt content variations along the water column are the result of a combination of heat and freshwater exchanges with the atmosphere and the lateral advection from the surrounding ocean and vertical mixing. For our purposes, their main conclusion is very interesting: they found that the anomalous production of deep water in winters 2004/05 and 2005/06 is linked to extreme winter air-sea heat and freshwater forcing only for 49%. Thus the lateral advection played a major role in setting the new deep water properties (see also Grignon et al., 2010).

Finally, following the final destiny of the MWs, at the Gibraltar Strait one can observe a synthesis of all the scales of motion relevant to interpret the observed Mediterranean variability (from tides to multidecadal variability): the properties of the final product depend on the atmospheric forcing that exhibits important interannual/decadal variability as well as possible long-term trends due to man-induced climate change or to natural internal variability. Therefore changes in the MWs properties must be reflected in the outflow at Gibraltar (Millot et al., 2006; García-Lafuente et al., 2007, 2009; Fusco et al., 2008). Moreover, the significant variability that has been recently observed in the AW salinity (Millot, 2007) is expected to have an important effect on the MTHC (Sannino et al., 2009a).

The non-homogenous distribution in space and time of in-situ ocean observations makes the numerical model simulation a key instrument to explore the internal variability of the Mediterranean. Despite their uncertainty, recently the analysis of regional numerical models (Roussenov et al., 1995; Artale et al., 2002; Pisacane et al., 2006; Sannino et al., 2009b) has shown their usefulness to understand the main processes that drive the Mediterranean variability. A number of regional climate model (RCM) systems have been developed in order to downscale the output from large-scale global climate model simulations and produce fine scale regional climate change information useful for these studies (Somot et al., 2008; Artale et al., 2009).

Pisacane et al. (2006) showed the transition from one equilibrium state, at low variability, to another, at very high variability, switching the only-ocean model from relaxation to mixed boundary condition. Similarly with the coupled model the same increase of variability is obtained (e.g EMT and the inversion of Ionian circulation together, as described in Borzelli et al., 2009, and Gačić et al., 2010) only when running the model without any constraints, namely when the sea surface salintiy patterns are the results of the free interaction between freshwater fluxes and the 3D ocean variability.

Very few studies have looked at the EMT as only an example of the complexity and high non-linearity of the ocean and its sensitivity to perturbations on a large range of scales. From this point of view the Mediterranean is a good example, its thermohaline circulation being the result of non-linear interactions between many physical processes, where the most relevant ones are the deep convection, the internal advection of salt and heat, the surface advection of freshwater, several topographic constraints and the external atmospheric forcing. Numerical experiments, more than observational analysis, may demonstrate that viewing many ocean phenomena (e.g. EMT, interannual variability of the deep convection) as purely atmosphere-driven events should be reviewed, and the role of internal variability in relation to advection-convection feedbacks should be reconsidered, paying more attention to the potential relevance of natural oscillations and trends, though without diminishing the role of the atmospheric forcing. Because of the sea's extreme sensitivity to perturbations on a large range of scales (see the spectral analysis of Marullo et al., 2011) it is hard to consider it in a stationary equilibrium, but more likely a multi-state of equilibrium or a continuum state of equilibrium, and in this context recent theoretical results about the internal long-term memory of ocean dynamics as the cause of the spectral behaviour of the observed and simulated sea surface temperature (Fraedrich et al., 2009) should be taken into account.

5. Outlook and Future Research Priorities

Significant advances have been made in the understanding of the thermohaline circulation and the forcings of the Mediterranean in recent years. However, there are still many issues to be addressed that should be seen as research priorities for the future. With a particular focus on the topics that have been described in this chapter, we schematically list these priorities and open questions below.

Related to "Changes in the Thermohaline Circulation of the Mediterranean Sea" priorities for future research should include attempts to answer the following questions:

- How long will it take the eastern Mediterranean to get back to the pre-EMT state (if this occurs at all)?
- What is the real impact of the EMT in the western Mediterranean?
- What is the cause of the observed increasing temperature and salinity of the subsurface water crossing the Sicily Channel?
- What is the nature and variability of the water masses flowing in and out through the Strait of Gibraltar ?
- To what degree does a change in the Mediterranean Outflow affect the oceanic circulation in the North-Atlantic and/or the deep water formation in the Arctic regions?

- Can we provide a realistic description of the long-term changes in the upper and intermediate layers and reconcile them with the warming and salting of the deep layers and the heat fluxes through the sea surface?
- Can new measurements be made leading to an agreed description of the surface circulation in the eastern Mediterranean?

Furthermore, as suggested by Millot (2007), studies about dense water formation and circulation, which take into account the interannual variability of the forcing functions, must take into account the interannual variability of the inflow, in particular, the observed increasing salt content of the inflowing Atlantic water. In terms of preconditioning, the salinification of surface and intermediate waters (due either to local processes or climate change) is likely to be one of the most important factors and could explain why the contribution by deep cascading from shelf regions seems to become more and more important.

Related to "The Forcings of the Mediterranean Sea", priorities for future research should include attempts to answer the following questions:
- Can we resolve the remaining imbalance in the basin mean heat budget through further improvements to the parameterizations for each of the four air-sea heat flux components ?
- To what extent can improved spatial resolution of the atmospheric forcing be achieved through dynamical downscaling of the various reanalyses products?
- What information do these downscaled fields provide about extreme wind forcings that may trigger dense water formation at the key deep convection sites?
- What are the main modes of temporal and spatial variability of the Mediterranean Sea circulation and how do they respond to different modes of atmospheric variability?
- Can we accurately quantify past, and foresee possible future, changes in the riverine freshwater inputs in order to assess their impacts on the circulation patterns in the Mediterranean Sea? Note this would require taking into account the complex inter-connections between human activities, environmental driving forces and climatic factors.

A more pervasive open issue is described in Section 4, addressing the variability at interannual to multi-decadal time scale. This issue arises from the fact that while some observed oceanic variability can be clearly related to forcing mechanisms, for other observed variability those mechanisms are less clear. Indeed, even if the external forcing were constant in time, the climate system would still display variability on many time scales. Attempts to address this issue and the questions listed above hold the promise of much exciting research in the decade ahead.

References

1. Adler R.F., Huffman G.J., Chang A., Ferraro R., Xie P., Janowiak J., Rudolf B., Schneider U., Curtis S., Bolvin D., Gruber A., Susskind J., Arkin P., Nelkin E. (2003). The version-2 global precipitation climatology project (GPCP) monthly precipitation analysis (1979-present). *J. Hydrometeor.* 4: 1147-1167.
2. Albérola, C., Millot, C., 2003. Circulation in the French Mediterranean coastal zone near Marseilles : the influence of the wind and the Northern Current. Cont. Shelf Res., 23 (6):587-610.
3. Allen, J.T., Smeed, D.A., Tintore, J. and Ruiz, S. (2001) Mesoscale subduction at the Almeria-Oran front. Part 1: ageostrophic flow. Journal of Marine Systems, 30, (3/4), 263-285. (doi:10.1016/S0924-7963(01)00062-8).
4. Allen, JT, Painter, SC, Rixen, M., 2008. Eddy transport of western Mediterranean intermediate water to the Alboran Sea. Journal of Geophysical Research, 113(C4), C04024.
5. Alpar, B. and Yüce, H., 1998. Sea-Level Variations and their Interactions between the Black Sea and the Aegean Sea. Estuarine, Coastal and Shelf Science, 46, 609-619.
6. Amitai Y., Lehan Y., Lazar A., Heifetz E., 2010. Surface circulation of the eastern Mediterranean Levantine basin - insights from analyzing 14 years of satellite altimetry data. Journal of Geophysical Research, doi:10.1029/2010JC006147, in press.
7. Andersen, J. J. and E. C. Carmack, 1984. Observations of Chemical and Physical Fine-structure in a Strong Pycnocline, Sea of Marmara. Deep-Sea Research, 21, 877-886.
8. Armi, L., and D.M. Farmer, 1988. The flow of Mediterranean Water through the Strait of Gibraltar, Prog. Oceanogr., 21, 1-105.
9. Arnell N. 2003. Effects of IPCC SRES emission scenarios on river runoff: a global perspective Hydrology and Hearth System Science, 7 (5), 619-641
10. Artale V, Iudicone D, Santoleri R, Rupolo V, Marullo S, D'Ortenzio F., 2002. Role of surface fluxes in OGCM using satellite SST. Validation and sensitivity to forcing frequency of the Mediterranean thermohaline circulation. J Geophys Res 107:3120, doi:10.1029/2000JC000452
11. Artale, V., Calmanti S., Malanotte-Rizzoli P., Pisacane G., Rupolo V., Tsimplis M., 2006. The Atlantic and Mediterranean Sea as connected systems. In: P. Lionello, P., Malanotte-Rizzoli & R. Boscolo (Eds), Mediterranean Climate Variability, Amsterdam: Elsevier, pp. 283-323
12. Artale, V., Calmanti, S., Carillo, A., Dell'Aquila, A., Hermann, M., Pisacane, G., Ruti, P., Sannino, G., Struglia, M., Giorgi, F., Bi, X.and Pal, J., and Rauscher, S., 2009. An atmosphere-ocean regional climate model for the Mediterranean area: assessment of a present climate simulation, Clim. Dyn., doi:10.1007/310 s00382-009-0691-8.
13. Astraldi M., G.P. Gasparini, L. Gervasio and E. Salusti, 2001. Dense water dynamics along the Strait of Sicily (Mediterranean Sea), Journal of Physical Oceanography 31, 3457–3475.
14. Astraldi M., S. Balopulos, J. Candela, J. Font, M. Gačić, G.P. Gasparini, B. Manca, A. Theocharis and J. Tintoré, 1999. The role of straits and channels in understanding the characteristics of Mediterranean circulation, Progress in Oceanography 44. 65–108.
15. Ayoub N., P.-Y. Le Traon and P. De Mey, 1998. A description of the Mediterranean surface variable circulation from combined ERS-1 and TOPEX/POSEIDON altimetric data, J. Mar. Syst. 18 (1–3), 3–40.
16. Aznar, R., Sotillo, M., Martín, M., Somot, S., Valero, F., 2010. Comparison of model and satellite-derived long-term precipitation databases over the Mediterranean basin: a general overview". Atmospheric Research 97 (1-2), 170-184, doi:10.1016/j.atmosres.2010.03.026
17. Basheck, B., U. Send, J. García-Lafuente, and J. Candela, 2001. Transport estimates in the Strait of Gibraltar with a tidal inverse model. J. Geophys. Res., 106, 31033-31044.
18. Beranger, K, Mortier, L, Crepon, M., 2005. Seasonal variability of water transport through the Straits of Gibraltar, Sicily and Corsica, derived from a high-resolution model of the Mediterranean circulation, Progress in Oceanography 66 (2-4), 341-364.

19. Beşiktepe, Ş. T., 2003. Density Currents in the Two-Layer Flow: An example of Dardanelles Outflow, Oceanologica Acta, 26, 243-253.
20. Beşiktepe, Ş., Özsoy, E. and Ü. Ünlüata, 1993. Filling of the Marmara Sea by the Dardanelles Lower Layer Inflow, Deep-Sea Res., 40, 1815-1838.
21. Beşiktepe, Ş., Sur, H. İ., Özsoy, E., Latif, M. A., Oğuz, T. and Ü. Ünlüata, 1994. The Circulation and Hydrography of the Marmara Sea, Prog. Oceanogr., 34, 285-334.
22. Bethoux J. P., Gentili B., 1999. Functioning of the Mediterranean Sea: past and present changes related to fresh water input and climatic changes. J. Mar. Sys., 20, 33-47.
23. Bethoux J.P., B. Gentili, D. Tailliez, 1998. Warming and freshwater budget change in the Mediterranean since the 1940s, their possible relation to the greehouse effect. Geophys. Res. Lett., Vol. 25, No. 7, 1023-1026.
24. Bethoux, J.P. and Gentili, B., 1996. The Mediterranean Sea, coastal and deep-sea signatures of climatic and environmental changes. J. Mar. Syst. 7, 383–394
25. Bethoux, J.P., B. Gentili, J. Raunet, D. Taillez, 1990. Warming trend in the western Mediterranean deep water. Nature, 347, 660-662.
26. Bethoux, J.P., X. Duriey de Madron, F. Nyffeler, and D. Tailliez, 2002. Deep water in the western Mediterranean: peculiar 1999 and 2000 characteristics, shelf formation hypothesis, variability since 1970 and geochemical inferences. J. Mar. Systems, 33-34, 117-131.
27. Beuvier, J., F. Sevault, M. Hermann, H. Kontoyiannis, W. Ludwig, M. Rixen, E. Stanev, K. Béranger, S. Somot, 2010. Modelling the Mediterranean Sea inter annual variability during 1961-2000: focus on the Eastern Mediterranean Transient (EMT). J. Geophys. Res., in press.
28. Bignami F., E. Böhm, E. D'Acunzo, R. D'Archino and E. Salusti, 2008. On the dynamics of surface cold filaments in the Mediterranean Sea, J. Mar. Sys., 74, 1-2, 429-442, doi:10.1016/j.jmarsys.2008.03.002.
29. Bignami F., R.Sciarra, S.Carniel, R.Santoleri, 2007. The variability of Adriatic Sea coastal turbid waters from SeaWiFS imagery, J. Geophys. Res., 112, C3.
30. Bignami F., S. Marullo, R. Santoleri and M.E. Schiano, 1995. Long wave radiation budget in the Mediterranean Sea. J. Geophys. Res. 100, 2501–2514.
31. Bogdanova, A.K., 1965. Seasonal fluctuations in the inflow and distribution of the Mediterranean water in the Black Sea, in Fomin, L.M.(Ed.) Basic Features of the Geological Structure, of the Hydrologic Regime and Biology of the Mediterranean Sea, Academy of Sciences, USSR Moscow, Engl. trans., 1969, Institute of Modern Languages, Washington DC, pp.131-139.
32. Borzelli, G., Manzella, G., Marullo, S., and Santoleri, R. 1999. Obervations of coastal filaments in the Adriatic Sea, J. Marine Systems, 20, 187–203.
33. Borzelli, G. L. E., M. Gačić, V. Cardin, and G. Civitarese, 2009: Eastern Mediterranean Transient and reversal of the Ionian Sea circulation, Geophys. Res. Lett., 36, L15108, doi:10.1029/2009GL039261.
34. Bozec A., Bouruet-Aubertot P., Beranger K., Crepon M., 2006. Mediterranean oceanic response to the interannual variability of a high-resolution atmospheric forcing: a focus on the Aegean Sea. J. Geophys. Res. Oceans 111, C11013, doi:10.1029/2005JC003427.
35. Brankart, J.M. and N. Pinardi, 2001. Abrupt cooling of the Mediterranean levantine intermediate water at the beginning of the 1980s: Observational evidences and model simulations. J. Phys. Oceanogr., 31, 8, Part II, 2307-2320.
36. Brenner, S., 1989. Structure and Evolution of Warm Core Eddies in the Eastern Mediterranean Levantine Basin, J. Geophys. Res., 94, 12593-12602.
37. Brenner, S., 1993. Long-term evolution and dynamics of a persistent warm core eddy in the Eastern Mediterranean Sea, Deep-Sea Res. II, 40, 1193-1206.
38. Bruno, M., J. J. Alonso, A. Cózar, J. Vidal, A. Ruiz-Cañavate, F. Echevaria, J. Ruiz, 2002. The boiling-water phenomena at Camarinal Sill, the Strait of Gibraltar, Deep Sea Res., Part II, 49, 4097– 4113.
39. Bryden, H. L., J. Candela, and T.H. Kinder, 1994. Exchange through the Strait of Gibraltar, Prog. Oceanogr., 33, 201-248.

40. Bryden, H.L., and H. Stommel, 1982. Origin of the Mediterranean outflow, J. Mar. Res., 40, Suppl., 55-71.
41. Bryden, H.L., and T.H. Kinder, 1991. Steady two-layer exchange through the Strait of Gibraltar, Deep-Sea Res., 38, S1, S445-S463.
42. Budillon, G., Lo Bue, N., Siena, G., Spezie, G., 2010. Hydrographic characteristics of water masses and circulation in the Northern Ionian Sea. Deep-Sea Research II 57 (5–6), 441–457.
43. Bunker A.F., H. Charnock and R.A. Goldsmith, 1982. A note on the heart balance of Mediterranean and Red Seas, Journal of Marine Research 40, 73–84.
44. Buongiorno Nardelli B., Santoleri R., Marullo S., Iudicone D., Zoffoli S., 1999. Altimetric signal and three dimensional structure of the sea in the Channel of Sicily, J. Geophys. Res., 104, 20585-20603.
45. Buongiorno Nardelli B., Sparnocchia S., Santoleri R., 2001. Small mesoscale features at a meandering upper ocean front in the western Ionian Sea (Mediterranean Sea): vertical motion and potential vorticity analysis, J. of Phys. Ocean., Vol. 31, 8, 2227-2250.
46. Buongiorno Nardelli, O. Cavalieri, M.-H. Rio and R. Santoleri, Subsurface geostrophic velocities inference from altimeter data: application to the Sicily Channel (Mediterranean Sea), J. Geophys. Res. 111 (2006), p. C04007 10.1029/2005JC003191.
47. Büyükay, M., 1989. The surface and internal oscillations in the Bosphorus, related to meteorological forces, M.Sc. Thesis, Institute of Marine Sciences, Middle East Technical University, 169p.
48. Canals, M., P. Puig, X. Durrier de Madron, S. Heussner, A. Palanques, and J. Fabres, 2006. Flushing submarine canyons, Nature, 444, 347– 354, doi:10.1038/nature05271.
49. Candela, J., C. D. Winant, and H. L. Bryden, 1989. Meteorologically forced subinertial flows through the Strait of Gibraltar, J. Geophys. Res., 94, 12,667– 12,679.
50. Castellari S, Pinardi N, Leaman K., 2000. Simulation of water mass formation processes in the Mediterranean Sea: Influence of the time frequency of the atmospheric forcing. J Geophys Res 105:24157–24181.
51. Çeçen, K., Beyazit, M., Sumer, M., Gucluer, S., Dogusal, M., Yüce, H., 1981. Oceanographic and hydraulic investigations of the Bosphorus: Section I, Final Report, submitted to the Irrigation Unit of the Turkish Scientific and Technical Research Council, Istanbul Technical University, (in Turkish), Istanbul, 166p.
52. CIESM (2009). Dynamics of Mediterranean deep waters. N° 38 in CIESM Workshop Monographs, edited by F. Briand, 132 pages, Monaco.
53. CIESM, 2005. Strategies for understanding mesoscale processes. CIESM Workshop Monographs n°27, 132 pages.
54. Cipollini P., S. Vignudelli, F. Lyard and L. Roblou, 2008, 15 Years of Altimetry at Various Scales over the Mediterranean, Remote Sensing of the European Seas, edited by Vittorio Barale and Martin Gade, ISBN: 978-1-4020-6771-6, 295-306 .
55. Criado-Aldeanueva, F., García-Lafuente, J., Vargas, J.M., Del Río, J., Sánchez, A., Delgado, J. and Sánchez, J.C., 2006. Wind induced variability of the hydrographic features and water masses distribution in the Gulf of Cádiz (SW Iberia) from in situ data. Journal of Marine Systems, 63, 130-140. doi:10.1016/j.jmarsys.2006.06.005.
56. Demirov E, Pinardi N., 2002. Simulation of the Mediterranean Sea circulation from 1979 to 1993. Part I. The interannual variability. J Mar Syst 33–34:23–50
57. Dijkstra H. A., and M. Ghil, 2005. Low-frequency variability of the large-scale ocean circulation: A dynamical systems approach, Rev. Geophys., 43, RG3002, doi:10.1029/2002RG000122, 2005
58. Dubois C., Sanchez-Gomez E., Braun A., Somot S., 2010. A gathering of observed air-sea surface fluxes over the Mediterranean Sea. Note de centre n°XXX. Groupe de Météorologie de Grande Echelle et Climat. CNRM. (in press)
59. Durrieu de Madron X., V. Zervakis, A. Theocharis and D. Georgopoulos, 2005. Comments on “Cascades of dense water around the world ocean”, Progress in Oceanography 64, 83–90.

60. El-Gindy A.A.H. and S.H.Sh. El-Din, 1986. Water masses and circulation patterns in the deep layer of the Eastern Mediterranean, Oceanologica Acta 9 (3), 239–248.
61. Elguindi N., Somot S., Dequé M., Ludwig W., 2009. Climate change evolution of the hydrological balance of the Mediterranean, Black and Caspian Seas: impact of climate model resolution. Clim.Dyn. doi: 10.1007/s00382-009-0715-4.
62. Eriş K.K., W.B.F. Ryan, M.N. Çağatay, U. Sancar, G. Lericolais, G. Ménot and E. Bard, 2007. The timing and evolution of the post-glacial transgression across the Sea of Marmara shelf south of İstanbul, Marine Geology 243, 57–76.
63. Farmer, D. M. and L. Armi, 1986. Maximal two-layer exchange over a sill and through the combination of a sill and contraction with barotropic flow, J. Fluid Mech., 164, 53-76.
64. Fekete B., Vorosmarty C.J, Grabs W., 2002. High-resolution fields of global runoff combining observed river discharge and simulated water balances, Gl. Biogeochem. Cycles, 16,3, 1042, 10.1029/1999GB001254.
65. Ferrari R. and C. Wunsch, 2010, The distribution of eddy kinetic and potential energies in the global ocean. Tellus, 62A, 92–108
66. Fielding, S., Crisp, N., Allen, J.T., Hartman, M.C., Rabe, B. and Roe, H.S.J., 2001. Mesoscale subduction at the Almeria-Oran front. Part 2: biophysical interactions. Journal of Marine Systems, 30, (3-4), 287-304, doi:10.1016/S0924-7963(01)00063-X.
67. Font, J., P. Puig, J. Salat, A. Palanques, and M. Emelianov, 2007. Sequence of hydrographic changes in NW Mediterranean deep water due to the exceptional winter of 2005, Sci. Mar., 71(2), 339– 346.
68. Fraedrich, K, R. Blender, X. Zhu, 2009. Continuum Climate Variability: Long-Term Memory, Scaling, And 1/F-Noise, International Journal of Modern Physics B, 23 (28-29), 5403-5416. doi: 10.1142/S0217979209063729.
69. Fuda, J.L., L. Bengara, S. Ben Ismail, C. Curtil, B. El Moumni, J. Font, D. Lefevre, C. Millot, I. Taupier-Letage, P. Raimbault, G. Rougier, C. Sammari and C. Tamburini, 2009. Recent dense water formation in the Med western basin, as observed by HYDROCHANGES. In Dynamics of Mediterranean Deep waters, CIESM workshop monograph, nº 38, 41-49.
70. Fuda, J-L., G. Etiope, C. Millot, C. Faveli, M. Calcara, G. Smriglio, E. Boschi, 2002. Warming, salting and origin of the Tyrrhenian deep water. Geophys. Res. Lett., 29, 18, 1886, doi: 10.1029/2001GL014072.
71. Fuda, JL, Millot, C, Taupier-Letage, I, U. Send and J. M. Bocognano, 2000. XBT monitoring of a meridian section across the western Mediterranean Sea, Deep-Sea Research Part I, 47, 11, 2191-2218.
72. Fusco, G., Artale V., Cotroneo Y., 2008. Thermohaline variability of Mediterranean Water in the Gulf of Cadiz over the last decades (1948-1999), Deep-Sea Research I 55, 1624–1638.
73. Fusco, G; Manzella, GMR; Cruzado, A, M. Gačić, G. P. Gasparini, V. Kovačević, C. Millot, C. Tziavos, Z. R. Velasquez, A. Walne, V. Zervakis, and G. Zodiatis, 2003. Variability of mesoscale features in the Mediterranean Sea from XBT data analysis. Annales Geophysicae 21(1), 21-32.
74. Gačić, M., G. L. E. Borzelli, G. Civitarese, V. Cardin, and S. Yari, 2010, Can internal processes sustain reversals of the ocean upper circulation? The Ionian Sea example, Geophys. Res. Lett., 37, L09608, doi:10.1029/2010GL043216.
75. García-Lafuente, J., E. Alvarez Fanjul, J.M. Vargas and A.W. Ratsimandresy, 2002. Subinertial variability in the flow through the Strait of Gibraltar. J. Geophys. Res., 107, doi:10.1029/2001JC0011004.
76. García-Lafuente, J., J.M. Vargas, F. Plaza, T. Sarhan, J. Candela, and B. Baschek, 2000. Tide at the eastern section of the Strait of Gibraltar, J. Geophys. Res., 105, 14197-14213.
77. García-Lafuente, J., A. Sánchez-Roman, G. D. del Río, G. Sannino and J. Sánchez-Garrido 2007. Recent observations of seasonal variability of the Mediterranean outflow in the Strait of Gibraltar. J. Geophys. Res., 112, C10005, doi: 10.1029/2006JC003992.
78. García-Lafuente, J., F. Criado-Aldeanueva, 2001. La climatología y la topografía del Estrecho de Gibraltar determinantes de las propiedades termohalinas del agua del Mar Mediterráneo

(Mediterranean climatology and Strait of Gibraltar topography determine the thermohaline properties of the Mediterranean water, (in Spanish). Física de la Tierra, 13, 43-54.
79. García-Lafuente, J., J. Delgado, A. Sánchez-Román, J. Soto, L. Carracedo, and G. Díaz del Río, 2009. Interanual variability of the Mediterranean outflow observed in Espartel sill, western Strait of Gibraltar, J. Geophys. Res., 114, C10018, doi: 10.1029/2009JC005496.
80. Garrett, Chris, Richard Outerbridge, Keith Thompson, 1993: Interannual Variability in Meterrancan Heat and Buoyancy Fluxes. Journal of Climate, 6, 900-910
81. Garzoli, S., Maillard, C., 1976. Hydrologie et circulation hivernales dans les canaux de Sicilie et de Sardaigne. Campagnes Amalthee (1967) Hydromed II (1968). Technical Report, Museum National d'Histoire Naturelle, Paris.
82. Gasparini G.P., Bonanno A., Zgozi S., Basilone G., Borghini M., Buscaino G., Cutitta A., Essarbout N., Mazzola S., Patti B., Ramadan A.B., Schroeder K., Bahri T. and Massa F., 2008. Evidence of a dense water vein along the Libyan continental margin. Ann. Geophysicae, 26: 1-6.
83. Gasparini G.P., D.A. Smeed, S. Alderson, S. Sparnocchia, A. Vetrano and S. Mazzola, 2003. Tidal and subtidal currents in the Strait of Sicily, Journal Geophysical Research 109, C02011.
84. Gasparini, J.P., A. Ortona, G. Budillon, M. Astraldi, E. Sansone, 2005. The effect of the Eastern Mediterranean Transient on the hydrographic characteristics in the strait of Sicily and in the Tyrrhenian Sea. Deep-Sea Res., I, 52, 915-935.
85. Georgievski, G., and E. V. Stanev, 2006. Paleoevolution of Euroasian watersheds: Water transport through the Bosporus Straits as an indicator of the Lateglacial-Holocene transition, Climate Dynamics , 26, 6, 631-644.
86. Gerin, R; Poulain, PM; Taupier-Letage, I, C. Millot, S. Ben Ismail, and C. Sammari. 2009, Surface circulation in the Eastern Mediterranean using drifters (2005-2007), Ocean Science, 5, 4, 559-574.
87. Gertman I., Pinardi N., Popov Y. and Hecht A., 2006. Aegean Sea water masses during the early stages of the Eastern Mediterranean Climatic Transient (1988-1990). Journal of Physical Oceanography, 36, 9, 1841–1859.
88. Gertman, I.F., I.M. Ovchinnikov, and Yu.I. Popov, 1994. Deep convection in the eastern basin of the Mediterranean Sea, Oceanology 34 (1), 19-24.
89. Gill A.E., 1982. Atmosphere-Ocean Dynamics, Academic Press, San Diego, California.
90. Gilman, C. and C. Garrett, 1994. Heat flux parameterizations for the Mediterranean Sea: the role of atmospheric aerosols and constraints from the water budget. J. Geophys. Res., 99, 5119-5134.
91. Gomis, D., M. N. Tsimplis, B. Martín-Míguez., A. W. Ratsimandresy, J. García-Lafuente and S. A. Josey, 2006: Mediterranean Sea level and barotropic flow through the Strait of Gibraltar for the period 1958-2001 and reconstructed since 1659, Journal of Geophysical Research, 111, C11005, doi:10.1029/2005JC003186.
92. Grassl, H., V. Jost, J. Schulz, R. Kumar, P. Bauer, and P. Schlüssel, 2000. A climatological atlas of satellite-derived air-sea interaction parameters over the worlds ocean, pp 120. Max-Planck Report No. 312. Max-Planck Institute for Meteorology, Hamburg, Germany.
93. Grayek, S., E.V. Stanev and R. Kandilarov, 2010. On the response of Black Sea level to external forcing: altimeter data and numerical modelling. Ocean Dynamics, 60: 123–140.
94. Gregg, M.C., Özsoy, E. and Latif, M.A., 2002. Flow, water mass changes and hydraulics in the Bosphorus. Journal of Geophysical Research 107, 1–23.
95. Gregg, M. C. and E. Özsoy, 1999. Mixing on the Black Sea Shelf North of the Bosphorus, Geophysical Research Letters, 26, 1869-1872.
96. Gregg, M. C., Özsoy E. and M. A. Latif, 1999. Quasi-Steady Exchange Flow in the Bosphorus, Geophysical Research Letters, 26, 83-86.
97. Grignon, L., D.A. Smeed, H.L. Bryden and K. Schroeder, 2010. Importance of the variability of hydrographic preconditioning for deep convection in the Gulf of Lion, NW Mediterranean. Ocean Sci., 6, 573–586, doi:10.5194/os-6-573-2010.

98. Groom S., Herut B., Brenner S., Zodiatis G., Psara S., Kress N., Krom M.D.,Law C.S., Drakopoulos P., 2005. Satellite-derived spatial and temporal biological variability in the Cyprus Eddy, Deep Sea Research, II, 52, 2990–3010.
99. Guibout P., Atlas hydrologique de la Mediterranee (Shom ed), Ifremer, Paris (1987) p. 150.
100. Güler, I., Yüksel, Y., Yalçıner, A. C., Çevik, E. and C. Ingerslev, 2006. Measurement and Evaluation of the Hydrodynamics and Secondary Currents in and near a Strait Connecting Large Water Bodies - A Field Study, Journal of Ocean Engineering, 33, 1718-1748.
101. Gulev, S., Josey, S. A., Bourassa, M., Breivik, L.-A., Cronin, M. F., Fairall, C., Gille, S., Kent, E. C., Lee, C. M., McPhaden, M. J., Monteiro, P. M. S., Schuster, U., Smith, S. R., Trenberth, K. E., Wallace, D. and Woodruff, S. D., 2010. Surface Energy and CO2 Fluxes in the Global Ocean-Atmosphere-Ice System, Plenary Paper for OceanObs'09, in press.
102. Gündüz, M. and E. Özsoy, 2004. Effects of the North Sea Caspian Pattern on Surface Fluxes of Euro-Asian-Mediterranean Seas, Geophys. Res. Letters, L21701, doi: 10.1029/2005GL024315.
103. Gunnerson, C. G., and Ozturgut, E., 1974. The Bosphorus. In: E. T. Degens, & D. A. Ross (Eds), The Black Sea – Geology, Chemistry and Biology (American Association of Petroleum Geologists, Tulsa, p. 103).
104. Gunnerson C.G. and E. Özturgut, 1974. The Bosphorus. In: The Black Sea—geology, chemistry and biologyAmerican Association of Petrology and Geologists 20, 99–114.
105. Lacombe H. and P. Tchernia, 1958. Températures et salinités profondes en Méditerranée en période d'été (fin Juin–fin Octobre), Bulletin Information du Comité d'Océanographie et d'Etude des Côtes X (4), 209–214.
106. Hamad, N; Millot, C; Taupier-Letage, I., 2005, A new hypothesis about the surface circulation in the eastern basin of the Mediterranean sea, Progress In Oceanography, 66, 2-4, 287-298
107. Hamad, N; Millot, C; Taupier-Letage, I., 2006, The surface circulation in the eastern basin of the Mediterranean Sea, Scientia Marina, 70, 3, 457-503
108. Hamlet A.F. and Lettenmaier D.P.,1999. Effects of climate change on hydrology and water resources in the Columbia river basin. Journ. Of American Water Res. Ass. 35, no.6, 1597- 1623
109. Hatzaki M., H.A. Flocas, D.N. Asimakopoulos and P. Maheras, 2007. The Eastern Mediterranean Teleconnection pattern: Identification and definition. Int. J. Climatol., 27, 727-737.
110. Hatzaki, M., Flocas, H. A., Giannakopoulos, C., and Maheras, P., 2009. The impact of the eastern Mediterranean teleconnection Pattern on the Mediterranean climate, J. Climate, 22, 977–992.
111. Hayes D., Testor P., Zodiatis G., Konnaris G., Hannides A., Mortier L., Beguery L., D'Ortenzio F., Mauri E., Lekien F., Gerin R., Poulain P. and Lazar A., 2010, Glider Transects In The Levantine Sea: A Study Of The Warm Core Cyprus Eddy. 39th Ciesm Congress, May, Venice
112. Hecht, A., N. Pinardi, and A. Robinson, 1988. Currents, water masses, eddies and jets in the Mediterranean Levantine Basin, J. Phys. Oceanogr., 18, 1320–1353.
113. Herrmann M., Somot S., 2011, submitted. Representation of wind variability and intense wind events in the Mediterranean sea : impact of the regional climate model configuration. Nat. Hazards Earth Syst. Sci.
114. Herrmann M., Sevault F., Beuvier J., Somot S., 2010. What induced the exceptional 2005 convection event in the Northwestern Mediterranean basin ? Answers from a modeling study. J. Geophys. Res., 115, C12051, doi: 10.1029/2010JC006162.
115. Herrmann, M. J., and S. Somot, 2008. Relevance of ERA40 dynamical downscaling for modeling deep convection in the Mediterranean Sea, Geophys. Res. Lett., 35, L04607, doi:10.1029/2007GL032442.
116. Herrmann, M., C. Estournel, M. Déqué, P. Marsaleix, F. Sevault, S. Somot, 2008a. Dense water formation in the Gulf of Lions shelf: Impact of atmospheric interannual variability and climate change. Cont. Shelf Res., 28, 2092-2112.
117. Herrmann, M., S. Somot, F. Sevault, C. Estournel, and M. Deque, 2008b. Modeling the deep convection in the Northwestern Mediterranean sea using an eddy-permitting and an eddy-resolving model: case study of winter 1986-87, J. Geophys. Res., 113, C04011, 25, doi:10.1029/2006JC003991.

118. Hopkins, T.S., 1978. Physical processes in the Mediterranean basins. In B. Kjerfve (Ed.), Estuarine transport processes.
119. Huck, T., A. Colin de Verdière, and A. J. Weaver, 1999. Interdecadal variability of the thermohaline circulation in box-ocean models forced by fixed surface fluxes. J.Phys. Oceanogr., 29, 865–892.
120. Hurrell J.W., Kushnir Y., Ottersen G., and Visbeck M., 2003. The Bookshelf: The North Atlantic Oscillation: Climatic Significance and Environmental Impact, American Geophysical Union (March 2003).
121. Ovchinnikov I.M., 1966. Circulation in the surface and intermediate layers of the Mediterranean, Oceanology 6, 48–59.
122. Ilıcak, M., Özgökmen, T. M., Özsoy, E. and Fischer, P. F., 2009. Non-hydrostatic Modeling of Exchange Flows Across Complex Geometries, Ocean Modelling, 29, 159–175.
123. IMS-METU, 1999. A Study of the Turkish Straits System Currents at Various Space – Time Scales, unpublished report, Institute of Marine Sciences, METU, Erdemli, Mersin, December 1999.
124. Iudicone D., R. Santoleri, S. Marullo and P. Gerosa, 1998. Sea level variability and surface eddy statistics in the Mediterranean Sea from TOPEX/POSEIDON data, J. Geophys. Res. 103(C2), pp. 2995–3012.
125. Johns, B, Marsaleix, P, Estournel, C, 1992. On the wind-driven coastal upwelling in the Gulf of Lions, Journal Of Marine Systems, 3(4-5), 309-320.
126. Jordi A. and D.-P. Wang, 2009. Mean dynamic topography and eddy kinetic energy in the Mediterranean Sea: Comparison between altimetry and a 1/16 degree ocean circulation model. Ocean Modelling 29 (2), 137-146, doi:10.1016/j.ocemod.2009.04.001
127. Josey, S.A., and R. Marsh, 2005. Surface freshwater flux variability and recent freshening of the North Atlantic in the eastern Subpolar Gyre. J. Geophys. Res., 110, C05008, doi:10.1029/2004JC002521.
128. Josey S.A, Kent E.C, Taylor P.K, 1999. New insights into the ocean heat budget closure problem from analysis of the SOC air–sea flux climatology. J. Clim. 12, 2856–2880.
129. Josey, S. A., 2003. Changes in the heat and freshwater forcing of the Eastern Mediterranean and their influence on deep water formation. J. Geophys. Res., 108(C7), 3237, doi: 10.1029/2003JC001778.
130. Josey, S.A., Pascal, R.W., Taylor, P.K., Yelland, M.J., 2003. A New Formula For Determining the Atmospheric Longwave Flux at Ocean Surface at Mid-High Latitudes. J Geophys. Res., doi:10.1029/2002JC00141.
131. Josey, S. A., S. Somot and M. Tsimplis (2011). Impacts Of Atmospheric Modes Of Variability On Mediterranean Sea Surface Heat Exchange J. Geophys. Res., doi:10.1029/2010JC006685, in press.
132. Kanarska, Y. and V. Maderich, 2008. Modelling of seasonal exchange flows through the Dardanelles Strait, Estuarine, Coastal and Shelf Science, 79, 449–458.
133. Kinder T.H., and H.L. Bryden, 1990. Aspiration of deep waters through straits in The Physical Oceanography of Sea Straits, L.J. Pratt ed., Kluwer Academic. Publ., London, 587 pp.
134. Klein B., Roether W, Manca BB, Bregant D, Beitzel V, Kovacevich V, Luchetta A, 1999. The large deep water transient in the eastern Mediterranean. Deep-Sea Res I 46:371–414
135. Klein B., W. Roether, B. Manca and A. Theocharis, 2000. The evolution of the eastern Mediterranean climatic transient during the last decade: the tracer viewpoint. CIESM Workshop Monographs, Trieste.
136. Korres, G., N. Pinardi, and A. Lascaratos, 2000. The ocean response to low-frequency interannual atmospheric variability in the Mediterranean Sea. Part I: Sensitivity experiments and energy analysis. J. Climate 13:705–731.
137. Krahmann, G. and F. Schott, 1998. Long term increases in western Mediterranean salinities and temperatures: anthropogenic and climatic sources. Geophys. Res. Lett., 25, 4209-4212.

138. Krichak, S.O., P. Alpert, 2005. Decadal trends in the East Atlantic/West Russia pattern and the Mediterranean precipitation, Int. J.Climatol , 25, 183-192.
139. Kutiel, H., and Benaroch, Y., 2002. North Sea–Caspian Pattern (NCP)—An upper level atmospheric teleconnection affecting the Eastern Mediterranean: Identification and definition: Theoretical and Applied Climatology, v. 71p. 17-28 doi: 10.1007/s704-002-8205-x.
140. Lacombe H. and P. Tchernia, 1960. Quelques traits généraux de l'hydrologie mediterranéenne, Cah. océanogr., 8, 527–547 XIe Année.
141. Lacombe, H., P. Tchernia, L. Gamberoni, 1985. Variable bottom water in the western Mediterranean basin. Prog. Oceanog., 14, 319-338.
142. Lacombe, H., Tchernia, P., and Benoist, G., 1958. Contribution à l'étude de la Mer Egée en période d'été. Bulletin d'Information du Comité Central d'Océanographie et d'Etude des Côtes, 8, 454–468.
143. Langlais C., B. Barnier, J.M. Molines, P. Fraunié, D. Jacob, S. Kotlarski (2009) Evaluation of a dynamically downscaled atmospheric reanalyse in the prospect of forcing long term simulations of the ocean circulation in the Gulf of Lions. Ocean Dynamics, 30, 270–286.
144. Larnicol G., P.-Y. Le Traon, N. Ayoub and P. De Mey, 1995, Mean sea level and surface circulation variability of the Mediterranean Sea from 2 years of TOPEX/POSEIDON altimetry, J. Geophys. Res. 100, 25163–25177.
145. Lascaratos, A., Sofianos, S. and G. Korres, 2002. Interannual variability of atmospheric parameters over the Mediterranean Basin from 1945 to 1994, CIESM Workshop Series, No. 16, edited by Frederic Briand, pp. 21-24.
146. Lascaratos, A., 1992. Hydrology of the Aegean Sea. In: H. Charnock, Winds and currents of the Mediterranean Basin (pp. 313–334). NATO Advanced Science Institute: atmospheric and oceanic circulation in the Mediterranean Basin. Reports in Meteorology and Oceanography, Harvard University no. 40, 1.
147. Lascaratos, A., 1993. Estimation of deep and intermediate water mass formation rates in the Mediterranean Sea. Deep-Sea Res. II, 40, 1327-1332.
148. Latif, M. A., Özsoy, E., Oğuz, T., and Ünlüata, U., 1991. Observations of the Mediterranean inflow into the Black Sea. Deep-Sea Res., 38(Suppl. 2), 711–723.
149. Leaman, K.D. and F.A. Schott, 1991. Hydrographic structure of the convection regime in the Gulf of Lions: Winter 1987. J. Phys. Oceanogr., 21, 575-598.
150. Lebeaupin Brossier C., K. Béranger, C. Deltel and P. Drobinski, 2011. The Mediterranean response to different space–time resolution atmospheric forcings using perpetual mode sensitivity simulations. Ocean Modelling, 36, 1-2: 1-25.
151. Lenderink G, Haarsma RJ, 1994. Variability and multiple equilibria of the thermohaline circulation associated with deep-water formation. J Phys Oceanogr 24:1480–1493
152. Lermusieaux P.F.J. and A.R. Robinson, 2001. Features of dominant mesoscale variability, circulation patterns and dynamics in the Strait of Sicily, Deep-Sea Res., Part 1, Oceanogr. Res. Pap. 48, 1953–1997.
153. Levitus, S., J.I. Antonov, T.P. Boyer, R.A. Locarnini, H.E. García, A.V. Mishonov, 2009. Global ocean heat content 1955-2008 in light of recently revealed instrumentation problems. Geophys. Res. Lett. 36, L07608, doi: 10.1029/2008GL037155.
154. Li L.Z. X., 2006. Atmospheric GCM response to an idealized anomaly of the Mediterranean sea surface temperature, Clim. Dyn., 27, 543-552, doi: 10.1007/s00382-006-0152-6.
155. Lionello, P., Malanotte-Rizzoli, P. and R. Boscolo (eds.), 2006. Mediterranean Climate Variability, Elsevier Science, 438 pp.
156. López-Jurado, J., C. González-Pola, and P. Vélez-Belchi, 2005. Observation of an abrupt disruption of the longterm warming trend at the Balearic Sea, Western Mediterranean sea, in summer 2005, Geophys. Res. Lett., 32, 6, L24606, doi: 10.1029/2005GL024430.
157. Lozier M. S. and N. M. Stewart, 2008. On the Temporally Varying Northward Penetration of Mediterranean Overflow Water and Eastward Penetration of Labrador Sea Water, Journal of Physical Oceanography, 38, 2097-2103.

158. Lucarini, V., Danihlik, R.,Kriegerova, I., Speranza, A., 2007. Does the Danube exist? Versions of reality given by various regional climate models and climatological data sets. Journ. Of Geophys. Res., 112, D13103, doi:10.1029/2006JD008360
159. Lucarini, V., Danihlik, R.,Kriegerova, I., Speranza, A., 2008. Hydrological cycle in the Danube basin in present-day and XXII century simulations by IPCCAR4 global climate models. Journ. Of Geophys. Res., 113, D09107, doi:10.1029/2007JD009167
160. Ludwig, W., Dumont, E., Meybeck, M., and Heussner, S., 2009. River discharges of water and nutrients to the Mediterranean and Black Sea : Major drivers for ecosystem changes during past and future decades ? Progress in Oceanography, 80, 199–217.
161. Ludwig, W., Bouwman, L., Dumont, E. and Lespinas, F., 2010. Water and nutrient fluxes from major Mediterranean and Black Sea rivers: past and future trends and their implications for the basin-scale budgets. Global Biogeochem. Cycles, Global Biogeochem. Cycles, doi:10.1029/2009GB003594, in press.
162. Ludwig, W., Meybeck, M., Abousamra, F., 2003. Riverine transport of water, sediments, and pollutants to the Mediterranean Sea. UNEP MAP Technical report Series 141, UNEP/MAP Athens, 111 pp. Available from: <http://www.unepmap.org/>.
163. Macdonald A., J. Candela and H.L. Bryden, 1994. An estimate of the net heat transport through the Strait of Gibraltar. In: P.E. Violette, Editor, Coastal Estuarine Stud. 46, AGU, Washington, D.C..
164. Malanotte-Rizzoli P., Manca B. B., d'Alcala M. R., Teocharis A., Bergemasco A., Bregant D., Budillon G., Civitarese G., Georgopoulos D., ichelato A., Sansone E., Scarazzato P. and Souvermezoglou E., 1997. A synthesis of the Ionian Sea hydrography, circulation and water mass pathways during POEM-Phase I. Progress in Oceanography, 39: 153-204.
165. Manca, B.B., Kovacevic, V., Gačić, M., Viezzoli, D., 2002. Dense water fomation in the southern Adroatic Sea and spreading into the Ionian Sea in the period 1997-1999. Journal of Marine Systems, 33-34, 133-154.
166. Manzella G.M.R., G.P. Gasparini and M. Astraldi, 1988. Water exchange between the Eastern and Western Mediterranean through the Strait of Sicily, Deep-Sea Research 35, 1021–1035.
167. Marcos, M. and M.N. Tsimplis, 2008. Comparison of results of AOGCMs in the Mediterranean Sea during the 21st century. J. Geophys. Res., 113, C12028, doi: 10.1029/2008JC0048420.
168. Mariotti A., Zeng N.,Yoon J., Artale V., Navarra A., Alpert P., Li L., 2008. Mediterranean water cycle changes: transition to drier 21st century conditions in observations and CMIP3 simulations Env. Res. Lett. 3 044001 doi:10.1088/1748-9326/3/4/044001.
169. Marsili, L.F. 1681. Osservazioni Intorno al Bosforo Tracio overo Canale di Constantinopoli Rappresentate in Lettera alla Sacra Real Maestá Cristina Regina di Svezia da Luigi Ferdinando Marsigli. Nicoló Angelo Tinassi, Roma. Translated into English by B. Soffientino and M.E.Q. Pilson.
170. Martin R.E., E. Leorri and P.P. McLaughlin, 2007. Holocene sea level and climate change in the Black Sea: multiple marine incursions related to freshwater discharge events, Quaternary International 167–168, 61–72.
171. Marullo S., E. Napolitano, R. Santoleri, B. B. Manca, R. Evans, 2003. The variability of Rhodes and Ierapetra gyres studied by remote sensing observation, hydrographic data and model simulations during LIWEX (october 1994-april 1995), J. Geophys. Res., C9, DOI:10.1029/2002JC001393.
172. Marullo S., V. Artale and R. Santoleri, 2011, submitted. The SST multidecadal variability in the Atlantic-Mediterranean region and its relation to AMO. J. of Climate.
173. Mertens, C., and F. Schott, 1998. Interannual variability in deep-water formation in the northwestern Mediterranean, J. Phys. Oceanogr., 28, 1410–1424.
174. Miller, A.R., 1963. Physical oceanography of the Mediterranean Sea: a discourse. Rapport du 17e Congrès de la Commision Internationale pour l'Exploration Scientifique de la Mer Mediterranée 17, pp. 857–871.

175. Miller, A.R., 1974. Deep convection in the Aegean Sea, in: Processes de formation des eaux océaniques profondes. Colloques Internationaux du CNRS 215, pp. 1–9.
176. Millot, C., and R. Gerin, 2010. The Mid□Mediterranean Jet Artefact, Geophys. Res. Lett., 37, L12602, doi:10.1029/2010GL043359.
177. Millot C. and I. Taupier-Letage, 2005a. Circulation in the Mediterranean Sea, The Handbook of Environmental Chemistry, Volume K, May 2005, Pages 29 - 66 DOI: 10.1007/b107143.
178. Millot C. and I. Taupier-Letage, 2005b. Additional evidence of LIW entrainment across the Algerian Basin by mesoscale eddies and not by a permanent westward-flowing vein. Progr. In Oceanogr., 66, 231-250.
179. Millot C., I. Taupier-Letage and M. Benzohra, 1990. The Algerian Eddies. Earth-Sci. Rev., 27, 203-219.
180. Millot C., J. Candela, J.-L. Fuda and Y. Tber, 2006. Large warming and salinification of the Mediterranean outflow due to changes in its composition. Deep-Sea Res., 53/4, 656-666. doi:10.1016/j.dsr.2005.12.017
181. Millot C., I. Taupier-Letage and M. Benzohra, 1997. Circulation off Algeria inferred from the Médiprod-5 current meters. Deep-Sea Res., 44, 9-10, 1467-1495.
182. Millot C., 1987. Circulation in the West Mediterranean Sea. Oceanol Acta, Vol.10, 143-149.
183. Millot, C., 1979. Wind induced upwellings in the Gulf of Lions. Oceanol. Acta, 2, 3, 261-274.
184. Millot, C., 1985. Some features of the Algerian Current. J. Geophys. Res., 90, C4, 7169-7176.
185. Millot, C., 1999. Circulation in the western Mediterranean Sea. J Mar Sys, 20, 423-442.
186. Millot, C., 2007. Interannual salinification of the Mediterranean inflow. Geophys. Res. Lett., 34, doi: 10.1029/2007GL031179.
187. Millot, C., 2008. Short-term variability of the Mediterranean in- and out-flows. Geophys. Res. Lett., 35, L15603, doi:10.1029/2008/GL033762.
188. Millot, C., 2009. Another description of the Mediterranean Sea outflow. Prog. In Oceanogr., 82(2), 101-124.
189. Millot, C., J. Candela, J-L. Fuda, Y. Tber, 2006. Large warming and salinification of the Mediterranean outflow due to changes in its composition. Deep-Sea Res. I, 53, 656-665.
190. Molcard, A., Pinardi, N., Iskandarami, M., Haidvogel, D.B., 2002. Wind driven general circulation of the Mediterranean Sea simulated with a Spectral Element Ocean Model. Dynamics of Atmospheres and Oceans, 35, 97-130.
191. Möller, L., 1928. Alfred Merz' hydrographische Untersuchungen im Bosphorus und Dardanellen. Veröffentlichungen des Instituts für Meereskunde an der Universität Berlin, 18 (Neue Folge A), 284.
192. Moretti M., E. Sansone, G. Spezie and A. De Maio, 1993. Results of investigations in the Sicily Channel (1986–1990), Deep-Sea Research II 40, 1181–1192.
193. Myers, P.G., K. Haines and S. Josey, 1998: On the Importance of the Choice of Wind Stress Forcing to the Modelling of the Mediterranean Sea Circulation. Journal of Geophysical Research, 103, C8, 15729 - 15749.
194. Nielsen J.N., 1912. Hydrography of the Mediterranean and adjacent waters, Report of the Danish Oceanographical Expedition 1908–1910, 1, 72–191, Copenhagen.
195. Nijssen B., O'Donnel G.M.,Lettenmaier D.P. Lohmann D., Wood E.F., 2001, Predicting the discharge of global rivers. J.Climate 14, 3307-3323.
196. Nittis K. and A.Lascaratos, 1998. Diagnostic and Prognostic Numerical Studies of LIW formation, Journal of Marine Systems, 18, 179-195.
197. Nittis, K., Tziavos, C., Thanos, I., Drakopoulos, P., Cardin, V., Gačić, M., Petihakis, G., and Basana, R., 2003. The Mediterranean Moored Multi-sensor Array (M3A): system development and initial results, Ann. Geophys., 21, 75-87, doi:10.5194/angeo-21-75-2003.
198. Nixon, S.W., 2003. Replacing the Nile: Are Anthropogenic Nutrients Providing the Fertility Once Brought to the Mediterranean by a Great River? Ambio 32, 30–39.
199. Oğuz, T., 2005a. Black Sea Ecosystem Response to Climatic Variations, Oceanography, 18 (2), 122-133.

200. Oğuz, T., 2005b. Hydraulic adjustment of the Bosphorus exchange flow, Geophys. Res. Letters, 32, L06604, doi:10.1029/2005GL022353.
201. Oğuz, T. and H. İ. Sur, 1989. A two-layer model of water exchange through the Dardanelles Strait, Oceanology Acta, 12, 23-31.
202. Oğuz, T., Özsoy, E., Latif, M. A., Sur, H. İ. and Ünlüata Ü., 1990. Modelling of Hydraulically Controlled Exchange Flow in the Bosphorus Strait, J Phys Ocean, 20, 945-965.
203. Ovchinnikov M., 1984. The Formation of Intermediate Water in the Mediterranean, Oceanology 24 (1984), pp. 168–173.
204. Ovchinnikov, IM, A. Plakhin, L.V. Moskalenko, K.V. Neglyad, A.S. Osadchiy, A.F. Fedoseyev, V.G. Krivoscheya, K.V. Voytova, 1976. Hydrology of the Mediterranean Sea, Gidrometeoizdat, Leningrad, 375 pp.
205. Özsoy E., Di Iorio D., Gregg M. and Backhaus J., 2001. Mixing in the Bosphorus Strait and the Black Sea Continental Shelf: Observations and a Model of the Dense Water Outflow, J. Mar. Sys., 31, 99-135.
206. Özsoy, E, Hecht A., Ünlüata U., Brenner S., Oğuz T., Bishop J., Latif M.A., Rosentraub Z., 1991. A review of the Levantine Basin circulation and its variability during 1985-1988, Dyn. Atmos. Oceans 15: 421-456.
207. Özsoy, E., 1999. Sensitivity to Global Change in Temperate Euro-Asian Seas (the Mediterranean, Black Sea and Caspian Sea): A Review, The Eastern Mediterranean as a Laboratory Basin for the Assessment of Contrasting Ecosystems, editors: P. Malanotte-Rizzoli and V. N. Eremeev, NATO Science Series 2, Environmental Security, 51, Kluwer Academic Publishers, Dordrecht, s. 281-300.
208. Özsoy, E. and Ü. Ünlüata, 1997. Oceanography of the Black Sea: A Review of Some Recent Results, Earth Sci. Rev., 42 (4), 231-272.
209. Özsoy, E., Latif, M. A., Beşiktepe, S., Çetin, N., Gregg, N. Belokopytov, V., Goryachkin, Y. and V. Diaconu, 1998. The Bosphorus Strait: Exchange Fluxes, Currents and Sea-Level Changes, in: L. Ivanov and T. Oğuz (editors), Ecosystem Modeling as a Management Tool for the Black Sea, NATO Science Series 2: Environmental Security 47, Kluwer Academic Publishers, Dordrecht, vol. 1, 367 pp + vol. 2, 385 pp.
210. Özsoy, E., M. A. Latif, H. İ. Sur and Y. Goryachkin, 1996. A Review of the Exchange Flow Regimes and Mixing in the Bosphorus Strait, in: F. Briand, (editor), Mediterranean Tributary Seas, Bulletin de l'Institut Oceéanographique, Monaco, Special Number 17, CIESM Science Series No. 2, Monaco.
211. Özsoy, E., M. A. Latif, S. Tuğrul, and Ü. Ünlüata, 1995. Exchanges with the Mediterranean, Fluxes and Boundary Mixing Processes in the Black Sea, In: F. Briand, (editor), Mediterranean Tributary Seas, Bulletin de l'Institut Oceéanographique, Monaco, Special Number 15, CIESM Science Series No. 1, Monaco p. 1-25.
212. Özsoy, E., Sözer, A., Gündüz, M., Yücel, İ., Yağcı, B., Mert, İ., Yıldız, H., Simav, M. and M. Elge, 2009. Meteorology and Oceanography Network of Excellence (MOMA) – Observation and Model Forecast Systems, 3rd National Defense Applications Modelling and Simulation Conference, Ankara, 17-18 June 2009, 27 pp.
213. Painter, S.C. and M.N. Tsimplis, 2003. Temperature and salinity trends in the upper waters of the Mediterranean Sea as determined from the MEDATLAS dataset. Cont. Shelf Res. 23, 1507-1522.
214. Parrilla, G., T.H. Kinder, and R. Preller, 1986. Deep and Intermediate Mediterranean water in the western Alborán Sea, Deep-Sea Res., 33, 1, 55-88
215. Pascual, A., M.-I. Pujol, G. Larnicol, P.-Y. Le Traon, and M.-H. Rio, 2007. Mesoscale mapping capabilities of multisatellite altimeter missions: First results with real data in the Mediterranean Sea, J. Mar. Sys., 65, 1-4, 190-211.
216. Pektaş, H., 1953. Surface currents in the Bosphorus and the Sea of Marmara, Publication of the Hydrobiology Research Institute, Faculty of Science, University of Istanbul, Hydrobiology Series, A, 1 (4), 154-169 (in Turkish).

217. Peliz, A., P. Marchesiello, A. M. P. Santos, J. Dubert, A. Teles-Machado, M. Marta-Almeida, and B. Le Cann, 2009. Surface circulation in the Gulf of Cadiz: 2. Inflow-outflow coupling and the Gulf of Cadiz slope current, J. Geophys. Res., 114, C03011, doi:10.1029/2008JC004771.
218. Peneva, E., E. Stanev, V. Belokopytov, and P.-Y. Le Traon, 2001. Water transport in the Bosphorus Straits estimated from hydro-meteorological and altimeter data: seasonal to decadal variability. J. Mar. Sys. 31, 21-33.
219. Pettenuzzo D., Large W.G., Pinardi N., 2010. On the corrections of ERA40 surface flux products consistent with the Mediterranean heat and water budgets and the connection between basin surface total heat flux and NAO" JGR-Ocean, 115 C06022, doi: 10.1029/2009JC005631.
220. Pierini, S., Dijkstra, H.A., Riccio, A., 2009. "A nonlinear theory of the Kuroshio Extension bimodality". Journal of Physical Oceanography, 39, 2212-2229.
221. Pike J.G., 1964. The estimation of annual runoff from meteorological data in a tropical climate. Journal of Hydrology 2, 116-123
222. Pinardi N., G. Korres, A. Lascaratos, V. Roussenov and E. Stanev, 1997. Numerical simulation of the interannual variability of the Mediterranean Sea upper ocean circulation. Geophys. Res. Letters 24, 425–428.
223. Pinardi N., Zavatarelli M., Arneri E., Crise A., Ravaioli M., 2004. The physical, sedimentary and ecological structure and variability of shelf areas in the Mediterranean Sea. The Sea Vol. 14 (A R. Robinson and K. Brink Eds.), Harvard University Press, Cambridge, USA, 1243-1330.
224. Pinot, J.M., J.L. López-Jurado, M. Riera, 2002. The Canales experiment (1996-1998). Inter-annual, seasonal and mesoscale variability of the circulation in the Balearic channels. Prog. In Oceanogr., 55, 335-370.
225. Pisacane G., V. Artale, S. Calmanti and V. Rupolo, 2006. Decadal Oscillations in the Mediterranean Sea: A Result of the Overturning Circulation Variability in the Eastern Basin? Climate Research, Vol. 31, N. 2-3.
226. Plakhin Y.A., 1971. Formation of distinct deep water in the Mediterranean by convective mixing, Oceanology 11, 524–529.
227. Plakhin, Y.A., 1972, Vertical winter circulation in the Mediterranean, Oceanology 12 (3), 344–351.
228. POEM Group, 1992. General circulation of the eastern Mediterranean sea, Earth Sci. Rev., 32: 285-309.
229. Pollak M.J, 1951. The sources of the deep water of the eastern Mediterranean Sea, J. Mar. Res. 10 (1), 128–152.
230. Poulain P.-M. and E. Zambianchi, 2007. Surface circulation in the central Mediterranean Sea as deduced from lagrangian drifters in the 1990s, Continental Shelf Research 27 (7), 981–1001.
231. Puillat I., I. Taupier-Letage and C. Millot, 2002, Algerian eddies lifetime can near 3 years, J. Mar. Syst. 31(4), 245–259.
232. Pujol M.-I., G. Larnicol, 2005. Mediterranean sea eddy kinetic energy variability from 11 years of altimetric data, Journal of Marine Systems, 58(3-4), 121-142, doi: 10.1016/j.jmarsys.2005.07.005.
233. Reverdin, G., E. Kestenare, C. Frankignoul, and T. Delcroix, 2007. Surface salinity in the Atlantic Ocean (30ºS–50ºN), Prog. Oceanogr., 73, 412, 311 –340.
234. Rhein, M., 1995: Deep water formation in the western Mediterranean, J. Geophys. Res., 100(C4), 6943– 6959.
235. Ribotti A., I. Puillat, R. Sorgente, S. Natale, 2004 .Mesoscale circulation in the surface layer off the southern and western Sardinia Island in 2000–2002, Chemistry and Ecology, 1029-0370, 20, 5, 345–363.
236. Rinaldi E., B. Buongiorno Nardelli, E.Zambianchi, R. Santoleri, P.-M. Poulain, 2010. Lagrangian and Eulerian observations of the surface circulation in the Tyrrhenian Sea, J. Geophys. Res., 115, C04024, doi:10.1029/2009JC005535.
237. Rio, M.-H., P. M. Poulain, A. Pascual, E. Mauri, G. Larnicol, and R. Santoleri, 2007. A mean dynamic topography of the Mediterranean Sea computed from altimetric data, in-situ

measurements and a general circulation model, J. Mar. Syst., 65, 484–508, doi:10.1016/j.jmarsys.2005.02.006.

238. Rixen, M., J-M. Bekers, S. Levitus, J. Antonov, T. Boyer, C. Maillard, M. Fichaud, E. Balopoulos, S. Iona, H. Dooley, M. J. García, B. Manca, A. Girgetti, G. Manzzella, M. Mikhailov, N. Pinardi, M. Zavatarelli, 2005. The Western Mediterranean Deep Water: a proxy for climate change. Geophys. Res. Lett., 32, L12608, doi: 10.1029/2005GL022702.
239. Robinson A.R., A. Hecht, N. Pinardi, J. Bishop, W.G. Leslie, Z. Rosentroub, A.J. Mariano and S. Brenner, 1987. Small synoptic/mesoscale eddies and energetic variability of the eastern Levantine basin, Nature, 327, 131-134.
240. Robinson, A. R., W. G. Leslie, A. Theocharis and A. Lascaratos, 2001. Mediterranean Sea Circulation. Encyclopedia of Ocean Sciences, Academic Press: 1689–1706.
241. Robinson, A.R., J. Sellshop, A. Warn-Warnas, W.J. Leslie, C.J. Lozano, P.J. Haley Jr., L.A. Anderson and P.F.J. Lermusiaux, 1999. The Atlantic Ionian Stream, Journal of Marine Systems 20, 129–156.
242. Roether, W., B. Klein, B.B. Manca, A. Thecharis, S. Kioroglou, 2007. Transient Eastern Mediterranean Deep waters in response to the massive dense water output of the Aegean Sea in the 1990s. Prog. in Oceanogr., 74, 540-571.
243. Roether, W., B.B. Manca, B. Klein, D. Bregant, D. Georgopoulos, V. Beitzel, V. Kovacevic, A. Luchetta, 1996. Recent changes in Eastern Mediterranean Deep waters. Science, 271, 333-335.
244. Roether, W., Schlitzer, R., 1991. Eastern Mediterranean deep water renewal on the basis of clorofluoromethane and tritium data. Dynamics of atmosphere and oceans, 15, 3-5, 333-354.
245. Rohling, E.J. and H. Bryden, 1992. Man-induced salinity and temperature increase in the western Mediterranean deep water. J. Geophys. Res., 97, NO. C7, 11191-11198.
246. Romanou, A., G. Tselioudis, C. S. Zerefos, C.-A. Clayson, J. A. Curry and A. Andersson, 2010. Evaporation - Precipitation variability over the Mediterranean and the Black Seas from satellite and reanalysis estimates, Journal of Climate, doi:10.1175/2010JCLI3525.1.
247. Roussenov, V., E. Stanev, V. Artale and N. Pinardi, 1995. A seasonal model of the Mediterranean Sea General Circulation, Journal of Geophysical Research ocean, vol. 100, no. C7, 13515-13538.
248. Rubino A. and D. Hainbucher, 2007. A large abrupt change in the abyssal water masses of the eastern Mediterranean. Geophys. Res. Lett., 34, L23607, doi:10.1029/2007GL031737.
249. Ruiz, S., A. Pascual, B. Garau, I. Pujol, and J. Tintoré, 2009. Vertical motion in the upper ocean from glider and altimetry data, Geophys. Res. Lett., 36, L14607, doi:10.1029/2009GL038569.
250. Ruiz, S., D. Gomis, M. G. Sotillo and S. A. Josey, 2008. Characterization of surface heat fluxes in the Mediterranean Sea from a 44-year high-resolution atmospheric data set, Global and Planetary Change, 63, 2-3, 258-274, doi:10.1016/j.gloplacha.2007.12.002.
251. Russo, A., S. Rabitti, M. Bastianini, 2002. Decadal climatic anomalies in the northern Adriatic Sea inferred from a new oceanographic data set. Marine Ecology, 23, suppl. 1, 340-351.
252. Ruti P.M., Marullo S., D'Ortenzio F. and Tremant M., 2007. Comparison of analyzed and measured wind speeds in the perspective of oceanic simulations over the Mediterranean basin: Analyses, QuikSCAT and buoy data, Journal of Marine Systems, 70(1-2), 33-48, doi:10.1016/j.jmarsys.2007.02.026.
253. Ryan W.B.F., Major C.O., Lericolais G., Goldstein S.L., 2003. Catastrophic flooding of the Black Sea. Annu. Rev. Earth Planet. Sci.31:525–54.
254. Salas J., C. Millot, J. Font and E. García-Ladona, 2002. Analysis of mesoscale phenomena in the Algerian Basin observed with drifting buoys and infrared images. Deep-Sea Res., 49, 2, 245-266.
255. Salat, J. and J. Font, 1987. Water mass structure near and offshore the Catalan coast during the winter of 1982 and 1983. Ann. Geophys., 5, 49-54.
256. Salat, J. and J. Pascual, 2006. Principales tendencies climatológicas en el Mediterráneo noroccidental a partir de más de 30 años de observaciones oceanográficas en la costa catalana. En: Clima, sociedad y medio ambiente, J.M. Cuadrats, M.A. Sanz, S.M. Vicente, S. Lanjeri, N.

de Luis, J.C. González (Eds.). Publicaciones de la Asociación española de Climatología (AEC), serie A, nº 5, 284-290.
257. Salat, J., M. Emelianov and P. Puig, 2009. From bottom water (Lacombe, 1985) to new-WMDW since 2005. Possible shifts in open sea deep convection. In Dynamics of Mediterranean Deep waters, CIESM workshop monograph, nº 38, 41-49.
258. Sammari, C., Millot, C., Prieur, L., 1995. Some aspects of the seasonal and mesoscale variabilities of the Northern Current inferred from the PROLIG-2 and PROS-6 experiments. Deep-Sea Res. 42 6 , 893–917.
259. Sammari, C; Millot, C; Taupier-Letage, I, A. Stefani, and M. Brahim, 1999. Hydrological characteristics in the Tunisia-Sardinia-Sicily area during spring 1995, Deep Sea Research Part I, 46 (10), 1671-1703.
260. Samuel-Rhoads, Y., Iona S., Zodiatis G., Stylianou S., Georgiou G., Hayes D., 2010. Sea Surface Temperature and Salinity rise in the Levantine Basin. 39th CIESM Congress, May, Venice.
261. Sánchez-Garrido, J.C., García-Lafuente, J., Criado Aldeanueva, F., Baquerizo, A. and Sannino, G. 2008. Time-spatial variability observed in velocity of propagation of the internal bore in the Strait of Gibraltar. J. Geophys. Res., 113, C07034, doi: 10.1029/2007JC004624.
262. Sanchez-Gomez E., Somot S., Josey S.A., Dubois C., Elguindi N., Déqué M., 2011. Evaluation of the Mediterranean Sea Water and Heat budgets as simulated by an ensemble of high resolution Regional Climate Models. Clim. Dyn. In press.
263. Sanchez-Gomez E., Somot S., Mariotti A., 2009. Future changes in the Mediterranean water budget projected by an ensemble of Regional Climate Models. Geophys. Res. Lett., 36, L21401, doi:10.1029/2009GL040120.
264. Sánchez-Román, A., G. Sannino, J. García-Lafuente, A. Carillo and F. Criado-Aldeanueva, 2009. Transport estimates at the western section of the Strait of Gibraltar: A combined experimental and numerical modeling study. J. Geophys. Res., 114, C06002, doi:10.1029/2008JC005023.
265. Sannino G., Herrmann M., Carillo A., Rupolo V., Ruggiero V., Artale V. Heimbach P., 2009b. An eddy-permitting model of the Mediterranean Sea with a two-way grid refinement at the Strait of Gibraltar. Ocean Modelling, 30, 1, 56-72, doi: 10.1016/j.ocemod.2009.06.002
266. Sannino, G., A. Bargagli, and V. Artale, 2004. Numerical modeling of the semidiurnal tidal exchange through the Strait of Gibraltar, J. Geophys. Res., 109, C05011, doi:10.1029/2003JC002057.
267. Sannino, G., A. Carillo, and V. Artale, 2007. Three-layer view of transports and hydraulics in the Strait of Gibraltar: A three-dimensional model study, J. Geophys. Res., 112, C03010, doi:10.1029/2006JC003717.
268. Sannino, G., L. Pratt and A. Carillo, 2009a. Hydraulic criticality of the exchange flow through the Strait of Gibraltar, J. Phys. Oceanogr., 39, 11, 2779-2799, doi:10.1175/2009JPO4075.1.
269. Sanz E. P. and Á. Viúdez, 2005. Diagnosing Mesoscale Vertical Motion from Horizontal Velocity and Density Data, J. Phys. Oceanogr., 35: 1744-1762.
270. Schlitzer R., W. Roether, H. Oster, H. Junghans, M. Hausmann, H. Johannsen and A. Michelato, 1991. Chlorofluoromenthane and Oxygen in the Eastern Mediterranean, Deep-Sea Research 38 (12), 1531–1551.
271. Schroeder K., Josey S.A., Herrmann M., Grignon L., Gasparini G.P., Bryden H.L., 2010. Abrupt warming and salting of the Western Mediterranean Deep Water after 2005: atmospheric forcings and lateral advection. J. Geophys. Res., doi: 10.1029/2009JC005749.
272. Schroeder K., Taillandier V., Vetrano A., Gasparini G.P., 2008a. The circulation of the Western Mediterranean Sea in spring 2005 as inferred from observations and from model outputs. Deep Sea Research, Part I, 55, 947-965.
273. Schroeder, K., A. Ribotti, M. Borghini, R. Sorgente, A. Perilli, and G.P. Gasparini, 2008b. An extensive Western Mediterranean Deep Water renewal between 2004 and 2006, Geophys. Res. Lett., 35, L18605, doi:10.1029/2006GL027121.

274. Schroeder, K., G.P. Gasparini, M. Tangherlini, and M. Astraldi, 2006. Deep and intermediate water in the Western Mediterranean under the influence of the Eastern Mediterranean Transient, Geophys. Res. Lett., 33, 21, L21607, doi:10.1029/2006 GL027121.
275. Send, U., J. Font, G. Krahmann, C. Millot, M. Rhein, and J. Tintoré, 1999. Recent advances in observing the physical oceanography of the western Mediterranean Sea. Progress in Oceanography, 44: 37-64.
276. SHOD, 2009. Turkish Straits Oceanography Atlas, Turkish Navy Navigation, Hydrography and Oceanography Office (in Turkish).
277. Shorthouse C.A. and N.W. Arnell, 1997. Spatial and temporal variability in European river flows and the North Atlantic Oscillation. In: FRIEND'97 — Regional Hydrology: Concepts and Models for Sustainable Water Resources ManagementA. Gustard, S. Blazkova, M. Brilly, S. Demuth, J. Dixon, H. van Lanen, C. Llasat, S. Mkhandi and E. Servat, Editors, International Association of Hydrological Sciences Publ. No. 246, 77–85.
278. Skliris, N., Sofianos, S., Lascaratos, A., 2007. Hydrological changes in the Mediterranean Sea in relation to changes in the freshwater budget: a numerical modelling study. Journal of Marine Systems 65, 400–416.
279. Smith, R.O., H.L. Bryden, and K. Stansfield, 2008. Observations of new western Mediterranean deep water formation using ARGO floats 2004–2006, Ocean Sci., 4, 133–149.
280. Smith, W. E., 1942. Some Observations on Water-levels and Other Phenomena Along the Bosphorus, Transactions of the American Geophysical Union, 27 (1), 61-68.
281. Somot S., 2005. Modélisation climatique du bassin méditerranéen: variabilité et scénarios de changement climatique. Ph-D thesis. Université Paul Sabatier, Toulouse- France. 333 pages
282. Somot S. , Sevault F., Déqué M., Crépon M., 2008. 21st century climate change scenario for the Mediterranean using a coupled Atmosphere-Ocean Regional Climate Model. Global and Planetary Change, 63(2-3), 112-126, doi:10.1016/j.gloplacha.2007.10.003
283. Somot S., Colin, J., 2008. First step towards a multi-decadal high-resolution Mediterranean sea reanalysis using dynamical downscaling of ERA40. Research activities in atmospheric and oceanic modelling. CAS/JSC Working group on numerical experimentation. Report No.38. (available at http://collaboration.cmc.ec.gc.ca/science/wgne/index.html)
284. Somot, S., Sevault F., Déqué M., and Crépon M., 2008, 21st Century Climate Change scenario for the Mediterranean using a coupled atmosphere-ocean regional climate model. Global and Planetary Change, 63 (2-3), Special Issue, 112-126.
285. Somot, S., Sevault, F., Déqué, M., 2006. Transient climate change scenario simulation of the Mediterranean Sea for the twenty-first century using a high-resolution ocean circulation model. Climate Dynamics 27, 851–879.
286. Soto-Navarro, J., F. Criado-Aldeanueva, J. García-Lafuente, and A. Sánchez-Román, 2010. Estimation of the Atlantic inflow through the Strait of Gibraltar from climatological and in situ data. J. Geophys. Res., 115, C10023, doi:10.1029/2010JC006302
287. Sözer, A., 2010. Numerical Modeling of the Bosphorus Exchange Flow Dynamics, Institute of Marine Sciences, Middle East Tchnical University, Erdemli, Mersin, Turkey (unpublished Ph.D. thesis in preparation).
288. Sözer, A. and E. Özsoy, 2002. A Three-Dimensional model of Bosphorus Strait Dynamics, The 2nd Meeting on the Physical Oceanography of Sea Straits, Villefranche, 15th-19th April 2002, 207-210.
289. Sparnocchia, S., G.M.R. Manzella, P. La Violette, 1994. The interannual and seasonal variability of the western Mediterranean Sea. In: La Violette, P.E. (Ed.), Seasonal and Interannual variability of the western Mediterranean Sea. AGU, Coastal and Estuarine Studies, 46, 177-194.
290. Sparnocchia, S., G.P. Gasparini, M. Astraldi, M. Borghini, P. Pistek, 1999. Dynamics and mixing of the Eastern Mediterranean outflow in the Tyrrhenian basin. Journal of Marine Systems, 20, 301-317.

291. Stanev, E. V., P.-Y. Le Traon, and E. L. Peneva, 2000. Sea level variations and their dependancy on meteolorogical and hydrological forcing: Analysis of altimeter and surface data for the Black Sea, Journal of Geophysical Research, 105(C7), 17,203–17,216.
292. Stanev, E. V., and E. L. Peneva, 2002. Regional sea level response to global climatic change: Black Sea examples. Global and Planetary Change, 32, 33-47.
293. Stashchuk, N. and K. Hutter, 2001. Modelling of water exchange through the Strait of the Dardanelles, Continental Shelf Research 21, 1361–1382.
294. Stashchuk, N. and K. Hutter, 2003. Modelling Gravity Current Flowing from the Bosphorus to the Black Sea, Geophys. Astrophys. Fluid Dynamics, 97, 1, 1–24.
295. Stemmann, L, Prieur, L, Legendre, L, Taupier-Letage I., Picheral M., Guidi L., Gorsky G., 2008. Effects of frontal processes on marine aggregate dynamics and fluxes: An interannual study in a permanent geostrophic front (NW Mediterranean), Journal Of Marine Systems, 70, 1-2, 1-20.
296. Stommel, H., 1972. Deep winter convection in the western Mediterranean Sea, in: Studies in physical oceanography: A tribute to Georg Wust on his 80th birthday, Vol. 2, edited by: Gordon, A. L., New York, NY, Gordon and Breach Science, 232 pp..
297. Stratford K, Haines K., 2002. Modelling changes in the Mediterranean thermohaline circulation 1987–1995. J Mar Syst 33–34:1–62.
298. Struglia M.V., Mariotti A, Filograsso A., 2004. River discharge into the Mediterranean Sea: climatology and aspects of the observed variability, J of Climate 17, 4740-4751.
299. Taupier-Letage I., I. Puillat, P. Raimbault and C. Millot, 2003. Biological response to mesoscale eddies in the Algerian Basin, Journal of Geophysical Research 108 (C8), p. 3245.
300. Taupier-Letage I. And C. Millot, 2010. Intermediate and deep circulations in the Eastern Basin of the Mediterranean: focus on its central part from the EGYPT observations (2005-2007). Rapp. Comm. Int. Mer Medit. 39: 190.
301. Taupier-letage, I., 2008. On the use of thermal infrared images for circulation studies: applications to the eastern Mediterranean basin.. In: “Remote sensing of the European Seas”, V. Barale and M. Gade Eds., Springer Verlag, 153-164.
302. Te Raa L. A. and H. A. Dijkstra, 2002. Instability of the Thermohaline Ocean Circulation on Interdecadal Timescales, Journal of Physical Oceanography, 32, 138-160.
303. Testor, P., K. Béranger, and L. Mortier, 2005b. Modeling the deep eddy field in the southwestern Mediterranean: The life cycle of Sardinian eddies, Geophys. Res. Lett., 32, L13602, doi:10.1029/2004GL022283.
304. Testor, P., U. Send, J.-C. Gascard, C. Millot, I. Taupier-Letage, and K. Beranger, 2005a, The mean circulation of the southwestern Mediterranean Sea: Algerian Gyres, J. Geophys. Res., 110, C11017, doi:10.1029/2004JC002861.
305. Testor, P; Gascard, J.C, 2003. Large-scale spreading of deep waters in the Western Mediterranean sea by submesoscale coherent eddies. Progress In Oceanography 66 (2-4), 211-230.
306. Theocharis A. and D. Georgopoulos, 1993. Dense water formation over the Samothraki and Limnos Plateaux in the north Aegean Sea (eastern Mediterranean Sea). Continental Shelf Res. 13, 919–939.
307. Theocharis A., D. Georgopoulos, A. Lascaratos and K. Nittis, 1993. Water masses and circulation in the central region of the Eastern Mediterranean: Eastern Ionian, South Aegean and Northwest Levantine, 1986–1987. In: Physical Oceanography of the Eastern Mediterranean SeaA.R. Robinson and P. Malanotte-Rizolli, Editors, Deep-Sea Res., II 40, 1121–1142.
308. Theocharis, A. and the CIESM initiative group, 2003. Long-term sustained observing system for climatic variability studies in the Mediterranean. In: Building the European capacity in operational oceanography, Proc. Third Int. Conf. EuroGOOS, Elsevier Oceanography Series, 69: 78-86.
309. Theocharis, A., K., Nittis, H. Kontogyannis, E. Papageorgiou, E. Balopoulos, 1999. Climatic changes in the Aegean Sea influence the Eastern Mediterranean thermohaline circulation (1986-1997). Geophys. Res. Lett., 26, 11, 1617-1620.

310. Tsimplis, M. N., E. Álvarez-Fanjul, D. Gomis, L. Fenoglio-Marc, and B. Pérez, 2005. Mediterranean Sea level trends: Atmospheric pressure and wind contribution, Geophys. Res. Lett., 32, L20602, doi:10.1029/2005GL023867.
311. Tsimplis, M.N. and M. Rixen, 2002. Sea level in the Mediterranean Sea: the contribution of temperature and salinity changes. Geophys. Res. Lett., 29(3), 2136.
312. Tsimplis, M.N. and S. A. Josey, 2001. Forcing of the Mediterranean Sea by atmospheric oscillations over the North Atlantic. Geophys. Res. Lett., 28, 5, 803-806.
313. Tsimplis, M.N. and T. F. Baker, 2000. Sea level drop in the Mediterranean Sea: An indicator of deep water salinity and temperature changes? Geophys. Res. Lett., 27, 12, 1731-1734.
314. Ünlüata, U ., Oğuz, T., Latif, M. A., and Özsoy, E., 1990. On the physical oceanography of the Turkish Straits, in: Pratt, L. J., (editor), The Physical Oceanography of Sea Straits, NATO/ASI Series, Kluwer, Dordrecht, 25-60.
315. Van Haren H., C. Millot and I. Taupier-Letage, 2006. Fast deep sinking in Mediterranean eddies. Geophys. Res. Let., 33, L04606, doi: 10.1029/2005GL025367.
316. Vargas-Yáñez, M., F. Moya, E. Tel, M.C. García-Martínez, E. Guerber, M. Bourgeon, 2009. Warming and salting in the western Mediterranean during the second half of the 20th century: inconsistencies, unknowns, and the effect of data processing. Sci. Mar., 73(1), doi: 10.3989/scimar.2009.73n1007.
317. Vargas-Yáñez, M., F. Plaza, J., García-Lafuente, T. Sarhan, J.M. Vargas, and P. Vélez-Belchí, 2002. About the seasonal variability of the Alboran Sea circulation. J. Mar. Systems, 35, 229–248.
318. Vargas-Yáñez, M., P. Zunino, A. Benali, M. Delpy, F. Pastre, F. Moya, M.C. García-Martínez, E. Tel, 2010. How much is the western Mediterranean really warming and salting?, J. Geophys. Res., 115, C04001, doi: 10.1029/2009JC005816.
319. Velaoras D. and A. Lascaratos, 2005. Deep water mass characteristics and interannual variability in the North and Central Aegean Sea, J. Mar. Syst. 53, 59–85.
320. Vignudelli, S., G. Gasparini, M. Astraldi, and M. Schiano, 1999. A possible influence of the north atlantic oscillation on the circulation of the western Mediterranean sea, Geophys. Res. Lett., 26, 623–626.
321. Vilibic I., and M. Orlic, 2001. Least squares tracer analysis of water masses in the South Adriatic, Deep Sea Res., Part I, 48 , 2297- 2330, doi:10.1016/S0967-0637(01)00014-0.
322. Viúdez, A., J. Tintoré, and R. L. Haney, 1996a. Circulation in the Alboran Sea as determined by quasi-synoptic hydrographic observations. Part I: Three-dimensional structure of the two anticyclonic gyres. J. Phys. Oceanogr. 26:684–705.
323. Viúdez, A., R. L. Haney, and J. Tintoré., 1996b. Circulation in the Alboran Sea as determined by quasi-synoptic hydrographic observations. Part II: Mesoscale ageostrophic motion diagnosed through density dynamical assimilation. J. Phys. Oceanogr. 26:706–724.
324. Vörösmarty, C.J., Fekete, B.M., Tucker, B.A., 1998. Global River Discharge 1807–1991, RivDIS v1.1. Available from: http://www.daacsti.ornl.gov//RIVDIS/guides/rivdis_guide.html. Last update: June 2004).
325. Whitehead, J. A., Jr, 1985. A laboratory study of gyres and uplift near the Strait of Gibraltar, J. Geophys. Res., 90, 7045– 7060.
326. Wunsch C., 1997. The vertical partition of oceanic horizontal kinetic energy. J. Phys. Oceanogr. 27, 1770–94.
327. Wüst, G., 1961. On the vertical circulation of the Mediterranean Sea. J. Geophys. Res., 66 (10), 3261-3271.
328. Xoplaki, E., J.F. Gonzalez-Rouco, J. Luterbacher, and H. Wanner, 2004. Wet season Mediterranean precipitation variability: influence of large-scale dynamics and trends. Climate Dynamics 23, 63–78.
329. Yin F, Sarachik ES, 1995. Interdecadal thermohaline oscillations in a sector ocean general circulation model: advective and convective processes. J Phys Oceanogr 25:2465–2484

330. Yüce, H., 1993a. Water level variations in the Sea of Marmara. Oceanologica Acta, 16, 4, 335-340.
331. Yüce, H., 1993b. Analysis of the water level variations in the eastern Black Sea. J. Coastal Res., 9, 4, 1075-1082.
332. Yüksel, Y., Ayat, B., Öztürk, M. N., Aydoğan, B., Güler, I., Çevik, E. O. and A. C. Yalçıner, 2008. Responses of the Stratified Flows to their Driving Conditions - A Field Study, Ocean Engineering, 35 (13), 1304-1321.
333. Zervakis V, Georgopoulos D, Karageorgis AP, Theocharis A., 2004. On the response of the Aegean sea to climatic variability: a review. Internat J Climatol 24: 1845–1858.
334. Zervakis, V., D. Georgopoulos and P. G. Drakopoulos, 2000. The role of the North Aegean in triggering the recent Eastern Mediterranean climate changes. J. Geophys. Res., 105, 26,103-26,116.
335. Zervakis, V, Papadoniou, G; Tziavos, C, and A. Lascaratos, 2003. Seasonal variability and geostrophic circulation in the eastern Mediterranean as revealed through a repeated XBT transect. Annales Geophysicae 21, 1: 33-47.
336. Zodiatis G, Theodorou A. and Demetropoulos A., 1998. Hydrography and Circulation in the area south of Cyprus in late summer 1995 and in spring 1996, Oceanologica Acta, 21, 3, 447-458.
337. Zodiatis G., 1991, The Water Masses and Deep Convection in the Cretan Sea during late winter 1987, Annales Geophysicae, 9: 367-376.
338. Zodiatis G., Hayes D., Gertman I., Samuel-Rhoads Y., 2010b. Cyprus warm eddy and the Atlantic water during the CYBO cruise 1995-2009. 39th CIESM Congress, May, Venice.
339. Zodiatis G., 1992, On the Seasonal Variability of the Water Masses Circulation in the NW Levantine Basin-Cretan Sea and Flows through the Eastern Cretan Arc Straits, Annales Geophysicae, 10: 12-24.
340. Zodiatis G., 1993a, Water Mass Circulation Between the SE Ionian - W Cretan Basins through the Western Cretan Arc Straits, Bollettino di Oceanologia Teorica ed Applicata, XI, 1: 61-75.
341. Zodiatis G., 1993b, Circulation of the Cretan Sea Water Masses (Eastern Mediterranean Sea), Oceanologica Acta, 16, 2: 107-114.
342. Zodiatis G., 1994. Advection of the Black Sea Water in the North Aegean Sea, The Global Atmosphere and Ocean System, 2,1, 41-60.
343. Zodiatis G., Drakopoulos P., Gertman I., Brenner S., and Hayes D., 2005a. The Atlantic Water Mesoscale Hydrodynamics in the Levantine Basin, 27th CIESM Workshop Monograph-Strategies for understanding mesoscale processes.
344. Zodiatis G., Drakopoulos P., Brenner S., Groom S., 2005b. Variability of the Cyprus warm core Eddy during the CYCLOPS project (2005) Deep-Sea Research Part II: Topical Studies in Oceanography, 52 (22-23), pp. 2897-2910.
345. Zodiatis G., Samuel-Rhoads Y., Hayes D., Stylianou S., Gertman I., Georgiou G., Soloyov D., 2010a. Interannual Variability in the Se Levantine Basin 1995-2009. EGU2010 General Assembly, May, Vienna.
346. Zodiatis, G. and G.P. Gasparini, 1996. Thermohaline staircase formation in the Tyrrhenian Sea. Deep-Sea Res., 43, 655-678.
347. Zodiatis, G., Drakopoulos, P., Brenner, S., Groom, S., 2003. CYCLOPS project: the hydrodynamics of the warm core eddy south of Cyprus. In: Yilmaz, A. (Ed.), Oceanography of the Eastern. Tubitak Publishers, Ankara, Turkey, pp. 18–23.
348. Zodiatis, G., Gertman I., Hayes D., Brenner S., 2007. The Atlantic water in the Levantine Basin 1995-2006. 38th CIESM Congress, April, Istanbul.
349. Zore-Armada, M. and T. Pucher-Petkovic, 1977. Some dynamic and biological characteristics of the Adriatic and other basins of the Eastern Mediterranean. In Symposium on the Eastern Mediterranean Sea IBP/PM-UNESCO. N. Huilings (Ed.), 396 pp. Acta Adriatica 28: 15-28.